UNIVERSITÀ DELLA CALABRIA

DIPARTIMENTO DI INGEGNERIA MECCANICA, ENERGETICA E GESTIONALE

DOTTORATO DI RICERCA IN INGEGNERIA CIVILE ED INDUSTRIALE

XXXI CICLO

Analysis of Static and Dynamic Meshing Behaviour of Lightweight Gears

Author:
Shadi SHWEIKI

Supervisor:
Prof. Domenico MUNDO

co-Supervisor:
Dott. Tommaso TAMAROZZI

February 2019

Declaration of Authorship

I, Shadi SHWEIKI, declare that this thesis titled, "Analysis of Static and Dynamic Meshing Behaviour of Lightweight Gears" and the work presented in it are my own. I confirm that:

- This work was done wholly or mainly while in candidature for a research degree at this University.
- Where any part of this thesis has previously been submitted for a degree or any other qualification at this University or any other institution, this has been clearly stated.
- Where I have consulted the published work of others, this is always clearly attributed.
- Where I have quoted from the work of others, the source is always given. With the exception of such quotations, this thesis is entirely my own work.
- I have acknowledged all main sources of help.
- Where the thesis is based on work done by myself jointly with others, I have made clear exactly what was done by others and what I have contributed myself.

Signed:

Date:

"After climbing a great hill, one only finds that there are many more hills to climb."

Nelson Mandela

Acknowledgements

The results shown in this thesis are partially founded by the People Programme (Marie Curie Actions) of the European Union's Seventh Framework Programme FP7/2007-2013/ under REA grant agreement no. 324336 DEMETRA: Design of Mechanical Transmissions: Efficiency, Noise and Durability Optimization.

Contents

List of Figures

List of Tables

A tutti quelli che non hanno mai smesso di lottare per realizzare i propri sogni.

Chapter 1

Introduction

Gears are seen as a symbol of mechanical industry, being applied in an enormous variety of mechanisms in many sectors. Gear have the goal of transmitting power between a driving shaft and the driven shaft, possibly at a different rotational speed, with the lowest possible losses. Being the transmitted power constant, neglecting all the losses, the torque at the different shaft is not constant if the speed changes. This aspect is particular relevant for the application of gears, allowing to change the rotational speed and consequently increasing or decreasing the transmitted torque.
This task is performed for any of the possible transmissions layout resulting in a huge variety of shapes and arrangements, spreading from small gears with a diameter of few millimetres to gears in the range of meters. This great variety in the design and in the characteristics comes from the wide application range, motivated by the great efficiency in transmitting power for different transmitted torques and by the relative compactness, allowing a convenient component packaging.
The application fields are extremely different in terms of working conditions. As example, very small gears are used to transmit power in mechanical watches. This task, even if not the most demanding in terms of transmitted loads, is extremely challenging due to precision requirements. Gears are also used almost in the totality of automotive gearboxes, allowing to the engine to operate in an ideal rotating regime for a vast range of vehicle speed. The gears used in wind turbines and marine industry are completely on the opposite side in terms of dimensions and delivered power. Even if the precision requirements are not as demanding as the ones used in the watches industry, the durability is the major concern. A fault can result in money loss due to the downtime or, even worse, in dramatically high reparation costs. The aviation industry is another application scenario for gears. The lightweight and durability requirements typical of planes and helicopter require an extreme accurate design, especially in terms of the coupling between the structure and the excitation coming from the gears. The dynamic behaviour represents a serious issue in these applications where, as example, the main gearbox is asked to reduce the rotational speed of the turbine from thousands of revolutions per minute to the hundreds allowed for the main rotor.
The fundamental role acquired by the gears in the mechanical industry is demonstrated also by the way in which it is perceived by the general society. In an editorial of the Journal of Mechanical Design, which is still actual [138], the gears are considered the most

representative icon of Mechanical Engineering by a survey. The iconic role of the gears is strengthened also by its inclusion in the emblem of the Italian Republic, as shown in Figure 1.1, where a metal gear represents the work activity, as stated by the first article of the Italian Constitution.

FIGURE 1.1: Emblem of the Italian Republic, where it is possible to notice the symbol of a gear. Reproduced from [147].

The iconic role of the gear is also due to the fact that gears are used since a long time ago in mechanics. The oldest known track of metallic gears, known as the Antikythera mechanism is dated back to first century before Christ. The name was given according to the one of the Greeck island where it was found in 1901, Figure 1.2. The mechanism was understood [38] [42] and replicated in a working copy.

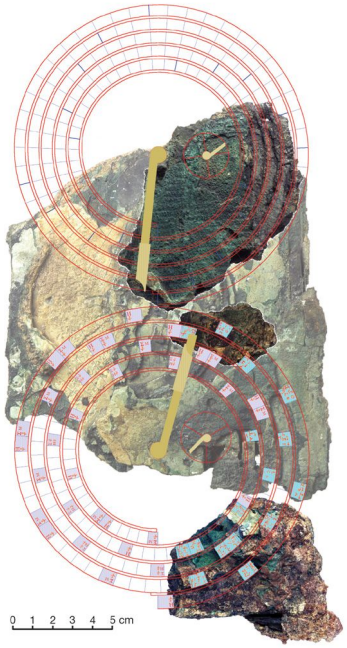

FIGURE 1.2: Main fragments of the Antikythera mechanism, dated circa 100 B.C. Reproduced from [42].

In spite of the many years of use in industry, gears still are the topic of many studies with goal to better understand the complex phenomena happening during the meshing process. In this dissertation the focus is limited to cylindrical gears with an involute profile, with the exception of deliberate micro-modifications applied on the theoretical shape of the tooth. More in detail, the object of this thesis work is bounded to the analysis of the dynamic behaviour of cylindrical gears where the shape of the gear body is modelled to achieve a reduction of the overall mass of the gear. The mass reduction, however, has also an influence on the mesh stiffness of the gear, generating additional dynamic components in the dynamic response. In this context the simulation of the dynamic behaviour of the transmission is particularly relevant, when high acoustic or durability standards have to be achieved.

In nominal conditions the meshing process involves only the kinematic relationship between conjugate profiles. Nevertheless manufacturing and assembly errors, together with the elastic deformations of the tooth when subject to the transmitted torque move the meshing process away from the pure kinematic contact. To accommodate this type of deviation a small amount of material, in the order of magnitude of microns, is removed from the tooth surface. The resulting surface can now accommodate small angular misalignments as well as the deformation of the teeth without resulting in high peaks of the contact pressure. The static and dynamic response of the transmission can be highly affected by the micro-geometry modifications, and a proper choice of the deliberate deviation from the theoretical profile is a key factor. The procedure to define the proper combination of macro and micro geometry of the gears is a kind of *black art* because of the extremely vast number of possible parameter combinations. It was only since the 50s

that efforts were spent to find an accurate modelling of the gear contact process to individuate the correct combination of kinematic and micro-geometry parameters limiting, in this way, the number of expensive physical prototypes.
In order to properly model the gear meshing, it is necessary to consider different and coupled effects, acting on multiple tooth pairs at the same time. The contact deformation with load-dependent non-linearities as well as sharp strain trend on the contact surface have to be properly considered when the gears are modelled. Extra complications arise from the coupling with the elastic deformations of the gear body that may be relevant in case of gears with lightweight design, and may have effect also on the way in which the different tooth pairs share the meshing loads. The environmental concerns, indeed, together with the raising fuel price push for lighter structure, in which the dynamic behaviour on the system is crucial to guarantee a reliable product. The three-dimensional nature of the meshing problem makes the situation even worse. This is obviously true when helical gears are considered, but the problem to analyse is three-dimensional also when spur gears operate in a condition different from the nominal one, such as the case of angular misalignment.
Different and established tools are available to simulate the static behaviour of the gears, both at component and at system level. The difference nowadays is limited only to the dimension of the problem. The context is different when time-domain simulations are considered, such as speed run-up simulations. In this case the standard approaches used in static simulations are not feasible any more, due to the dimension of the problem. Different approaches are developed, based on assorted hypothesis and numerical techniques.
The challenges in the simulation of mechanical transmissions will be discussed in detail in Section 2.5, but it is however worthwhile to summarize the biggest ones here. The fluctuation in the meshing loads generated during the engagement and disengagement of the meshing teeth is responsible for some of the transmission failures and in many cases generates high noise and vibration levels in the transmission, affecting in this way the performances of the system in terms of durability and comfort. A big challenge is therefore to predict the coupling between the dynamic excitation coming from the teeth and the modal behaviour of the structure, allowing to establish the proper modifications already in the early design phase.
A whole category of problems is represented by the vibrations generated by the meshing loads when no contact losses happen. The typical acoustic signature is a tonal noise called *whine* at a frequency related to the meshing frequency of the gears. This type of noise is even amplified when the tonal components is sufficiently close to a system resonance. The goal for any simulation tool here is to properly model the mesh stiffness allowing to represent in a correct manner the different orders in which the meshing loads can be decoupled. A reliable representation of the mesh stiffness is important also to replicate the natural frequency of the mode shape involving a mutual deflection of the meshing teeth. In this case, indeed, the compliance of the gear body is not only an excitation for the system, but it also modifies the transmission response. The importance of the correct

representation of the coupling with the structure is evident. In case of planetary transmission, for example, the load sharing between the planets is directly affected by the ring and the supporting structure flexibility.
Another category of problems lies in the simulation of the meshing process when contact losses occur. The non-linearities generated by the clearance introduce the typical *jumps* in the amplitude of the frequency response. In this case the acoustic signature has not a defined frequency any more, because of the broadband nature of the impacts events. In this condition the gears are said to *rattle*. The dangerous overloads generated when the contact is restored, together with the definition of the conditions when the contact loss may occur, are the main concerns for the simulation tools.
Besides the whine and rattle phenomena, the improvement of the system efficiency is a important task for the designers. The attention given to the transmissions efficiency is pulled by the increased oil price and the regulation on the pollutant emissions. The physical phenomena that contribute in wasting mechanical energy in a transmission are mainly related to friction and to the interaction of the gears with the surrounding fluids. The complexity of the phenomena is so big to constitute an entire branch of study that is not treated in this dissertation.
The argumentations in favour of the importance of gear dynamics simulations can be supported by a sentence in the conclusions of a PhD dissertation [52] stating that the bigger becomes the size of a wind turbine (and its transmission), the more important becomes the detailed design of microgeometry modifications.

1.1 Context of the present thesis work

The pursuit for lightness of the mechanical transmissions, together with the structures in general, increases the dynamic coupling between the components of the system, requiring more sophisticated simulation techniques. On the other hand, competition between the manufacturers has raised the requirements in terms of reliability and acoustic comfort. An example of the increased requirements in terms of acoustic comfort is given by the automotive field. Electric cars and hybrid vehicles in electric mode are particularly sensitive to the transmission noise since the noise coming from the internal combustion engine is no longer present, making impossible to cover the gear whine or rattle noise.
The biggest concern for the wind turbine industry is reliability as testified by the related literature [53][104][10]. As additional proof of the importance given to this issue by the manufacturers, an industrial dedicated consortium is established to increase the knowledge about the causes of the expensive failures using advanced simulation and condition monitoring techniques [68].
Prediction of the global response of the system is required to address the distributed flexibility of the components coupled with the non-linear gear contact. Finite Element (FE) analysis can accomplish this task in a very accurate way, but the computational cost is too high: static simulations of a single meshing period on a standard workstation require a computational time that is in the order of hours, using general purpose non-linear FE

software. This time can drop to minutes if the same problem is addressed by specialized FE formulations expressly designed for gear contact simulation [101].
The trade-off to accept if the designers want to achieve more feasible computational times is to move towards analytical formulation. Different lumped-parameters models, up-to 21 degrees of freedom, are available in literature [153]. Different and more recent formulations have been developed to take into account the three-dimensional nature of the meshing process [136] [40]. This type of formulation has the biggest drawback in the exclusion of the flexibility modelling of key components, such as shafts and the housing. These models however have still the ability to investigate detailed dynamic behaviour of lightweight gears, when combined with FE simulation tools, as it will be shown in Chapter 3.
Multibody modelling brings the accuracy of the model at a higher level thanks to the possibility of including flexible mode shapes in the simulation, still in a reasonable simulation time. An efficient multibody approach is used in Chapter 4 to simulate the static behaviour of lightweight gears while the same approach, but this time applied to the dynamic analysis of a complete transmission, is used in Chapter 5.

1.2 Contribution to the state of the art

Main contributions of the presented work to the state of the art can be listed as follows:

1. The dynamic contribution due to the lightweighting is analysed exploiting the computational efficiency given by the lumped parameters formulations. An accurate representation of the variable mesh stiffness, including the contribution coming from the particular shape of the gear body, is computed using non-linear FEM simulation in a pre-processing phase. In this way, long time-transient simulation such as run-up events, can be performed showing the additional frequency components generated by the mesh fluctuations.

2. A general purpose commercial MB simulation environment, such as Siemens Simcenter 3D Motion, is further extended to include the analysis of the lightweight gears. The limited increase in the computational costs is justified by the higher level of accuracy that the formulation can provide. The hybrid FE-Analytical gear contact model allows to represent the bulk contribution to the mesh stiffness by using the FE discretisation. At the end of the simulation, the displacement field of the nodes of the FE mesh can be recovered and used for strain analyses. This type of discretisation allows additionally to consider with great accuracy the contribution to the mesh stiffness of the geometry of the gear body, which is particularly relevant in the case of lightweight gears.

3. A gear precision test-rig available in the headquarters of Siemens PLM software in Leuven, and developed jointly by the University of Calabria, Siemens Industry Software NV and the Katholieke Universiteit of Leuven is used for an experimental validation of the proposed method. It allows to validate the simulation results both

in terms of transmission error and also for what concerns the strain levels at the tooth tooth. The strain validation can prove that the strength levels in the gear body are correctly replicated in the simulations no matters what is the lightweight shape.

4. A transmission with a layout typical of the front wheel driven cars is analysed. The commercial MB software allows to include in the analysis the flexible representation of the transmission housing, and the stiffness of the bearing units. A system level analysis of this type allows to investigate the behaviour of the gears when they operate in condition different from the nominal ones. Angular misalignment may occur when the different components are deformed under load. The inclusion of the dynamic behaviour of the housing highlights the coupling effects between the housing and the excitation coming from the gears. This excitation is even richer in components when lightweight geometries are considered.

The outlined points are further justified and clarified hereafter.
The numerical solution of the differential equation representing a system where meshing gears are present requires the solution of a contact problem for each time-step of the time discretisation, and especially in case of speed sweep analyses the simulated time may be long. On the other hand the meshing frequency is directly proportional to the rotational frequency by the number of teeth. This leds quickly to a huge number of timesteps to solve for a transient analysis.
Analytical tools may help to address this difficult tasks, but the accuracy they can provide is limited and directly dependent to the formulation itself. This accuracy can be improved by tuning the formulation. Since the modelling of the meshing stiffness is crucial to accurately replicate the excitation loads acting on the bearing units, particular attention is given to this phase. In Chapter 3 this task is addressed by performing non-linear static FE simulations on the analysed gear pairs. The FE method, providing the highest level of accuracy among all the simulations techniques, is used to generate a transmission error curve for a discrete number of angular positions for each gear pair. All these steps are limited to a pre-processing phase and have to be performed only once for each torque and gear pair. The database created in this way is efficiently exploited during the dynamic simulations, where only 2D or 3D (in the case in which the load-dependency is included) curves are interpolated. This type of formulation intrinsically includes the effects of the gear lightweighting. Such effects in the form of additional orders in the waterfall plot of the speed-sweep analyses are not taken into account by any of the analytical formulations available in literature.
A step further in terms of accuracy is provided by the approach included in Simcenter 3D Motion, where the extension of the formulation to lightweight gears is included in a commercial MB software. This type of formulation does not require any interpolation of the mesh stiffness during the transient simulation. A good computational efficiency is achieved by computing the non-linear deformation due to the Hertzian loads using an analytical description of the displacement field close to the contact area. The global

linear deformation of the gear is modelled using an approach based on the FE discretisation, that indirectly provides a nodal displacement vector that is used to recover the strain field in the gear, excluding the Hertzian deformation. The additional advantage of the FE formulation is a direct dependency of the bulk compliance to the body geometry, represented by the elements mesh. The fluctuation on the mesh stiffness function due to holes and slots in the gear body are well represented, and this is extremely important when lightweight gears are considered. The analysis of lightweight gears is experimentally validated, proving the capabilities of the methodology.This approach allows to simulate relative long events (compared to impact simulations) due to the great computational efficiency and put the focus on the dynamic effects due to the lightweighting that were not analysed before due to the lack of proper simulation tools.
The computational efficiency of the method is still so high to allow to perform speed-sweep analysis at a system level on an automotive transmission using a flexible representation of the housing.

1.3 Dissertation Structure

The current introduction chapter states the rationale and provides an overview of the static and dynamic behaviour of ligthweight gears when the latters are used in mechanical transmissions. The advantages and disadvantages of the considered formulation are also discussed.

Chapter 2 The chapter provides a detailed discussion on the current state of the art. The advantages and disadvantages of the methodologies currently available for simulating transmission dynamics are compared. The three main categories in which the simulation techniques are divided are discussed: analytical, Finite Element and multibody approaches. From the formulations themselves it appears that FE models are not suitable for time domain simulations at system level, due to the dimension of the model. In this chapter, a section is focused on the main industrial application fields for the different simulation techniques. Industrial needs in each specific context are discussed.

Chapter 3 This chapter investigates the dynamic effects of mass reduction on a pair of spur gears. A one Degree-of-Freedom (DOF) analytical model of a mechanical oscillator with clearance type non-linearity and linear viscous damping is used to perform the investigations. Among analytical models, one-dimensional (1D) description aims at studying the torsional gear vibrations around the rotational axes and can be used to simulate either gear whine or gear rattle phenomena. High computational efficiency is reached by using a spring-damper element with variable stiffness to model the gear meshing process. The angle-dependent mesh stiffness function is computed in a preparation phase through detailed Finite Element (FE) simulations and then stored in lookup tables. The look-up tables are then interpolated during the dynamic simulation allowing for high computational efficiency. Nonlinear

contact effects and influence of material discontinuities due to lightweighting are taken into account by FE simulations with high level of detail. Finally, the influence of gear body topology is investigated through a sensitivity analysis, in which analytical functions are defined to describe the time-varying mesh stiffness.

Chapter 4 In this chapter the transmission error and the strain field are analysed for two gear pairs, with different lightweight designs, reflecting the common industrial practice. The methodology used for the analysis is based on a hybrid FE-Analytical approach implemented in a multibody environment which allows to achieve a good accuracy with a low computational effort. The specific formulation allows to well describe the deformation field of the gear body from which the strain values can be computed at specific locations in the FE model. The numerical method used in this work is validated both in terms of transmission error and strain field, using the results obtained from an experimental campaign performed on a high-precision gear test rig.

Chapter 5 In this part of the dissertation a model of automotive transmission is analysed, using the approach described in Chapter 4 that allows to consider a detailed description of the gear stiffness in a flexible multibody model. The mesh stiffness description is crucial to evaluate the impact of the gear blank topology when lightweight design is considered or if a gear with a particular shape (like the differential housing, to whom the gear crown is fastened) is used in the transmission. The flexible formulation, on the other side, improves the accuracy of the results including effects such as the deformation of the housing under the meshing loads together with the coupling with its dynamic response. In this chapter the dynamic meshing loads are used to predict the acoustic response of the transmission in terms of acoustic pressure in a spatial location. The acoustic signature shows a different trend depending on the blank topology.

In the remaining part of the dissertation the conclusions are given in the last chapter followed by the references on which the dissertation is based.

Chapter 2

State of the Art

2.1 Introduction

Initial studies aimed to systematically investigate the dynamics of spur gears can be found in the works of Tuplin [129], Reswick [109], Strauch [125], Zeman [149], Abramov [4] and Utagawa [133] from the 50s, even if gears have been used in mechanical industry for a long time before.
The work of Harris [51], later assisted by Munro [141], deserves to be cited in the references because of its fundamental contribution to the understanding of the sources of gear meshing vibrations. In his work Harris showed that what he called *static error* is affected by profile modifications that he introduced deliberately. He investigated the influence of the profile modifications on the static behaviour of the meshing gears. An important conclusion arisen from his work is that the gear vibrations are generated from the load transition from one tooth pair to the subsequent. The static error showed a variability which depends on the transmitted load, while its variability for a specific load was limited allowing to introduce a quantitative microgeometry modification in order to reduce the relative displacement.
It has to be noted that the computational resources at that time did not allow to proceed to extensive simulation campaigns. Therefore the experimental part was fundamental for this investigation: around 16800 photoelatic stress patterns were created and analysed in order to perform this technical in-depth analysis.
Harris also stated that the damping has a key role in determining the amplitude of the vibrations close to the resonance, where the dynamic loads can overcome the external loads leading to contact loss at critical speed.
In the work of Gregory [141], based on the PhD dissertation of Munro [90], a more refined analysis was performed. What was early defined as *static error* evolved in *static transmission error*. The latter was referenced as the "*the angular displacement of the mating gear from the position it would occupy if the teeth were rigid and unmodified*". This definition has to be applied for any instantaneous angular position of one gear. The definition however still did not include any reference to the alignment nor the spacing of the teeth. The importance of this definition however lies in the consideration of the TE as one of the main sources of vibrations of meshing gears. A set of dynamic simulations were performed, using a lumped-parameter model. Even if the treatment was still affected by the

limited computational resources of the time, it was possible to calculate and to measure non-linearities due to loss of contact showing a good qualitative agreement for both TE and tooth loads. The dynamic overloads appeared to be more than five times higher than the load applied in nominal conditions. The two works presented above represent a suggested reading for anyone who is approaching the field of gear dynamics, even if they deal with the limitations proper of the years where initial steps of the gear dynamics research were taken.
Additional useful references for the interested researcher are the book about gear noise and vibration written by Smith [123], the book on gear geometry written by Litvin and Fuentes [81] together with the handbook on practical gear design of Dudley [36].
Most of the more recent analytical representations aimed to model the gear dynamic behaviour are based on the same principle as the one developed in [141]. An example can be found in the work of Nevzat [151], where the gear bodies are considered as rigid entities. The contact between the meshing teeth is lumped in a spring-damper system, which connect the two gears along the line of action.
A distinction between the loads acting on the gears can be done following the categorization made by Helsen [53]. In this work the dynamic loads that cause the vibration response of the system are divided into internal and external excitation. This distinction depends on whether the dynamic loads are generated directly by the meshing of the rotating gears or by the coupling with the system in which the gears are used. Typical examples are the power generators, the power users or the couplings with the dynamic behaviour of the supporting structure of mechanical power transmission.
The physical phenomena causing the vibrations are determined by whether the dominant excitation is internal or external, and the purpose of the model is to properly model this effect. In the works of Dion [35] and Ziegler [156] the dynamic behaviour caused by different external excitations is investigated. It can be pointed out that external excitations can lead to contact loss and consequently to repeated teeth impacts. This is especially true when lightly loaded gears are analysed. In this case the gears are reported to *rattle* and this condition is directly amenable to the backlash between the teeth. The main characteristics of the noise produced by the gears in rattle condition is a broadband frequency spectrum typical of impact events. This type of phenomena is analysed in the works of Kahraman [64] and Liu [82], where the focus is on the nonlinear behaviour induced by the clearance which is captured by using time-integration schemes.
When the dynamic effects are less relevant, the teeth usually do not loose contact and the internal excitation is dominant in the dynamic behaviour of the system. Its acoustic response is represented by a tonal noise known as gear *whine*. The behaviour of the gears in this case is dominated by the mesh stiffness periodic variation, which generates a tonal excitation at the tooth-passing frequency, as reported by [153] and Morgan [87].
The technique used by the different approaches to model the mesh stiffness variation is a key feature that distinguishes one approach from the others. Another distinction can be made by considering the level of detail used to represent all the flexible components of

the transmission which have a tremendous influence on the behaviour of the transmission. This consideration is supported by the works of Harris [57] and Campbell [21].
In order to properly model the dynamic coupling with the different components and the gears, a higher number of degrees of freedom is required, thus resulting in a consequent higher computational cost. The number of degrees of freedom in the model can be considered therefore as an indicator of the complexity and reflects the level of detail of the model. In the simplest approaches only a few degrees of freedom are required to catch the rotation of the gears which interact through a spring-damper element [153].
The goal of simple approaches for gear whine applications is to model only the variable mesh stiffness, which is sufficient to reproduce the dynamic behaviour of the gear pair. The latter includes both the effects of the elastic tooth deflections as well as the ones of the tooth profile micro-modifications as pointed out by Umezawa [130] and Cai [20], [19]. The assumptions of rigid bodies and supports, together with a one-dimensional representation of the meshing force acting in the direction of the line of action, allows to simplify these models.
The inclusion of degrees of freedom in the plane orthogonal to the rotational axis of the gears, made by Ambarisha [8], had the aim of investigating the effects of bearings and shaft flexibilities, which are modelled using a lumped parameters approach. The limitation to a orthogonal motion, however, still represents a limitation to the applicability of this type of approaches. This is motivated by the consideration that the contact phenomena between the teeth lie in a region which has a non-negligible extension in the axial direction, therefore the relative orientation between the gears (misalignments) may have a huge influence on the behaviour of the transmission.
The lack of accuracy introduced by in-plane models is recovered by considering the models proposed by Velex [136] and Eritenel [40] were the rotational degrees of freedom allow to consider the 3 dimensional nature of the meshing behaviour.
In the investigation of the shuttling influence, intended as shifting of the location of the resultant contact force acting on the tooth flank along the axial direction, the neglecting the out-of-plane rotational degrees of freedom in the model can bring to unacceptable lack of accuracy. Shuttling, indeed, is originated from the fluctuations of the contact point position along the axial direction, leading to a 3D motion field of the gears, as showed by Helsen [53]. The model used by Nishino [93] to represent shuttling phenomena consists in a couple of spring-damper systems representing the mesh stiffness. A relative phase between the two curves introduces this fluctuating behaviour for the considered gear pair. Different considerations have to be taken into account when these approaches are adopted. Firstly, the simplicity of the equation of motion stands on a huge jeopardisation of the actual physical phenomena acting in the transmission bringing on a reduction of the accuracy of the simulation. The accuracy is decreased also by the rigid modelling of the surrounding structure as well as rigid representation of the gear bodies. An additional drawback can be found in the need for a tailoring phase, which is required in order to include the most relevant effects. The complexity of this phase reflects the complexity of the system.

The use of FE based techniques to model the gear meshing process offers the main advantage of including the gear body flexibility in the simulation environment. Informations can be found in the work of Kabur [67], Lin [80] and Li [70]. The Finite Elements method offer a great level of accuracy for the solution of gear-related problems but at a very high computational cost. This is mainly due to the extremely refined node distribution on the tooth surfaces required to properly discretize the contact. The non-linear nature of the contact problems adds complexity to the FE formulation resulting in extremely long computational time. Due to the listed limitations, currently this type of simulation is limited to static analysis at gear pair level and is not used for long time events, such as speed sweep analysis, nor in the case of complex systems where transmissions with multiple stages are considered.
Considering the exceptional accuracy provided by the FE discretization, and the limitation due to the dimension of the problem, the focus of the researchers is targeted on developing the formulation in order to decrease the computational cost. Following this effort, very interesting achievements were obtained by Vijayakar [139]. In his work he combined an analytical formulation of the close-field contact deformation based on the Bussinesq [148] solution with a FE formulation of the far-field displacements. The resulting method does not require a fine FE mesh to model the contact loads, resulting in a notable reduction of the degrees of freedom. However despite the increased efficiency, the method is still not applicable in speed-sweep analysis.
The trade-off between the accuracy of the solution and the computational cost can be found using multibody simulation tools. The main advantage is the possibility to model complex systems, in which the distributed flexibility of the different main components such as shafts and housings can be modelled. The hypothesis of rigid gear bodies helps to increase the computation efficiency. Well established techniques, such as modal reduction techniques, move in the same direction by reducing the overall dimension of the problem, such as the well established approach proposed in [12]. In this framework, a 3D multibody formulation was proposed in [23] allowing to apply the forces generated during the meshing process in the correct direction. The limitations of the method lie in the lack of treatment for the relative misalignments between the gears and for the backlash, which make this approach inapplicable for the analysis of different types of non-linear phenomena typical of the gears. The main limitation however is the consideration of a constant mesh stiffness, neglecting its fluctuation. This limit was overcome by Ebrahimi [37], who developed a tool to keep track of the variable number of meshing teeth. In that work, the hypothesis of constant mesh stiffness for a single tooth is made together with the assumption that the displacement of each tooth lies in the direction tangential to the gear blank. By following this approach, no coupling between the deformed teeth is considered. An estimation of the mesh stiffness based on FE simulations was proposed by the same authors.
The high-speed dynamic analysis of meshing gears at system level is still a complex task from the simulation point of view.

2.2 Analytical models

The analytical representations of the meshing gears represent the root of the research about gear dynamics. They have been developed for many different applications. Single degree-of-freedom models of a gear pair represent the starting point for the more detailed 3D formulations. The interest which is still around this type of models can be partially explained by the low computational requirements due to the small number of degrees-of-freedom and by the easy implementation of the lumped parameters formulation. This type of formulation represents an advantage when the duration of the simulated events is relevant but on the other side these tools require an experienced user in order to proper tailor the few equations to the specific application. A good knowledge of the specific gear-related theory as well as a proper engineering judgement is required to avoid under-estimating potentially dangerous effects. These formulations moreover stand on an analytical description of the mesh stiffness that, being the dominant feature of a gear pair, may cause wrong results. Its modelling therefore is crucial for the accuracy of the results.

2.2.1 One-dimensional models

This class of formulations performs very well when the focus is exclusively on the vibratory behaviour of the gears around their rotational axes. Their applicability is limited exclusively to the configurations where the translational motions together with the rotations out of the gear plane can be considered negligible when compared to the rotational one. Depending on the formulation used to represent the gear contact phenomena, the analytical models can reproduce gear whine as well as the non linear behaviour typical of when gears loose contact.
The general implementation consists of rotating masses which are lumped into inertia moments around the rotational axis. A spring-damper element is used to connect two masses. Its formulation can be either a rotational spring and damper as well as a translational one parallel to the line of action of the gear pair, being any rotational displacement of the gears representable as a linear motion along the line of action. In this case the TE corresponds directly to the relative displacement of the gears, intended here as the deviation of the relative motion from the ideal purely kinematical one.
The work of Mahalingam [84] from 1974 is an example of whine study of a gear train. The analysis is performed by analysing the rotational modes and the natural frequencies. In the more recent model of Ozguven [153], the static TE is used to compute the dynamic response of the gear pair. In the same work the loss of contact is taken into account by considering it as a negative contact force. The experimental comparison shows also how the contact losses happen when the gear mesh frequency becomes close to the natural frequency of the gear pair.
Room for further improvements can be found in the simulation of the gear dynamics using a forced response approach. The simplest approaches do not consider the parametric

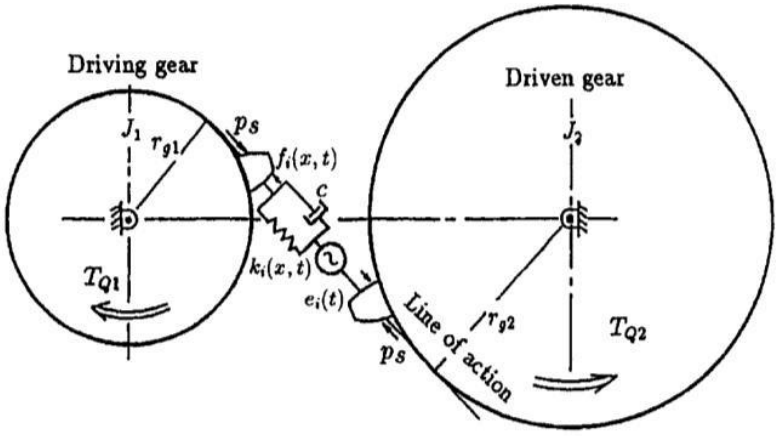

FIGURE 2.1: One-dimensional gear pair rotational model used by Cai. Reproduced from [20].

excitation due to the time-varying mesh stiffness. A work by Kahraman [64] uses a similar constant stiffness formulation to study the non-linear response of a spur gear pair. The non-linearity due to the clearance is modelled in a clever way by setting the mesh stiffness equal to zero when the gears are assumed to move in the backlash range. The analytical formulation is solved using two different solution schemes and showed the typical jumps in the frequency response. A good agreement with experimental results is achieved.

A formulation that includes a time-varying mesh stiffness can be found in the work of Cai [20] [19], whose model is represented in figure 2.1, that extended the results obtained in the works of Umezawa [130] but adapting the formulation to the consideration of involute teeth whose profile shape is no more a straight segment, such as the teeth of a rack. The used approach is based on the standard model with one degree-of-freedom per gear and a mass concentrated in the inertia moments of the gears, conventionally used in this type of applications, and expressed by equation 2.1. An additional contribution is the inclusion of the profile deviation through a displacement excitation in series to the spring-damper element. In this model it can be appreciated the distinction of the two contributions to the TE represented by the elastic deformations and the displacement due to the deviation from the theoretical involute shape due to deliberate microgeometry modifications as well a manufacturing errors.

$$\begin{cases} m\ddot{x} + c\dot{x} + \sum_{i=1}^{n} f_i(x,t) = p_s \\ f_i(x,t) = k_i(x,t)[x_s + x + e_i(t)] \end{cases} \tag{2.1}$$

where $x = x(t)$ represents the dynamic relative displacement on the line of action. Considering the single degree of freedom model, the displacement represents the dynamic relative displacement between the gears and therefore is the TE of the gear pair. The

equivalent mass of the gears represented by term m is obtained after dividing each inertia moment J_{i} by the related base radius r_{i}:

$$m = \frac{m_1 m_2}{m_1 + m_2} \qquad m = \frac{J_i}{r_i^2} \qquad i = 1, 2 \tag{2.2}$$

The second term in the system $f_i(x, t)$ indicates the force contribution, which is generated by the elastic deflections, and the contributions due to profile deviations from the pure involute, which is treated as an imposed displacement.The effect of pairs of teeth which can engage at the same time is taken into account by the summation. The terms, which determine the elastic force, are:

- $k_i(x, t)$, the instantaneous stiffness for the i-th pair of teeth;
- $x_s = p_s/k$, the average displacement given by the total contact force divided by the average total meshing stiffness;
- $e_i(t)$, the sum of the profile deviations for the two teeth belonging to the i-th pair.

In this type of models a crucial aspect that determines the accuracy of a specific formulation is the modelling of the single tooth pair mesh stiffness $k_i(x, t)$. Cai bases its investigation on the formulation suggested by the ISO standard 6336 [132], which provides a stiffness value at the pitch point. This value is then extended including its variation due to the movement of the contact point along the tooth profile by assuming an exponential function as variation law. Unavoidably, a high level of approximation is introduced at this stage. In this PhD dissertation different approaches are used to model the tooth pair stiffness and the results are reported in the subseqent chapters.
The utility of the analytical one-dimensional models lies in the possibility to estimate the TE values in the dynamic range as well as the dynamic loads and total contribution given by the contact force.
Higly cited works considering both clearance-type nonlinearity due to backlash together with an analytical formulation of the timevarying stiffness are the ones of Blankenship [15] and Kahraman [62]. In these studies the forced response of a mechanical oscillator is investigated reproducing the jumps phenomena. This kind of non-linear effects are reproduced with a good accuracy when compared with the experimental results. In the work reported in[35], an analytical model is used to study the dynamic behaviour under contact loss conditions of a non-engaged gear pair in an automotive transmission. The excitation comes from a fluctuating acceleration of the input shaft, while the other shaft was connected to a rotating inertia. The proposed model was capable to well replicate the experimental results in term of kinematic of the impacts, having determined the dissipative terms in an experimental campaign. In the paper by Andersson [9] a rotational model was used to investigate the influence of the onset of a new tooth pair into contact. In the paper a quantitative description of the contact pressure was provided. This paper is remarkable for the approach used to model the mesh stiffness, which was originally developed in the PhD dissertation of Vedmar [134] but used under static conditions exclusively. The low computational times make this formulation particularly suited for

optimization process, that requires large simulation campaigns. The problem of the optimisation of the tooth profile was addressed using rotational models by Lin in [76], where a system represented by a gear pair connected to a motor and a generator was built. The results are evaluated in terms of the different response obtained by applying different microgeometry modifications (linear or parabolic). The studies performed by Faggioni [41] and Bonori [17] were aimend to perform an optimization process to choose the best trend for the microgeometry optimisation, focusing on the dynamic TE.

2.2.2 Two-dimensional models

As already pointed out in the previous section the performances of an one-dimensional model are acceptable only if the translational motion of the gears is negligible. In this case the non-linearities together with the amplitudes of the dynamic response are well replicated, under the assumption that the time-varying mesh stiffness is properly modelled. In the vast majority of the applications, however, the deflections of bearings, shafts and supporting structures are not negligible, being the radial stiffness of such components similar to the one of the meshing gear [65] [72] [74] [75] [49]. The aim of these models is to include the stiffness of these components by including extra spring-damper elements. Of course, any rotational misalignment which is not in the plane orthogonal to the rotational axes can not be caught by these formulations. Taking as reference [152], Ozguven extended the rotational formulation used in [153] to include the effects of the bearings and shafts compliance. The conclusion of this work is that when the mesh stiffness is coupled with the one of the surrounding elements, the bearing reaction force shows a different shape with respect the mesh forces that they have to support.
Some authors included the translational displacements also in the models aimed to represent the non-linear behaviour of the gear pair. The result is a coupling effects between the pure rotational vibration and the translational one, as reported by Walha [142]. In this work the authors show how the bearing reaction forces can be affected by the impacts between the teeth. The work of Siyu [122] deserves to be cited because it shows how the stiffness of the additional components affect the backlash value impacting in this way on the non-linear behaviour of the system.
Similar to the rotational models also the planar ones have been used in the optimization of the dynamic behaviour of the transmission by investigating the optimum amount of profile microgeometry modifications. An example of these approaches can be found in the work of Liu [82], whose model is reproduced in Figure 2.2, where the problem is faced in the case of a multi-mesh transmission. In this work the effects of the clearance were also introduced because of the presence of the idle gear, that not being externally loaded is more susceptible to contact losses by moving in the backlash. The aim of the work is to reduce the non-linear phenomena, and the results show the reduction of the internal excitation. The fidelity of the model was assessed by a comparison with planar FE model.

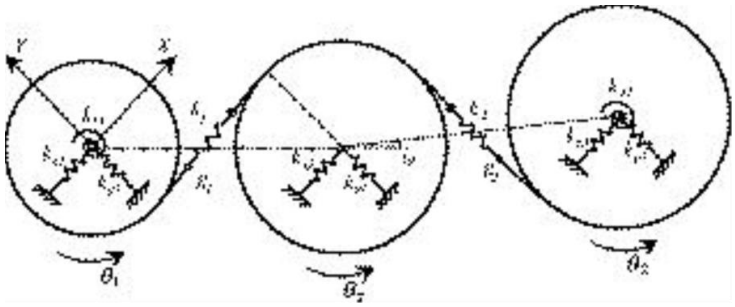

FIGURE 2.2: Two-dimensional idler-gear system model used by Parker. Reproduced from [82].

2.2.3 Three-dimensional models

It is trivial to notice that many phenomena can not be investigated with the use of planar models, that prevent the gears from tilting out of the plane perpendicular to the rotational axis. This type of motion is particularly relevant for the dynamic response of the transmission because a whole class of mode shapes can now be included in the analysis. Moreover misalignment-related effects, which have a huge impact on the durability performances of the gears such as stress concentration and the sensitivity to micro-modification in the axial direction, are now properly considered.
The simplest category of 3D models can be individuated in the representations that neglect the distribution of the contact loads along the tooth width. In these models the contact is lumped in a spring-damper system along the actual line of action of the gear pair. This representation allows to include the axial component of the contact force in the helical gears that generates a bending moment out of the rotational plane. In the case of spur gears there is not any axial components, but additional excitation can come from the bending of the other components. Even if any rigid motion of the gears can be taken into account by the model, still the local effects due to the microgeometry modifications along the width are not captured. Examples of this type of representation are found in the work of Kahraman [61] and of Kabur [67]. These studies proved the importance of considering the interaction between the meshing gears and the deflection of the surrounding elements, resulting in a coupling between all the rigid motions of the gears.
The consideration of the distribution of the contact pressure along the width of the gear results in more refined formulations. An example is represented by the paper of Velex [137]. Here the pressure distribution is obtained by introducing different springs in the axial direction, each of them representing the stiffness of a thin slice of the tooth. In a paper by Baud [13] the same model is used to prove the importance of the load distribution along the tooth thickness. The assumption of the work is that the method is applicable only for thin gears where the helix angle has a low value. The reason can be found in the non-consideration of the coupling effects between the slices. This hypothesis is supported by the experimental validation. The limits of the formulation were overcome by

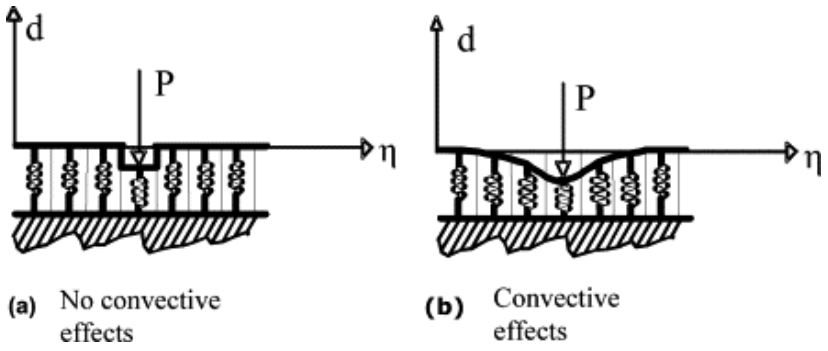

FIGURE 2.3: Representation of convective effects due to contact shear. Reproduced from [6].

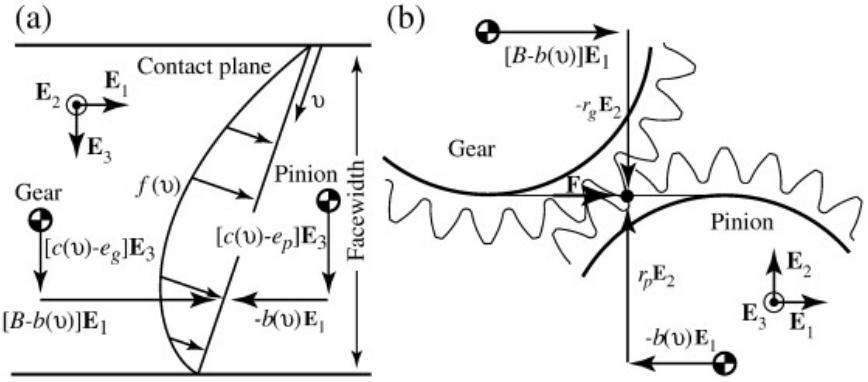

FIGURE 2.4: Distributed load and the position vectors from the pinion and gear mass centers. (a) Front view and (b) side view. Reproduced from [39].

Ajmi [6] that introduces the Pasternak elastic foundations to keep track of the convective effects. Figure 2.3 explains the main idea behind this approach. A more recent formulation is the one of Eritenel [40] [39] where the actual pressure distribution is used to investigate partial contact losses in the instantaneous contact lines. Even in this work the 3D modelling of the transmission is fundamental together with a representation of the distribution of the mesh loads.

2.2.4 Models for planetary gear trains

The modelling of planetary gears follows a similar approach to the ones described in the previous sections. The models used spread from mono-dimensional types to the more refined formulations. The particular configuration of planetary gear stages, however, introduces a particular dynamic behaviour. The source of these phenomena can be found in the coupling effects originating when the multiple planets mesh together with the sun and the ring gear. This mutual interaction and angular symmetry between the contact forces open the doors to the improvement of the overall dynamic response of the

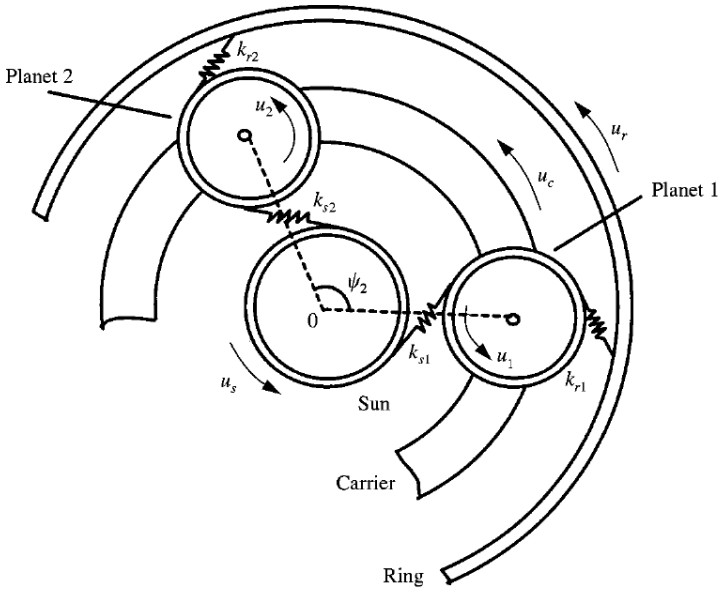

FIGURE 2.5: Rotational model for planetary gear sets. Reproduced from [79].

transmissions. Figure 2.5 shows an application of a rotational model used by Lin [79] to investigate the effects of the instantaneous variation in the mesh stiffness. The results of the investigation show the relation between the instability phenomena and the angular phase introduced between the planet-ring and planet-sun mesh. The influence of the mesh phasing is remarkably high to completely avoid the instability in specific conditions, thanks to the symmetry between the mode shapes. The geometrical relationship that governs the mesh phasing in the epicyclic gear trains are discussed in another work by the same authors [100].

The nonlinear dynamic response originated by the contact loss was investigated by Al-Shyyab [7] using a simple rotational model. The paper shows that the contact losses occur in a similar way as the ones obtained for isolated spur gears.

An important requirement for planetary transmission is an equal load distribution among the planets. Improvements in this direction can be achieved by a careful choice of the position of all the gears in the transverse plane. Singh in [121] provided a physical explanation for these effects including also the clearance in the models. In order to include in the investigations the motion in the transverse plane, planar models have been developed. In a study by Kahraman [61] the difference between rotational and planar models are investigated. The more complex formulation of the planar models allows to include the dynamic effects due to the translational mode shapes. Saeger in [117] shows how reduce the excitation coming from the meshing loads with a proper mesh phasing. This kind of investigation is carried out by using a planar model. A representation is reported in Figure 2.6.

A classification of the planar mode shapes with different mesh phasing was performed by Lin in [78] and [77]. In these works a distinction is made between modes that involve a motion of all the gears (rotational and translational modes) in the system and others

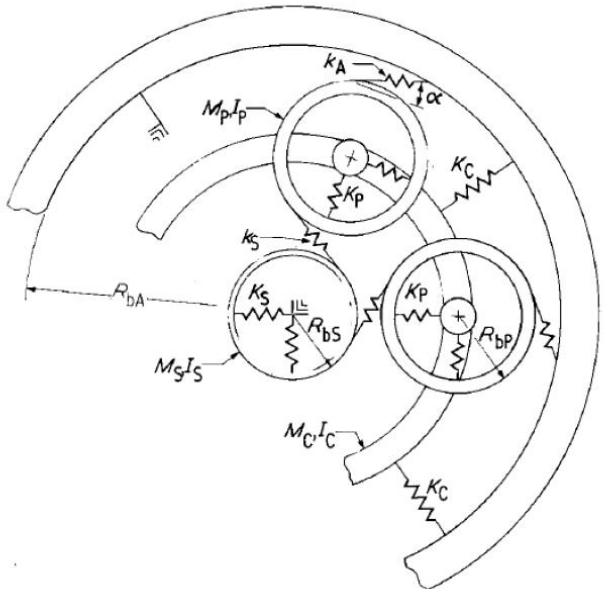

FIGURE 2.6: Two-dimensional model for planetary gear sets. Reproduced from [117].

that involve exclusively a motion of the planets (planets modes). Chaari [26] studied the modulation sidebands generated by machining errors in the planetary gears. The effects of eccentricity and profile errors consist in an increase of the response amplitude at the meshing frequency. When the analysis of helical planetary gears is addressed a three-dimensional model is required due to the tilting component of the meshing force present in helical gears. This additional component excites the dynamics of the system also in the out-of-plane direction. Such model can be found in the paper of Kahraman [61] and is reported in Figure 2.7 The classification of the planetary mode shapes made by Lin is extended by Eritenel [40] using a three-dimensional formulation, obtaining similar results but adding the out-of-plane components.

2.3 Finite Elements models

Finite Elements models allow to accurately simulate the meshing process relaxing some of the restrictions applicable to the analytical techniques. Generally the analytical models are based on a lumped formulation of the stiffness of the meshing gears. This intrinsically introduces an approximation by neglecting the distributed stiffness of the gear. This approximation can become very important if for example lightweight gears are analysed. The increased compliance due to the lightweighting makes the coupling between the deformation of the gear body and of the teeth extremely relevant and its approximation may therefore lead to incorrect results. The FE formulations implicitly take into account these effects without any need for further assumptions.
This type of advantage is somehow balanced by the computational cost of the formulation. An extremely refined geometrical discretization of the contact surfaces on the teeth is required to properly model the sharp strain gradient generated by the Hertzian loads.

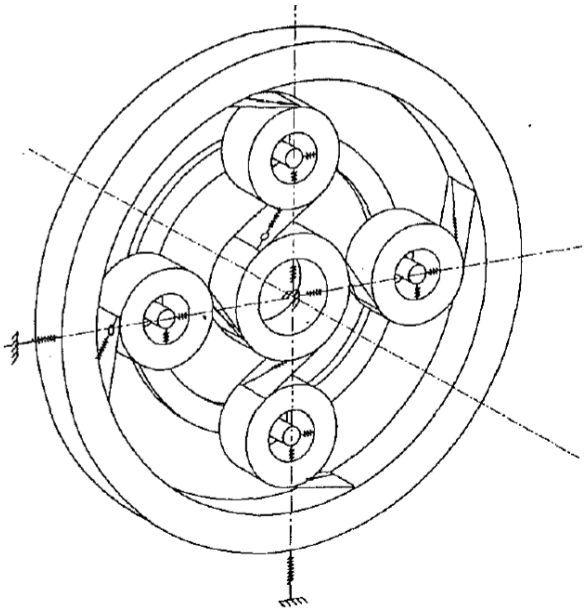

FIGURE 2.7: Three-dimensional model for planetary gear sets. Reproduced from [61].

The size of the problem, in this way, is considerably increased. The time required for a simulation, therefore, is several orders of magnitude higher than the one needed by analytical formulations. The application of this method for transient three-dimensional analyses is still generally un-practical.

2.3.1 Static Analysis

The different physical phenomena acting at the same time during the meshing of two or more gears make the simulation of this process a difficult task.
The deformation path of a gear subject to meshing loads is the result of multiple phenomena on different scales. On the micro scale the local contact loads cause to the tooth a deformation path which interests a small portion of the tooth surface but is relevant on the overall deformation. This contribution is superimposed to the global linear deformation of the elastic tooth and gear body. References explaining the different contributions affecting the static deformation of the meshing gears can be found in the works of Conry [28] and Stegemiller [124]. The difficulties to properly catch the deformation caused by the contact loads arise from the different and coupled features of the contact deformation, which is:

- non-linear with load;
- affected by relative positioning of the teeth (misalignments);
- extremely sensitive to local curvature.

The analytical tools described in the previous sections show lack of accuracy when used to model all these phenomena, due to their complexity and to the huge variety of possible combinations between all the geometrical and kinematical parameters (addendum over

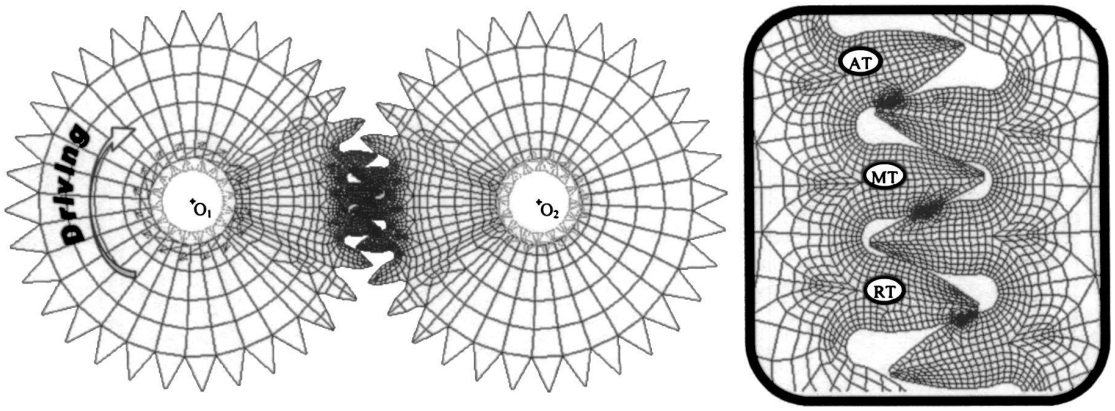

(a)

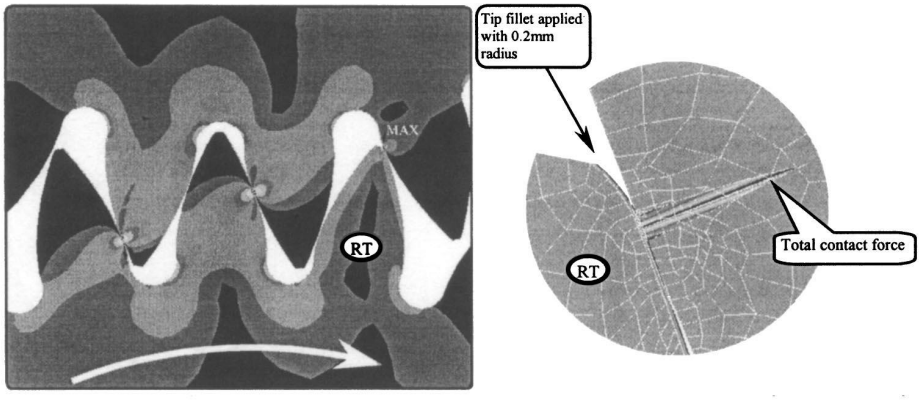

(b)

FIGURE 2.8: 2.8(a) Planar FE mesh for gear contact and 2.8(b) contact stress gradients. Reproduced from [143].

dedendum ratio, addendum modification, face width size, helix angle, pressure angle, etc.) of the gears. All these features are modelled by FE method which provides, therefore, accurate results for the TE curves and stress patterns without any need for a-priori assumptions.

The work of Wang [143] is a good example of how planar FE simulations are used to compute static TE and mesh stiffness curves when profile modifications are applied to the gear teeth. In figure 2.8 the FE model used is shown and can give an idea of the level of mesh refinement required to properly model the sharp contact stress gradients on the teeth and to provide an accurate discretisation of the tooth geometry when a profile modification is applied. A different approach was developed by Vedmar in his PhD thesis [134], where the local Hertzian contribution on the mesh stiffness is analytically computed based on the local curvature of the tooth.

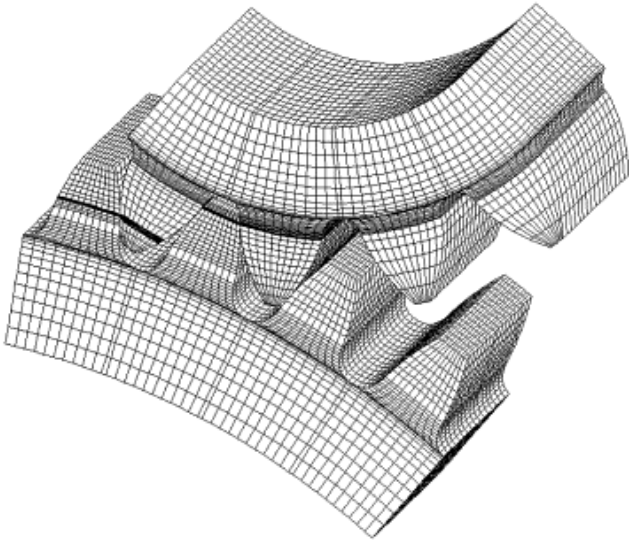

FIGURE 2.9: Three-dimensional FE mesh for gear contact. Reproduced from [69].

An example of three-dimensional FE simulations of the effects of manufacturing and assembly errors, as well as tooth modifications, can be found in the paper written by Li [69]. The refinement of the mesh used to provide such accurate results can be appreciated in Figure 2.9.
The high computational cost of FE simulations is due not only to the high number of degrees of freedom required to discretize the contact area, but also to the fact that the contact behaviour is non-linear, therefore additional iterations are required to solve the problem at each time-step.
The limited application as design tools of FE simulations leave the room to their use as benchmark for the analytical models. This kind of aplication can be found in the work of Pedrero [103] and Sainsot [113]. In this way the analytical dynamic models have their mesh stiffness and Static TE verified. Faggioni [41] used this scheme of each new value of microgeometry modification iterated in the optimization scheme. In the work of Korta [66] FE simulation were used in a multi-objective optimization strategy. Due to the high computational time required for the non-linear FE simulations, response surface models were used, allowing in this way to check a large number of possible solutions in a relative short times.

2.3.2 Dynamic Analysis

The application of FE analysis to dynamic time domain simulations has an obstacle in the simulation time. The dimension of the problem joined with the small time step required to ensure the convergence of the contact problem lead to enormous simulation durations. The application therefore is to investigate very short events in the order of a few milliseconds.

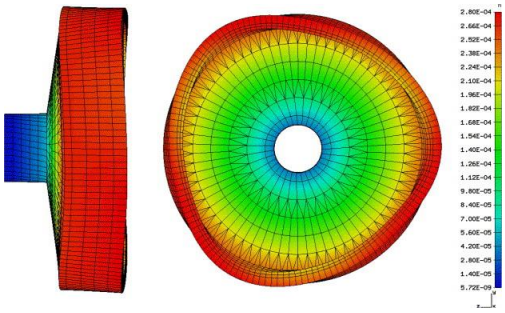

FIGURE 2.10: Deformation of a ring gear meshing with three planets Reproduced from [3].

Dynamic FE simulations were carried out by Lin [80] to investigate the propagation of elastic waves after an impact event. The simulations consist in a load applied in a short time interval and an initial speed difference. Considering the small portion of the gear subjected to the impact effects, only a fraction of the whole gear consisting in the meshing teeth and the surrounding is analysed. What emerges from the investigation is that the higher is the initial separation, the lower is the impact duration, while the contact forces appear higher. When the initial speed difference condition is considered, the impact duration seems not to be affected by the increasing values of the speed difference. The contact forces, instead, appear higher. Similar investigations were performed by Ziegler in [156] and in [155], where different approaches from pure FE are also analysed in order to reduce the computational time without affecting the accuracy of the results. In this work, the FE simulation used as reference case lasts around 8 days on a standard desktop machine for simulating 13 impacts in 20 ms.

Being the solution of the contact problem the most expensive part in the simulation of the gear meshing process, Abousleiman [3] proposed an approach where the FE discretization of the deformable ring gear is combined with an analytical gear contact formulation, as shown in Figure 2.10. The FE formulation allows to model the ring distributed stiffness coupled with meshing loads. This investigation shows how the distribution of the load on the tooth surface is heavily affected by the ring flexibility.

The analytical description of the contact problem was also used by Vijayakar [139] who combined the Bussinesq solution for a point load on a half-space with the FE representation of the global displacement field of the gear. This approach consists of a match of the analytical solution with the FE results on an interface surface. The analytical description of the contact loads eliminates the need for highly refined mesh in the contact regions. An example of a FE mesh suited for this approach is reported in Figure 2.11. The gains on the computational time of the planar formulation allow to apply the method to time-domain analysis of a spur gear pair. The predicted dynamic results matched very well with the experimental ones when the jumps in the frequency response are considered, as reported

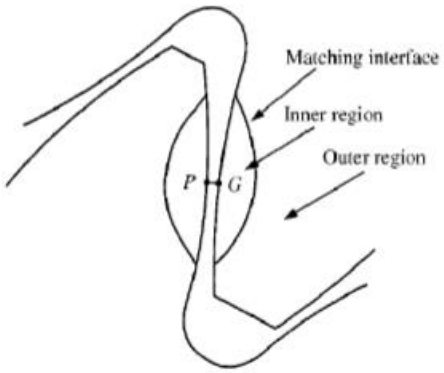

(a)

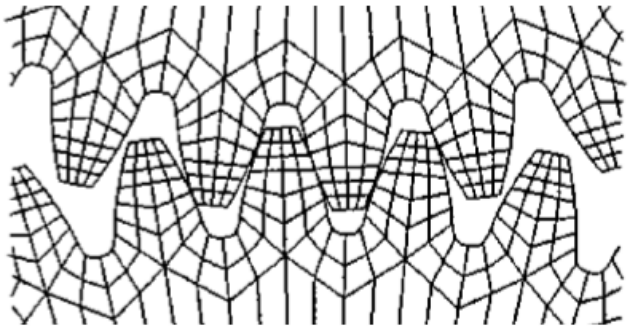

(b)

FIGURE 2.11: Hybrid modelling approach by Vijayakar: 2.11(a) Inner region described by analytical contact solution and outer region described by finite elements; 2.11(a) Planar FE mesh, to be compared with Figure 2.8. Reproduced from [139].

by Parker [101] and Tamminana [127]. Similar level of accuracy in the experimental validation was also achieved for planetary gear sets [99]. It has to be pointed out, however, that despite the increased computational efficiency, three-dimensional time domain simulations where high speed events are considered still require very high computational time, limiting this type of three-dimensional application.

2.4 Multibody models

Multibody models are used to simulate the interaction between different bodies, subject to different boundary conditions and mutually connected by joints. The definition of body, in dynamic field, consists in the modelling of a physical entity through its inertia properties defined in a reference frame. The simulation representation of a body can be either rigid or flexible. Flexible multibody models can have different representations of the flexibility. In most of the cases, the internal degrees of freedom of a body are represented using FE discretization. In order to reduce the size of the system matrices, standard practice is the use of modal reduction techniques [12]. By considering the dynamic content only up to a chosen frequency it is possible to efficiently simulate the dynamic behaviour in the considered frequency range without heavily affecting the accuracy of the solution.
Multibody techniques have, therefore, the potential to represent the most suited tool to simulate the dynamic of the transmission at system-level, under the condition that the meshing forces between the gears are accurately modelled. A more detailed revision of MB models for the simulation of the meshing process, with a focus on the dynamic stress recovery is given in Paragraph 4.1.

2.4.1 Rigid-body models

Following the rigid-body approach, any distributed compliance of the gear bodies and teeth is lumped into spring-dampers elements. In his work Cardona [23] developed a simplified model, reported in Figure 2.12, that enables to represent the direction of the total contact force. On the other hand neglecting the stiffness variation in the meshing cycle, does not allow to consider the internal excitation generated from the loaded rotating gears. The purpose of such a simplified model is to analyse the force path in the whole transmission and also to recover preliminary information on the system natural frequencies, under a given configuration in terms of angular position. The work of Ebrahimi [37] overcame this limitation by accounting for the variable instantaneous number of teeth in contact, still keeping a rigid-body formulation. The model consists of a rigid body to which all the teeth are connected by means of tangential spring-damper elements, as shown in Figure 2.13. In this model the stiffness variation due to the translation of the contact point along the tooth profile is still neglected, together with the non-linear stiffening effects. In the work of Palermo [95] the limitations due to th consideration of a constant mesh stiffness were overcome thanks to the development of a multibody element that can represent the meshing gears without any limitation on their relative

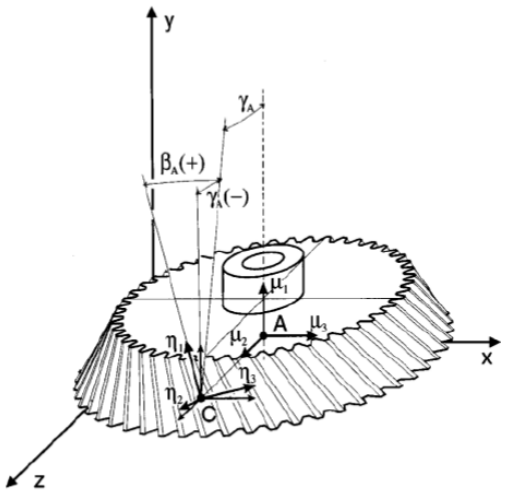

FIGURE 2.12: Rigid-body model for total contact force orientation and contact point positioning. Reproduced from [23].

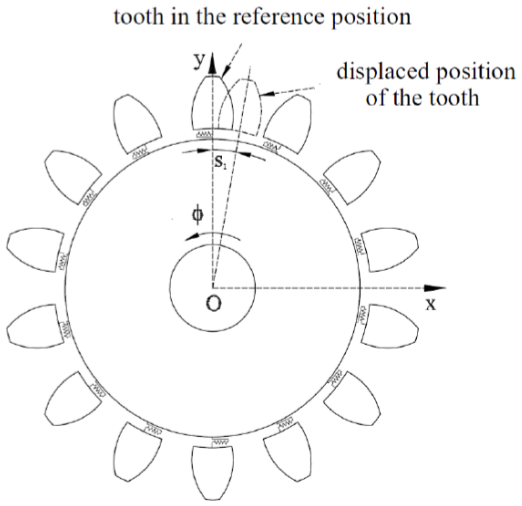

FIGURE 2.13: Independently meshing teeth model by Ebrahimi and Eberhard. Reproduced from [37].

displacement. The representation of the TE-based mesh stiffness is done off-line in a pre-processing phase thanks to gear dedicated tools. Different sets of TE curves are generated corresponding to different working conditions of the gears in terms of transmitted load and relative position. The curves are then interpolated during the dynamic analysis to obtain the actual value of the mesh stiffness.
Simulation tools capable to predict the gear behaviour at system level are available in many commercial multibody solvers such as Romax [102], Simpack [89], MSC [50], AVL [92] and Siemens PLM [120]. The latter formulation is described more in detail in Chapter 4. The simulation technique used by Romax is based on a forced response computation in frequency domain [58]. The detailed gear mesh simulation is performed statically, and linearized around each operation point. Simpack uses an approach [115] in which the user can upload an user defined mesh stiffness or use a curve based on the ISO 6336 norm. MSC approach lies on a simplified dynamic simulation using a description of the gear contact based on an external software [5]. A similar approach is used in AVL software, but this time the external software [54] is called during the dynamic simulation using a dynamic link library.

2.4.2 Flexible-body models

Flexible multibody approaches allow to consider the distributed flexibility in the gear body, allowing to investigate its effect on the static behaviour as well as on the dynamic one by including the mode shapes and relative natural frequencies of the whole gear pair under meshing conditions.
Flexible multibody models can provide the highest level of accuracy when used to simulate gear dynamics. At the same time, given the accurate representation of the teeth and body compliance, detailed contact models are required, which are generally expensive from the computational point of view. Due to the non-linear FE representations, flexible multibody formulations have limited applicability due the un-feasible computational time.
The flexible multibody formulation proposed by Vinayak [140] lies on a combination of FE discretization and theory of plates to reduce the overall size of the numerical problem (Figure 2.14). The resulting linearized time-invariant formulation is the result of a reduction phase from the original non-linear time-variant problem. The correlation with the experimental data in terms of forced response is good and highlights the influence of the body compliance on the dynamic behaviour of the meshing gears.
A planar flexible multibody formulation for spur gears was proposed by Lundvall [83], that includes friction effects. This work is based on a separation between the small deformation of the gear and the rigid-body motion. The deformation of the gear is computed using a FE mesh, coupled with the contact problem, which is solved using a node-to-node approach. The results obtained with such a methodology, in terms of dynamic TE for different microgeometry modifications, proved similar to the ones provided by 3D analytical representations. A clear advantage of the method is that no a-priori assumptions are made during the simulations.

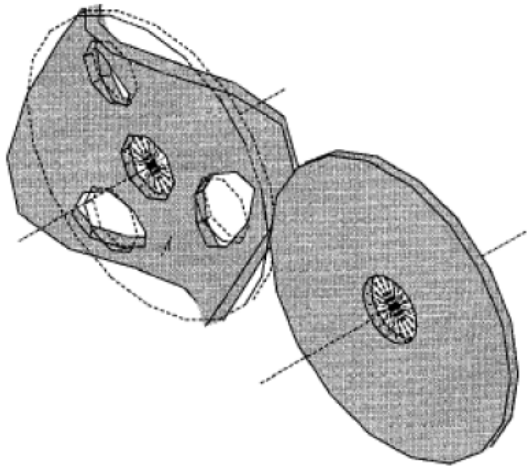

FIGURE 2.14: Gear body mode of vibration captured in the model by Vinayak and Singh. Reproduced from [140].

The formulation developed by Ziegler [156][155] has the aim to reduce the computational efforts by reducing the system matrices using modal modes. The non-linear FE dynamic simulations were taken as reference and show a good correlation with the experiments. Since only normal modes are included in the model, the agreement of the proposed formulation with the FE results can be obtained only by including a large number of modes. Despite the high number of modal shapes included in the reduction space, the formulation proved still efficient when compared with pure FE formulations. An interesting outcome of the work is the comparison of the computational time for the different computational techniques, including flexible multibody, FE and rigid multibody. Data is reported in table 2.1.

TABLE 2.1: Comparison of the computational effort required for impact simulations performed by Ziegler and Eberhard. [155]

	Model preprocessing time	**Integration time 13 impact (20ms)**	**Disk requirements**	**Memory requirements**
FE	0	~8 days	~1 GB	~1 GB
MB	0	5 s	~100 MB	~500 MB
Modal MB	28 h	~9 minutes	~8 GB	~100 MB

2.5 Simulation Challenges in Different Application Domains

Gear dynamics study is relevant in many application thanks to the large use of mechanical power transmission with gears in the industry. In the present paragraph is provided a disclosure on the present applications where gears have an important role. The attention given to the gears in the mechanical transmission field is mainly due to the need for

investigations made to prevent failures in such a sensitive component to dynamic loads. Secondary, the excitation generated during the gear meshing is a source of vibrations and noise in the transmission, therefore gear dynamics has a relevant importance not only on the durability side but also in defining the comfort level. The dynamic working conditions of the transmission are also fundamental to define the lubrication regime between the teeth. The interaction between the rotating gears and the lubricant determines the efficiency of the whole system. Energy losses, indeed, are caused not only in the contact regions where elasto-hydrodynamic lubrication and oil squeeze losses happen but also in other surfaces of the gears, where the windage losses are caused by the huge amount of oil moved by the gear. This topic however is not in the scope of this thesis, and the interested reader can find a relevant number of publications in the literature.
In the current industrial age, the importance of the gears is particularly evident in the automotive, wind turbine and aerospace fields, among all the others. These fields, however, present different design requirements due to the extremely different working conditions of the gears in terms of operating speed and transmitted loads. But, before illustrating the specific application details and issues, it is necessary to explain the process behind the phenomena together with the simulation tools aimed at simulating the effects in a virtual environment. The durability requirements of a transmission impose to perform simulation cycles [135] [44] [154] to determine the loads that the gears have to withstand in dynamic conditions, possibly including the flexibility effects of the different components in order to accurately replicate the working conditions. The recovery of the stress field in the design stage, in sensitive regions of the gears, helps also to determine how far the gear is from the failure point. In a standard transmission the regions that are more sensitive to the applied loads, because of the stress concentration gradients, are the teeth root and the rolling elements in the bearings. It is important to notice that, while for the bearings standardised and detailed application specifications are made available by the manufacturers, the gears have to be designed depending on each application case. Different types of failure may happen to the gears, which are caused mainly by the contact stress on the tooth surface and by the stress amplified by the fillet curve at the tooth root [34]. What is know as *macropitting* is recognized to be among the most common failure mechanism. It is generated by the cyclic loading of the tooth. In the highest shear pressure point caused by the Hertzian stress, which is slightly below the tooth surface, a crack starts to nucleate. The nucleation process may lead to the detachment of small metal pieces creating craters on the tooth surface. A similar phenomena but at an one-order-of-magnitude smaller scale is recognized as *micropitting*. The modest entity of micropitting allows to consider it among the wear-related phenomena. This phenomenon can be reduce by using better lubricants and hardened tooth surfaces. The phenomenon called *scuffing* (also known as "*scoring*") is generated by a poor lubrication that can let the two metal surfaces to slide on each other without any oil layer in between. When this occurs, the effects are superficial scratches in the sliding direction caused by the metal-to-metal contact. Root cracks, on the other side is not generated by the superficial contact stress field, but from the bending stress that, due to its cyclic components, may cause a fatigue loading and let a crack to

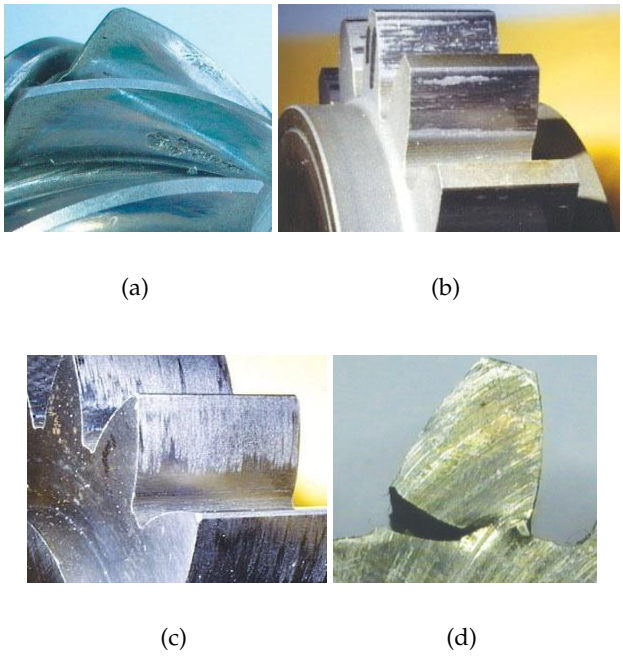

(a) (b)

(c) (d)

FIGURE 2.15: Typical gear failures: 2.15(a) pitting, 2.15(b) micropitting, 2.15(c) scuffing, 2.15(d) root crack. Reproduced from [34].

nucleate in the fillet region.

An accurate modelling of the transmission response is relevant when simulations for diagnostics are addressed. In this context the simulations can help in locating the appropriate instruments to obtain a clear view of the transmission health, and react with sufficient advance to prevent any failure. On the other hand, accurate models can help to recover quantities that can not be directly measured (e.g. the contact pressure), by receiving as input measured signals from accessible locations. Due to the typical layout of a mechanical transmissions, sensors cannot be directly applied on the gears, therefore the transfer path between the meshing teeth and the sensor locations is crucial. The simulation models have therefore to properly include the dynamics of the whole system allowing to isolate, from the entire response, the signal component due to the defect in the gear. The whole dynamic response of the transmission and, in particular, the spectral signature is a very powerful indicator of the system status. In this view, beside the simulation technique, the signal processing theory gained importance in the researcher works [33][106][14], motivated by real case applicability for determining faults in transmissions. The advantages of these techniques is that the transmission has not to be dismounted and could be working, while its response is analysed.

A good health indicator among the different measurable quantities is the mesh stiffness, whose instantaneous decrease indicates a potential cracked tooth [25]. Change in the trend of other quantities, such as TE or dynamic contact force, have been observed, when one of the described defect is present.

From the comfort point of view, acoustic simulations can help the designer to tune the

system in order to increase the comfort level for the final user. This can be done by reducing the acoustic pressure due to the transmission contribution at the location of the user's ears. The way in which a noise can be perceived by a person is investigated by the psychoacoustics [18].
Acoustic simulations generally are based on a dynamic simulation of the meshing gears, which provide the input, for the subsequent acoustic simulation. Coupled vibro-acoustic simulations are avoided due to the high computational cost when the coupling between the air and the mechanical components is taken into account. In the work of Abbess [2], however, the coupling between the air and the housing dynamics is investigated.
The acoustic response of the transmission is strictly related to the corresponding dynamic regime of the rotating gears. In case of gear whine, the excitation has a frequency content at precise frequencies corresponding to the meshing frequency and its multiples. When lightweight gears are analysed, additional orders may appear due to the stiffness variation caused by the holes. Typical analysis for gear whine applications are made in the frequency domain. The purpose of this analysis is to find possible matches between the frequency of the excitation and the natural frequencies of the transmission. If this circumstance happens, amplification of the radiated noise may happen but even more catastrophic events are possible leading to a failure of the transmission. They are made out of *slices*, as shown in Figure 2.5, where each slice is a Fourier transformation of the transmission response in a time window at a given (possibly constant) speed. The analysis is performed for the different speed levels in the working range of the transmission, filling the plot with the different slices. For this Purpose waterfall plots are an extremely useful tool that helps the designer to distinguish between the internal excitation coming from the gears and the natural frequencies of the transmission. The excitation generated by the meshing teeth is linearly dependent on the rotating speed. Resonances of the system, excluding gyrscopic effects, are independent from the speed, therefore when observing the plot in the frequency-speed plane, the excitation appears as a straight vertical line. This type of clear distinction between the excitation and resonance is much less evident when rattle phenomena occur. The response of the transmission in this case has a broadband spectrum due to the happening impacts, as shown in Figure 2.17.

2.5.1 Automotive

In the automotive field, the passengers acoustic comfort is heavily affected by the transmission dynamics. Both gear whine and gear rattle represent noise sources that may annoy the occupants. The increasing number of electric and hybrid vehicles sold in the last years amplifies the problem [94]. When the electric motor of a hybrid vehicle is spinning, while the internal combustion engine is switched off, the transmission is loaded while in the interior cabin the combustion noise is no longer present with its masking action. The acoustic signature of the car interior is therefore dominated by the whine noise with its annoying tonal component. Gear rattle is a non-negligible issue as well. Diesel engines exhibit a higher level of torque fluctuations that may favourite the contact loss between the gear teeth and the subsequent impacts. The conditions that generate gear rattle are

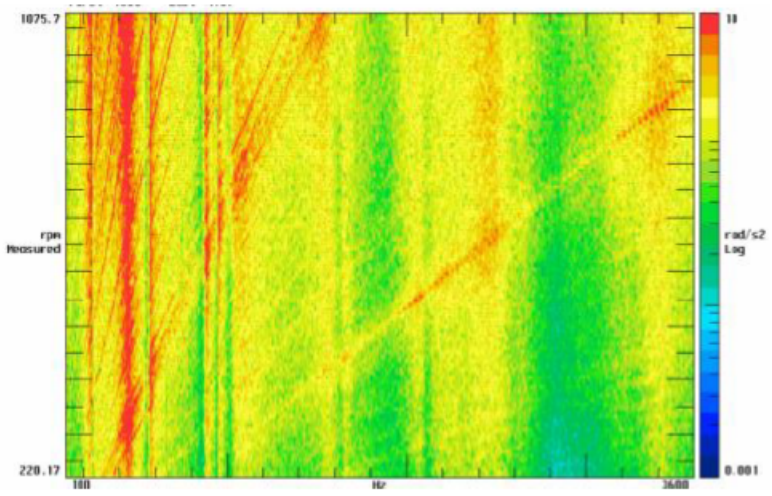

(a)

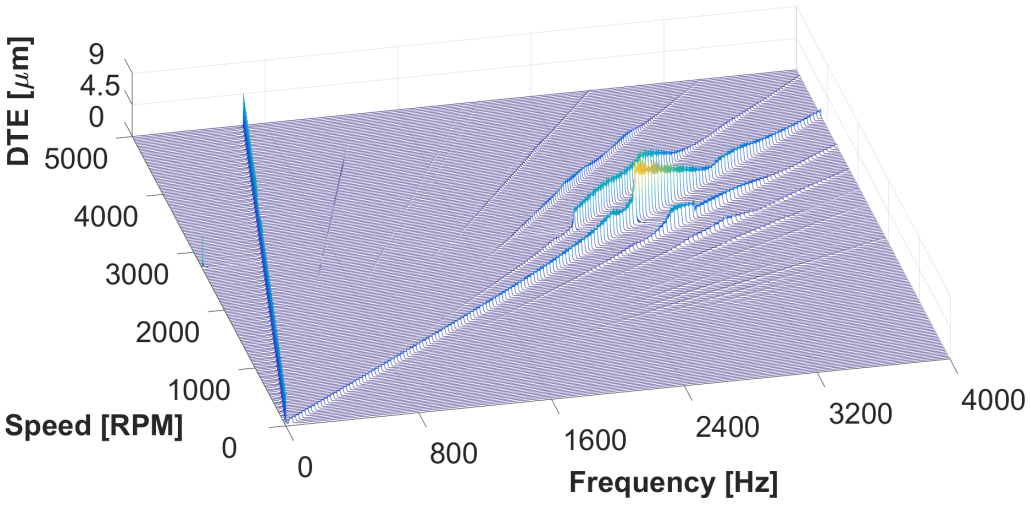

(b)

FIGURE 2.16: 2.16(a) two-dimensional colormap waterfall plot, 2.16(b) Three-dimensional waterfall plot. Reproduced respectively from [58] and [118].

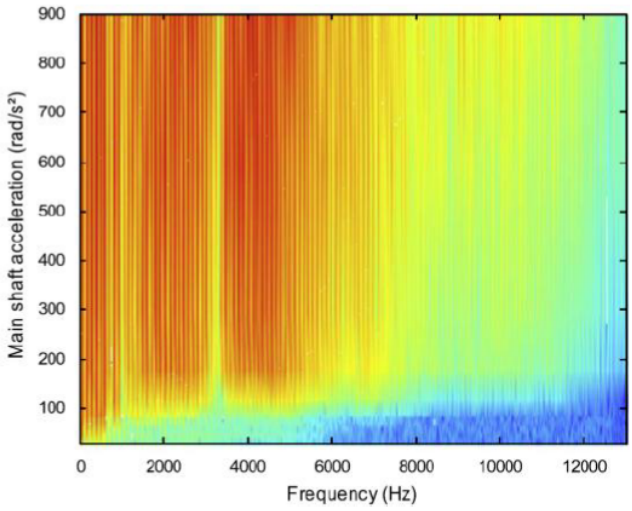

FIGURE 2.17: Shaft response due to gear rattle. Reproduced from [35].

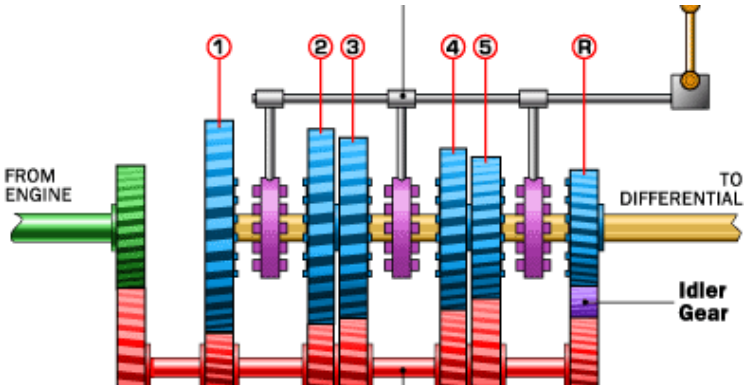

FIGURE 2.18: Typical arrangement for a 5-speed manual transmission. Reproduced from [86].

particularly favourable when low torque levels are transmitted by the transmission, especially when idling. A standard industrial solution to limit the occurring of gear rattle is equipping the car with a dual-mass flywheel (DMF) [146].
From the simulation point of view, different approaches are available in this context. Manual transmissions (Figure 2.18) that imply the engagement of a single gear pair at each time do not represent a major problem. On the other hand, automatic transmission (Figure 2.19) or complex gearboxes for hybrid cars are designed with multiple planetary stages that make simulation of the transmission response more challenging. The resulting coupling with the surrounding structure together with the load sharing between the planets must be captured in order to provide accurate results. The lightweight trend, which is relevant in the last years, imposes a weight saving apporach in all the design aspects of a car, resulting in lighter but more compliant structures. When applied to gear bodies, lightweighting impose holes in the body that enrich the transmission response with additional low frequency orders and modulation sidebands. The simulation tools have to be able to catch these effects together with the mutual coupling between them.

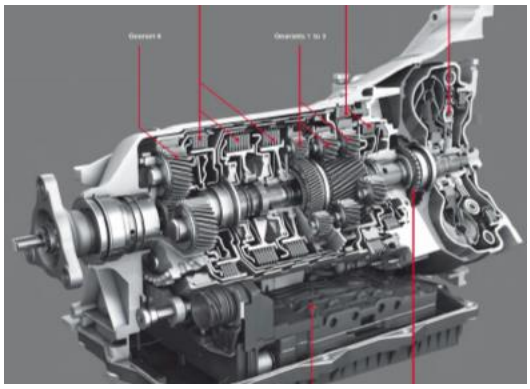

FIGURE 2.19: 8-speed automatic transmission ZF 8HP. Reproduced from [150].

System level simulations is the required modelling strategy to capture the coupling between the different phenomena.

2.5.2 Wind Turbines

In the wind turbine field the performance in terms of durability represents the main concern, being the maximum acoustic emissions imposed by regulations [55]. Taking as reference the wind energy industry, according to Pinar [105], in a typical wind turbine the gearbox is recognized to be the component with the second lowest failure rate, but on the other side it is responsible for up to 40% of the total downtime, being the repairing time the longest compared to all the components. This type of failure may led to lubricant fire, which is then spread along the whole nacelle components, causing a complete destruction of the whole turbine. A higher level of reliability of the gearbox can be reached if the dynamic overloads are properly caught, together with the actual working conditions in terms of misalignments under load. When a wind turbine gearbox is modelled, the challenge is the complexity of the transmission. Typical layouts combine planetary stages with standard ones, being the speed difference between the input and out shafts huge. The typical layout for turbines below 3MW of rated power consists of a planetary stage followed by a couple of fixed axis stages [30] (Figure 2.20). More powerful turbines have a gearbox composed by two planetary stages and a high-speed standard stage; an example can be found in the GE 2P 2.9 wind turbine transmission, reported in Figure 2.21. This layout is necessary due to the very low rotational speed of the blades typically below 1 Hz (60 rpm), that due to the inertial loads can not rotate at higher speed, and to the high frequency of the generator shaft that has to be close to the grid frequency, around 1500 rpm. The complexity of the system is amplified by the flexibity effects of the different components, that was observed for the behaviour of both the bearings and the gears [31]. It is clear the need for system level simulations, including flexible coupled formulation for the shafts and the supporting structures. Additionally, the contribution of the ring gear flexibility as well as the one coming from the bearings stiffness has to be included. In some investigations [98][53] the deformation of the ring gear in planetary stages proved to be relevant in the transmission response. The bearing models in particular determine

FIGURE 2.20: General Electric 1P 2.3 wind turbine transmission, having one planetary stage and two conventional parallel helical stages. Reproduced from [43]

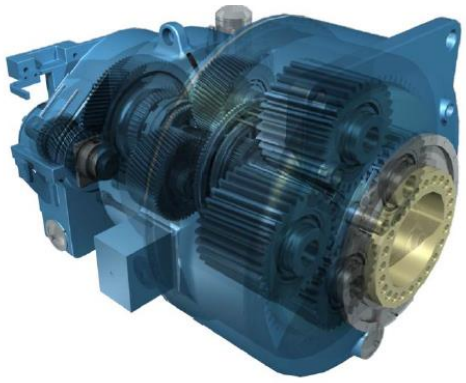

FIGURE 2.21: General Electric 2P 2.9 wind turbine transmission, having two planetary stages and one conventional parallel helical stage. Reproduced from [43].

the features of the corresponding transfer path analysis [73][73][74][49][48]. The noise radiation in wind turbine applications is structure-borne mainly. The configuration of the blades and of the tower is similar to a resonance box, that amplifies the excitation coming from the mechanical loads generated in the gearbox [123]. The interest of the manufacturers in the acoustic emissions of wind turbines is justified by a potential commercial advantage in delivering a turbine, in which the acoustic noise is lower than the level imposed by the regulations. This goal can be achieved both by reducing the excitation in the gearbox and by altering the amplification features of the tower and the blades. The first approach consists in fine tuning the microgeometry on the gear teeth, allowing to lower the TE in the working conditions. This can be obtained only if the loads inside the transmission are accurately reproduced in the simulations. Also in this case, system-level simulations are mandatory because of the mutual coupling between the load paths and the displacement of the components due to the compliance of the supporting structure, shafts and bearings. Additionally the amplitude of the response can be reduced by altering the acoustic characteristics of the tower and the blades. For example, by tuning the stiffness and inertial properties it is possible to shift the resonance frequency crossed by the excitation orders, as to lower the response for that given frequency range. Also in this case the system level formulation, with the accurate representation of the flexibility, is the starting point for this tuning process. The correct representation of the TE in order domain gives the orders of the excitation, which has to be coupled with the system's response modelled on the basis of the stiffness and inertial properties.

2.5.3 Aerospace

Gearboxes are present in helicopters as well as in jet engines. Due to their presence in crucial components, the durability is a critical concern. Acoustics is important for the comfort of the occupants but also because quieter transmissions allow to use less insulating material saving weight. In helicopter applications the main transmission connects the engine units to the main rotor. The blades are connected to the main rotor and require adequate low rotational speed for aerodynamic and structural reasons, typically in the order of 300 rpm. On the other hand the jet engines operate at an extremely high rotational speed, which can reach easily 30000 rpm. The main transmission has therefore the challenging task of providing such a high transmission ratio in the order of 1:100 with strictly weight and packaging requirements. The most convenient layout is based on the use of one or even multiple planetary stages, due to they high power density (Figure 2.22). A different gearbox is used to deliver power to the tail rotor, where spiral bevel gears are used. The oil and fuel pumps are driven by the accessory transmission [11], consisting of spur gear pairs. Due to the high durability requirements, health monitoring of the transmission is particularly advanced, relying on numerous sensors in the transmission and signal processing techniques [107][108]. The data coming from the accelerometers placed directly in the gearbox housing, in order to be in the closest position possible to the excitation source, is processed by the Monitoring System (HUMS) with the aim to alert the pilot if abnormal signal is recorded [114]. The acoustic level inside the cabin is a serious

FIGURE 2.22: Cutaway of an Agusta A109 helicopter transmission displayed at Sint Truiden Air Base, Belgium.

concern. The main gearbox, being connected directly to the helicopter roof, transmits vibration directly to the interior cabin through the structure [88]. The excitation coming from the gearbox may be rich in the contribution number. The lightweighting design in helicopters is quite extreme, therefore the holes in the gears, coupled with the many stages present, contribute to increase the number of orders originated from the transmission. According to [88] the frequency range where the transmission excitation dominates the internal noise goes from 0 to 8kHz, as shown in Figure 2.23, reaching an amplitude of 100dB [123]. A lower level of emitted noise is an advantage, especially for the market of VIP helicopters [145]. The absorbing material used to limit the interior noise increases

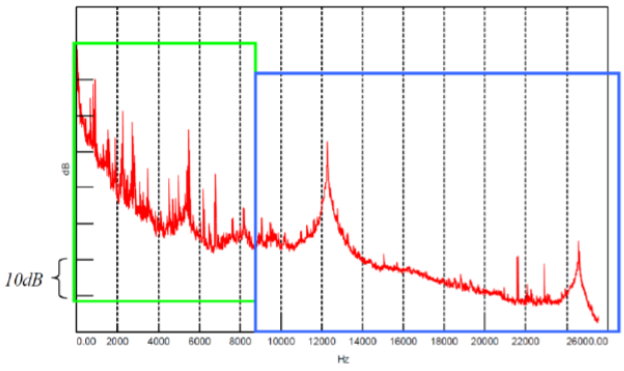

FIGURE 2.23: Sound pressure autopower in a helicopter cabin under steady-state operational condition. Reproduced from [88].

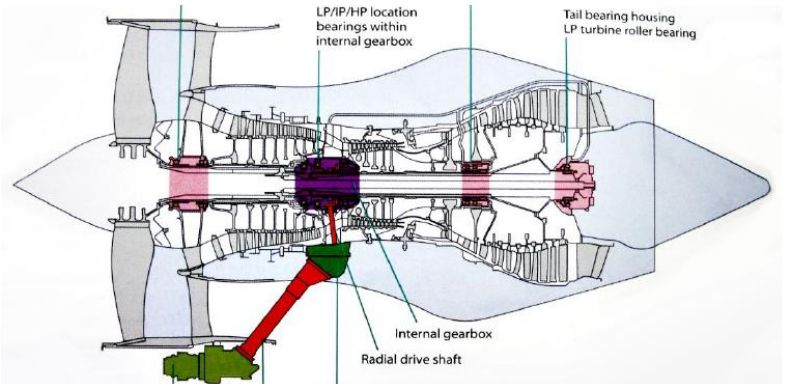

FIGURE 2.24: Typical transmissions arrangement in a jet engine. Reproduced from [112].

the overall weight, with all the connected disadvantages. A quiter transmission helps to limit the use of insulating material, allowing to design lighter helicopters.
In the area of jet engine transmissions, the focus is no more on the generated noise. The sound emissions from the blades, together with the aerodynamic noise generated by the plane itself is much higher than the one coming from the transmission. The focus on the transmission has the scope to monitor the gearbox health for condition monitoring and durability reasons [110]. A typical arrangement of the transmissions in jet engines applications [112] is reported in Figure 2.24. An accessory gearbox has the function to extract power during the operation, or by using it in the opposite direction, power can be provided to start it. An angled shaft is used to connect the core shaft to the external gearbox, therefore spiral bevel gears have to be used. The output power is then delivered at the appropriate speed using a spur gear drive. The choice of spur gears is motivated by weight saving purposes. The absence of trust loads generated during meshing allows to avoid the use of axial bearings, but the sharper stiffness variation makes the dynamic excitation higher and closer to possible jump-phenomena. System level simulations are mandatory also in this field due to the strong coupling between the gear excitation and the dynamic response of the structure, made extremely compliant due to the lightweighting.

2.6 Gear Lightweighting

Trends for emission limitations and fuel saving impose a more efficient energy exploitation in many sectors of mechanical engineering. Lightweighting is one of the strategies that can be adopted to reach this goal. Besides the environmental requirements, lightweighting is a key aspect in all the applications where the weight is a crucial aspect for the overall performance of the system, such as in aerospace and automotive industries. Geared power transmissions, which are key components in many mechanical systems, are not excluded from such a lightweighting trend. Common lightweighting strategies are based on the reduction of gear thickness as well as on the manufacture of holes in the web of the gear. Although the use of lightweight gears in the transportation sector and in general machinery is continuously increasing, design problems

related to the dynamic strength of such transmissions are not yet fully solved [70], requiring the development of simulation models able to predict the impact of different design choices (e.g.,web thickness, number, position, and shape of the holes) on their vibration behaviour. During gear meshing, complex phenomena occur simultaneously, such as nonlinear load-dependent contact deformations, friction, clearance, and time-varying mesh stiffness. As reported in section 2.3 three-dimensional FE simulations for gear meshing analyses represent the most detailed simulation approach available nowadays [2]. In this case no special treatments are required to model the lightweighting effects. On the other side analytical formulations and lumped-parameter modelling have been widely used to analyse gear dynamics thanks to their computational efficiency and capability to capture nonlinear phenomena in the dynamic behaviour [5]. In comparison with FE approaches, lumped-parameter models have a high computational efficiency as key advantage, but an adequate description of the time-varying meshing stiffness and of the related dynamic excitation is required to enable accurate predictions of the system behaviour. Given the general nature of the method, detailed FE simulations enable mesh stiffness calculations and loaded tooth contact analysis without a priori assumptions, but at the cost of very high computational load. For this reason, hybrid approaches, combining FE and analytical modelling, have been developed [14, 15]. A combination of FE and lumped-parameter models was used by Ren et al. [17] to study the dynamic behaviour of a coupled gear-shaft-bearing-housing assembly by using the impedance synthesis method. In solid, axisymmetric gears, the TE curve and the mesh stiffness function are typically dominated by the harmonic content at the meshing frequency. One of the effects of gear lightweighting is the occurrence of additional harmonic components at lower frequencies, originating from the non-uniform distribution of mass and stiffness along the gear blank.

Chapter 3

Combining FEM and Analytical Modelling for Static and Dynamic Analysis of Lightweight Gears

3.1 Introduction

In this chapter the static and dynamic behaviour of lightweight gears is analysed combining non-linear FE simulations and a lumped parameter model. The nonlinear FE simulations are used to compute the Static Transmission Error (STE) curves for different gear pairs, from which the angle-dependent mesh stiffness is derived. In this manner the accuracy typical of the FE method is exploited to derive STE curves that show the dependency with the body topology of the gear pairs. Typical fluctuations in the mesh stiffness due to the non-uniform distribution of the material around the hub can be represented and taken into account. In this way the effects of several shapes of the gears body can be analysed in the static field as well as during dynamic simulations. The statically computed curves are then used in a 1D lumped-parameter model to simulate the dynamics of different lightweight gear pairs differing for the shape of the body, while the kinematical parameters are kept constant.
The advantages of the approach described in this chapter, which is already investigated in the work of Shweiki et al. [118] is that detailed and time-consuming simulations are limited in a preprocessing phase without affecting the computational efficiency of the analytical model, while the dynamic effects of the different gear topologies are well captured by the latter model.
In order to present the capabilities of the method to properly model the static and dynamic behaviour of gear pairs when different lightweighting strategies are adopted, different case studies are presented including two different strategies for gear weight reductions are analysed. The first lightweighting approach consists in a gear where the web thickness is reduced resulting in a rimmed axisymmetric gear. A second lightweighting approach is based on material removal from the web through a series of holes or slots, which result in a rotational symmetry for the lightweight gear that influences the mesh stiffness and the TE of the gear pair.

3.2 STE Estimation in Lightweight Gears by Nonlinear FE Simulations

An analysis of how different strategies for lightweight design influence the static response of a gear pair is done by estimating the STE curves through nonlinear FE simulations, for which high-detail models of the meshing gears have been built.
Four case studies, consisting of different gear pairs, are analysed. In each pair, a solid blank gear is meshing with a lightweight gear, with a different layout. The four gear pairs analysed through nonlinear FE simulations are shown in Figure 3.1. In the gear pairs of Figures3.1(a) and 3.1(c), the blank of the lightweight gear is axisymmetric; that is, mass reduction is achieved by reducing the depth of the rim, while in the other two case studies gear lightweighting is achieved through eight circular holes and three slots in the blank, as shown in Figures 3.1(b) and 3.1(d), respectively. The last gear pair represents a case of extreme lightweight design, which will be analysed along with the others to highlight the effects of increased blank flexibility on the mesh stiffness and, subsequently, on the dynamic response of the system. The two lightweight gears with axisymmetric geometry, shown in Figures 3.1(a) and 3.1(c), have been designed as to have the same overall mass of the lightweight gears with 8 holes and 3 slots, respectively. Gear (a) can be directly compared to gear (b), except for the absence/presence of the holes and their effect on blank stiffness; the same holds for gears (c) and (d).
The FE models of the four meshing gear pairs, shown in Figure 3.1, were created by using 8-node hexahedral elements, while the main design specifications are reported in Table 3.1.

TABLE 3.1: Main design parameters of the analysed gears

Parameter	**Units**	**Value**
Tooth number	[-]	57
Module	[mm]	2.6
Pressure angle	[deg]	20
Tip diameter	[mm]	154.5
Root diameter	[mm]	141.7
Face width	[mm]	23
Contact ratio	[-]	1.45
Working centre distance	[mm]	150
Material	[-]	Steel

In the FE model of the gear pairs, supporting shafts were represented as infinitely rigid by rigidly constraining all the DOFs of the gear bore nodes to a master node located in the centre of the gear and constrained with rigid body elements. A loading torque equal to 350Nm was applied to the master node located at the pinion centre, for which the rotational DOF was left unconstrained. With the aim of generating STE curves, different nonlinear FE static simulations were performed for each gear pair, by positioning the

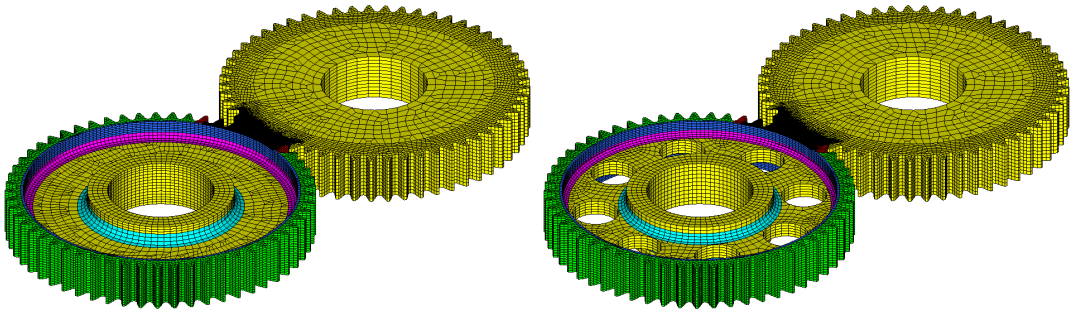

(a) Gear pair A

(b) Gear pair B

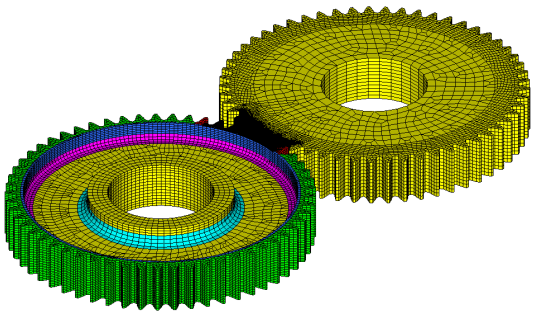

(c) Gear pair C

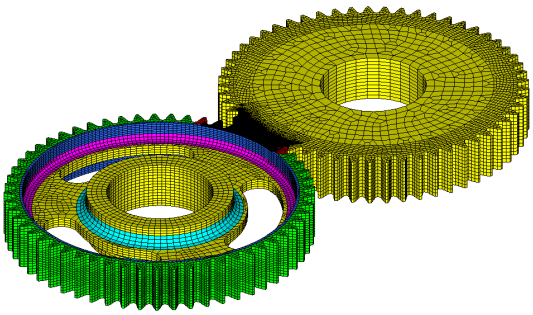

(d) Gear pair D

FIGURE 3.1: FE models of the four gear pairs analysed: (a) and (c) have an axisymmetric design for the lightweight gear, while 8 holes and 3 slots enable mass reduction in (b) and (d), respectively, with different degrees of discrete rotational symmetry. Gears (a) and (b) are designed to have the same total mass; the absence/presence of the holes cause different effect on blank stiffness; the same holds for gears (c) and (d).

two gears in a discrete number of equally spaced angular positions in the angular period of the gear pair. In each angular configuration, one point of the STE curve is computed according to the following equation:

$$TE = r_{bG}\theta_G - r_{bP}\theta_P \tag{3.1}$$

where θ_P and θ_G represent the rotation of the pinion and of the gear, respectively, while r_{bP} and r_{bG} are their base radii. In the specific cases analysed in this chapter, θ_P is the final rotational displacement of the pinion master node after load application, while is equal to zero, considering the constraining condition of the gear, in which the master central node is held stationary during the simulations. Having identical tooth geometry, the two gears have the same base radius.

In order to reduce the computational time, the FE model of each gear was divided into regions of different mesh size. In the regions close to the tooth contact area, where a

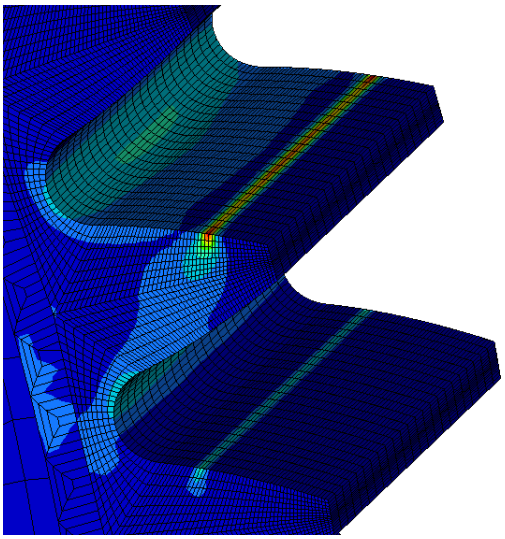

FIGURE 3.2: Example of stress distribution estimated by nonlinear FE simulation for the lightweight gear shown in Figure 3.1(b) in a given configuration.

detailed description of the geometry is required to properly capture contact phenomena, the element size was set to 0.11 mm, based on a convergence analysis [56]. Considerably coarser mesh was created in the regions that are sufficiently far from the meshing teeth. Since the computational complexity is strictly dependent on the number of nodes in the model, several models were created for each non axisymmetric gear, as to limit the number of teeth with fine mesh to 5, that allow for simulating 3 meshing cycles. A total of 7 and 19 models were created for the gear with 8 holes and with 3 slots, respectively. An example of the results obtained from the nonlinear FE simulations in a region of an axisymmetric gear close to the meshing area is shown in Figure 3.1, while Figure 3.2 highlights the effects of material removal from the blank on the local and on the global deformation of the lightweight gear with holes. It appears, in fact, that lack of material in the region close to the meshing teeth causes higher deflections compared to the situation in which the meshing teeth are close to a region of the web in which no holes are present. By post-processing the results of the static simulations, the STE curves for each pair of meshing gears were derived. From the STE curves shown in Figure 3.5, it is possible to appreciate that the effects of blank topology of the lightweight gear on the mesh stiffness of the gear pairs are significantly different in the four case studies. Figures 3.5(a) and 3.5(c) show the STE curves estimated for the gear pairs of Figures 3.1(a) and 3.1(c), respectively. The two curves are periodic with the mesh frequency and do not exhibit lower frequency harmonic components. The effects of the holes and of the slots are clearly visible in the curves of Figures 3.5(b) and 3.5(d), where the additional low-frequency components significantly change the shape of the curves. Such observations are confirmed by the results of the FFT analysis shown in Figure 3.3, where the frequency content of the STE curves for the nonaxisymmetric gears shows the presence of low-frequency components, with an angular frequency equal to the number of material discontinuities in the blank (holes or slots) and its multiples. From the static results shown above, the mesh stiffness that

will be used as input for the dynamic simulations is derived. For the purpose of calibrating the analytical model, the gears are lumped into rigid bodies with inertia and stiffness proprieties derived from the FE models and reported in Table 3.2.

TABLE 3.2: Main properties of the gears that will be used in the analytical model for dynamic simulations.

Parameter	**Gear A**	**Gear B**	**Gear C**	**Gear D**
Gear inertia $[kg * m^2]$	0.0041	0.0041	0.0038	0.0038
Mass $[kg]$	1.72	1.72	1.68	1.68
Average mesh stiffness $[N/m]$	$2{,}72 * 10^8$	$2{,}18 * 10^8$	$2{,}42 * 10^8$	$1{,}35 * 10^8$
Average resonant frequency $[Hz]$	3258	2962	3030	2345
STE at meshing frequency $[\mu m]$	3.776	3.663	3.921	3.894
STE at blank angular frequency $[\mu m]$	0	1.794	0	9.584

3.3 Lumped Parameter Modelling and Dynamic Analysis of Gear Pairs with Lightweight Design

The model described by the following equations is derived from the one proposed in [15] and is intended to describe the relative motion between two gears in dynamic conditions. The joints are supposed to be perfectly rigid, so that no motion of the gears is allowed except for the rotation along their rotational axis. Gear meshing is modelled by a single spring-damper system acting along the line of action of the gear pair. The use of one single spring representing both the blank stiffness and the teeth contact stiffness can be justified by the consideration that the meshing frequency and its harmonics are almost identical for all the gear pairs analysed here, indicating that in static condition the contribution to the TE of the tooth stiffness is not significantly affected by the holes or the slot in the gear body. Additional dynamic contributions coming from the tooth mode shapes are neglected in this work, the focus being on the impact of blank topology on the dynamic behaviour of the gear pair, which can be captured by the torsional model used in this work. In this way, the relative motion between the gears is described as a linear displacement along the line of action. Consistently, the applied torque and the rotational inertia are converted, respectively, in a linear force acting along the line of action and in an equivalent mass.The transformation from a rotational inertia to an equivalent mass is done considering the gears as homogeneous discs, and extracting their inertia properties from a CAD model, while the equivalent mass of the 1 DOF system, which is represented in Figure 3.3, is calculated starting from the mass values estimated for each gear.

The dynamic behaviour of this 1-DOF system, which considers a pair of identical gears, is governed by the following equation of motion:

$$m\ddot{x} + 2\zeta\dot{x} + k[PC(t)]g[x(t)] = F(t) \tag{3.2}$$

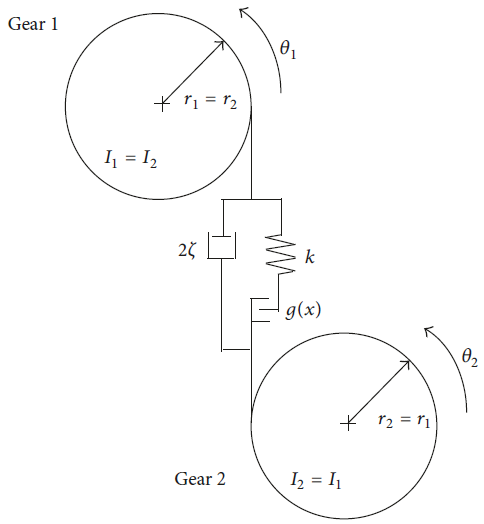

FIGURE 3.3: Representation of the 1D dynamic model of meshing cylindrical gears.

where x is the linear relative displacement of the equivalent gear pair along the line of action and represents the Dynamic Transmission Error (DTE) in the system; $\dot{x}$ and $\ddot{x}$ are its first and second time derivatives; m is the equivalent mass of the system; and ζ is a damping coefficient introduced in the model to consider losses during tooth meshing. The model parameter $k[PC(t)]$ is intended to represent the time-varying mesh stiffness derived from the STE curves calculated as described in Section 3.2.The mesh stiffness is a function of the instantaneous position of the contact point $PC(t)$ along the mesh cycle, which is derived as

$$PC(t) = \frac{1}{\theta_{\mathrm{P1}}}\left[\theta_1(t) - floor\left(\frac{\theta_1(t)}{\theta_{\mathrm{P1}}}\right)\theta_{\mathrm{P1}}\right] \tag{3.3}$$

where $\theta_1(t)$ is the actual value of the rotational angle and θ_{P1} is the angular period of the STE curve. The obtained value of PC is between 0 and 1. When an axisymmetric gear is analysed, the angular period corresponds with the length of the meshing cycle, because no harmonic components due to the gear body discontinuities are present in the STE curve of the gear pair. In this case, the variability of the mesh stiffness is given mainly by the variable number of tooth pairs in contact, which results in a dominant harmonic component in the STE at themeshing frequency and additional harmonic components.When gears with material discontinuities in the blank, that is, holes or slots, are analysed, the angular period has to be extended in order to capture the entire frequency content of the STE curve. An entire revolution of the gear has to be analysed in the case in which the teeth number is not an integer multiple of the hole number, while symmetry exploitation

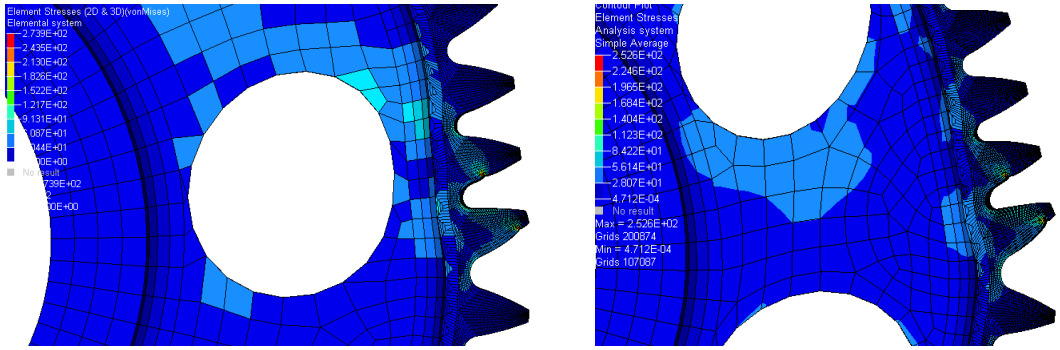

(a) (b)

FIGURE 3.4: Example of stress distribution and static deformation of the gear with 8 holes in two angular configurations of the gear pair: loaded teeth are close (a) and far away (b) from a hole in the blank.

can be sought in those cases where the tooth number is a multiple of the hole number, as for the case of the gear with 3 slots. The periodic mesh stiffness is derived as a function of the rotational angle from the STE curves through the following equation:

$$k(PC) = \frac{F_{tt}}{STE(PC)} \tag{3.4}$$

where F_{tt} is the magnitude of the tangential contact force used for estimating the STE curves. The hypothesis behind this approach is that the dependencies of the obtained STE values with the transmitted load are negligible in a small load interval around the nominal condition. No microgeometry modifications are applied on the teeth and the nonlinear dependencies of the STE with the applied load are not taken into account. The applied torque corresponds to the one used in the STE calculation phase. In line with the assumption of perfect joints, no further dependencies of the STE on the relative misalignment between the gears are considered. The mesh stiffness values are stored as function of the relative angular position of the gears in lookup tables, which are then interpolated during the dynamic simulation.

The formulation of eq. 3.2 allows also modelling the backlash b between the gears introducing the restoring function $g[x(t)]$, which is the following function of the equivalent relative displacement between the gears [15]:

$$g[x(t)] = \begin{cases} x(t) - b, & x(t) > b \\ 0, & |x(t)| \leq b \\ x(t) + b, & x(t) < -b \end{cases} \tag{3.5}$$

The restoring function allows considering contact losses between the teeth, by bringing

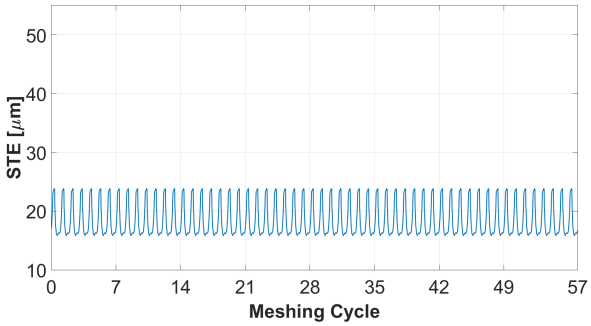

(a)

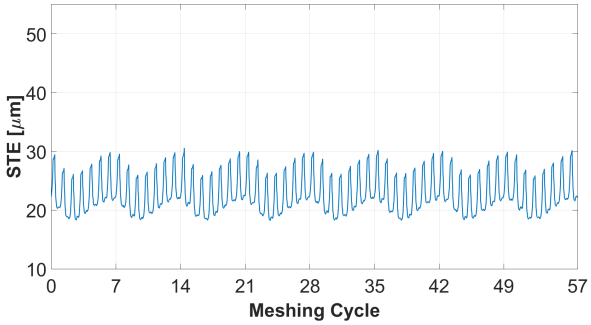

(b)

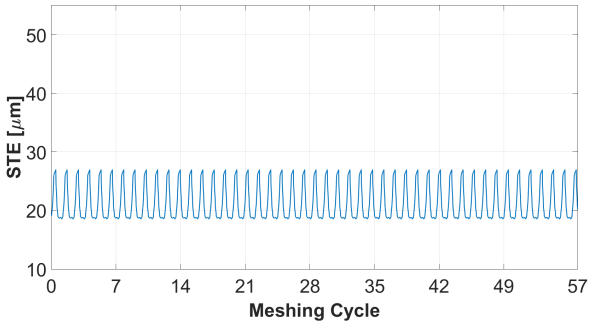

(c)

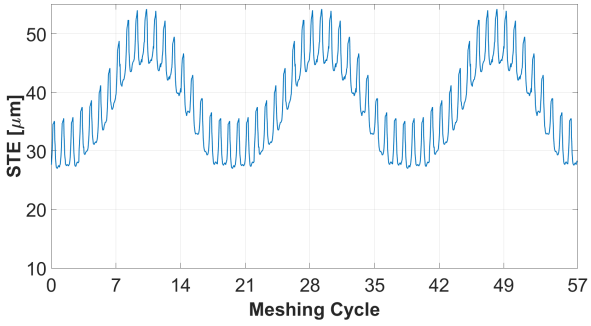

(d)

FIGURE 3.5: STE curves of the analysed gear pairs computed through non-linear FE simulations for the gear pairs (a), (b), (c), and (d) in Figure 3.1.

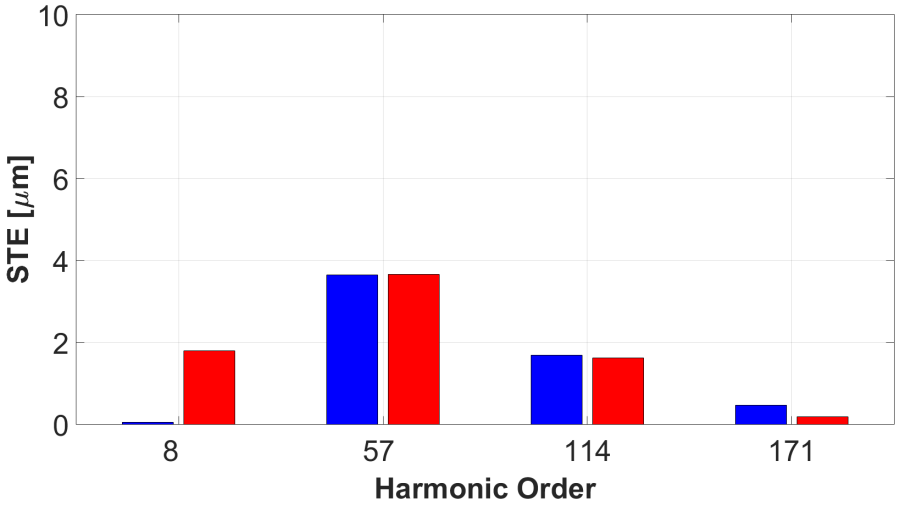

(a)

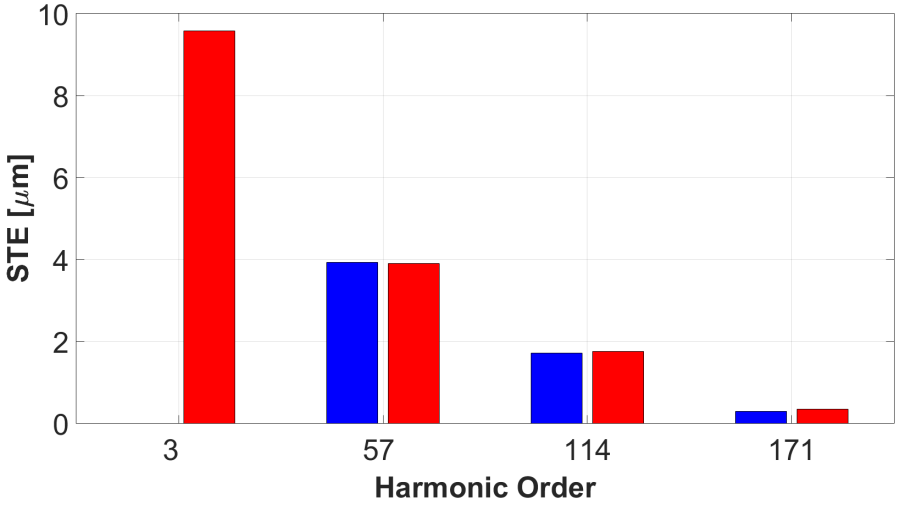

(b)

FIGURE 3.6: Amplitude of different harmonic components obtained from FFT of the STE curves computed for gear pairs (a and b) (a) and for gear pairs (c and d) (b). The rotational speed is kept constant in each simulation. Blue histograms refer to the axisymmetric gears.

the value of the mesh stiffness to zero when the relative displacement is below the backlash threshold. This condition means that there is no contact between the teeth and consequently no elastic meshing force acting on the bodies. When the instantaneous relative displacement assumes a value higher than the imposed backlash, the restoring function allows considering only the effective penetration between the teeth in contact, subtracting the backlash from the estimated relative displacement.
The external force $F(t)$ in eq. 3.2 represents the loading force in the system. In general, a time-varying load can be considered in the model, but in the work presented in this chapter it is considered to be constant, based on the assumption that the imposed value of transmitted torque by the gears is constant. The instantaneous acceleration value $\ddot{x}$ is computed numerically by using a fixed step explicit Runge-Kutta algorithm. Dynamic simulations are performed considering a constant applied torque of 350Nm and a linearly increasing speed from 0 to 5000 rpm in 200 seconds. The fixed time-step is set to 2microseconds and corresponds also to the sampling period. This grants a maximum observable frequency of 250 kHz, which is sufficiently high to reconstruct impulsive phenomena and to capture the significant harmonics of the gear mesh frequency.
The actual value of the rotational speed given as revolutions per minute is converted into a meshing frequency value by considering the teeth number.The position along the mesh cycle is obtained by integrating the instantaneous meshing frequency value.
The obtained time histories of the DTE are then analysed in terms of root mean square (RMS) of the oscillating component in each mesh cycle versus the meshing frequency. One model is created for each of the four gear pairs, with inertia and stiffness (STE) properties derived as described in Section 3.2. The RMS of the steady-state oscillating component of the estimated DTE is reported in Figure 3.7. The results of Figures 3.7(a) and 3.7(c), corresponding to the two axisymmetric gears, and of Figure 3.7(c), corresponding to the gear with 8 holes, show a clearly visible jump in correspondence with the resonance frequency. The jump phenomena, which are due to loss of contact and are a typical clearance-type nonlinearity, disappear in the dynamic response of extremely flexible gear pair 3.7(d), in which the lightweight design is achieved through three slots.
By comparing the DTE estimated for gear pairs (a-b) and (c-d), which have identical inertia properties, different amplitude in the RMS of the dynamic response is observed in the analysed frequency range. It is worth to notice also that the nonaxisymmetric design has a lower average mesh stiffness as compared to the axisymmetric gear with the same mass reduction. For a given mass reduction, the lower value of the average mesh stiffness determines a frequency shifting towards lower values and a modification of the amplitude of jump phenomena in the dynamic response. Loss of contact phenomena appear less significant in gear pairs with nonaxisymmetric lightweight gear and disappear for the gear pair (d).
A thorough comparison can be done considering the waterfall diagrams shown in Figure 3.8. When the gear lightweighting is achieved by discontinuities in the gear blanks, the low-frequency harmonic components of the STE shown in Figure 3.3 cause additional excitation orders, while sideband effects showup in the regions where the meshing order

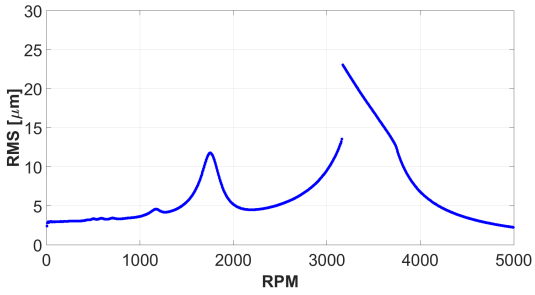

(a)

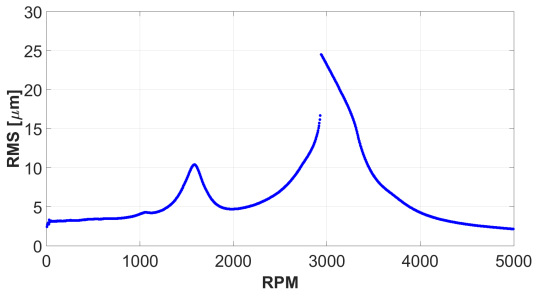

(b)

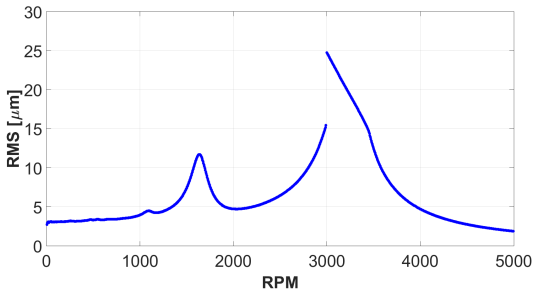

(c)

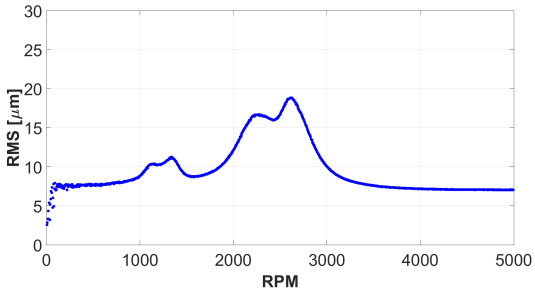

(d)

FIGURE 3.7: RMS of DTE obtained by using the different STE curves computed for the four gear pairs shown in Figure 3.1.

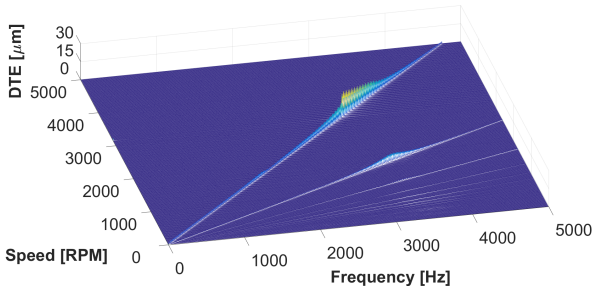

(a)

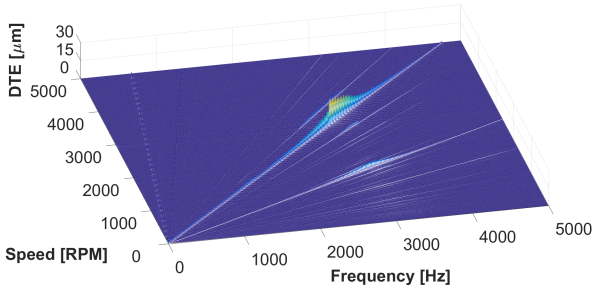

(b)

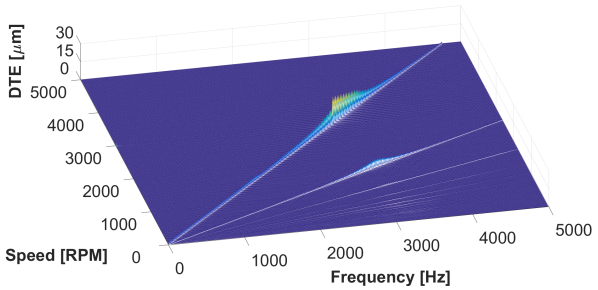

(c)

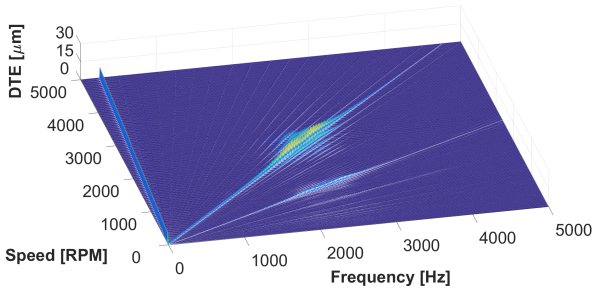

(d)

FIGURE 3.8: Waterfall diagram of the DTE for the four gear pairs analysed.

excites the resonance of the system.
To further analyse the effects of lightweight design on the dynamic behaviour of each gear pair, constant-velocity simulations, at a speed where the meshing frequency is slightly below the gear pair resonance frequency, have been executed. The results are summarized in Figure 3.9(a) for gear pairs (a) and (b) and in Figure 3.9(b) for gear pairs (c) and (d), which show the results of the FFT analysis of the DTE curves estimated for the four gear pairs in steady-state conditions. Only the amplitude of the meshing order and its sidebands, along with the orders due to the holes, are reported.
Gear pairs (b) and (d) (red) exhibit a different dynamic behaviour as compared to the gear pairs with an axisymmetric design (blue). Due to the additional excitation orders shown in the waterfall diagrams, significant harmonic components due to the holes and slots are observed at low frequencies. Specifically, for the extreme lightweight design of gear pair (d) in Figure 3.9(b), the system response excited by the order of the slots is comparable with the one of the meshing order, even if the latter excites the resonance of the system. Clear sidebands around the meshing frequency and its harmonics can be appreciated as well.

3.4 Parametric Study

The simulation results shown in the previous sections demonstrated that the presence of holes in the gear blank influences the average value of the mesh stiffness and the shape of the STE curve, in which an important harmonic component shows up at the angular frequency of the gear blank geometry (linked to the number of holes), on top of the harmonic component at the meshing frequency (linked to the number of teeth). With the aim of investigating the impact of such modifications of the STE curves on the dynamic response of the gear pair, a parametric model of the STE curve is defined in equation 3.6

$$STE(PC) = STEav + STEh * cos(Nh * PC) + STEm * cos(Nt * PC) \tag{3.6}$$

TABLE 3.3: Ranges in which the STE parameters are varied.

	Units	**STEav**	**STEh**	**STEm**
Min	[μm]	18	0	2
Max	[μm]	38	10	6

where $STEav$ is the mean STE value, while $STEh$ and $STEm$ are the harmonic components at the hole angular order and at the meshing order, respectively. $Nh = 8$ and $Nt = 57$ are the number of holes and the number of teeth, respectively, while the ranges that have been set for the three STE parameters are shown in Table 3.3.

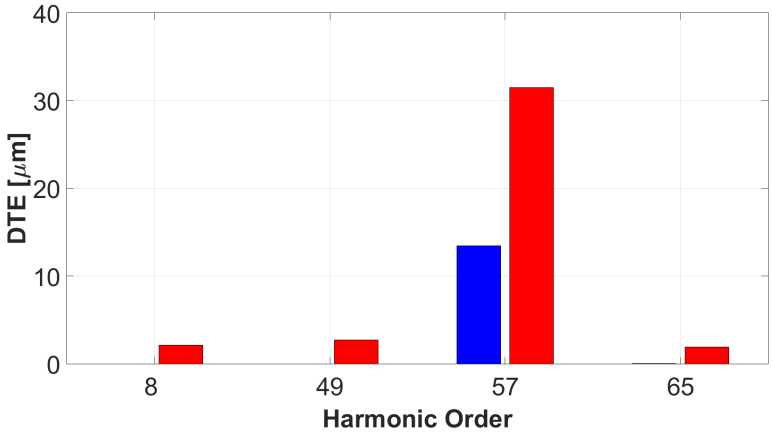

(a)

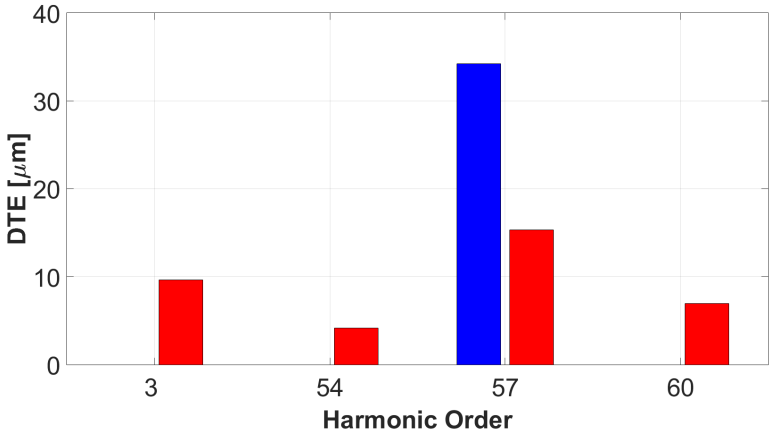

(b)

FIGURE 3.9: Amplitude of different harmonic components obtained from FFT of the STE curves computed for gear pairs (a and b) 3.9(a) and for gear pairs (c and d) 3.9(b). The rotational speed is kept constant in each simulation. Blue histograms refer to the axisymmetric gears.

The STE curves, analytically generated through the relation 3.6 and by varying the parameters in the ranges of Table 3.3, are represented in Figure 3.10. The harmonic component in the STE curve with the angular frequency corresponding to the number of discontinuities in the gear web is intended to represent the harmonic fluctuation in the STE curve due to the presence of the discontinuities. Its amplitude is changed from curve to curve in order to replicate the effect of positioning and sizing of holes in real design. The harmonic component of the STE curve at the tooth meshing frequency is mainly due to the change in the instantaneous number of meshing teeth between 1 and 2 in the case studies illustrated in this chapter. From each of the analytically generated STE curves, one mesh stiffness function is derived and used in the gear pair model of eq. 3.2. In all the simulations, the damping coefficient is varied in such a way that a modal damping ratio of around 6% for the equivalent Linear Time-Invariant (LTI) system is obtained. The inertia values are kept constant during the analysis, being the focus of the simulation campaign on the relative importance of the harmonic content of the internal excitation.

3.4.1 Effect of the Average STE Value

The results shown in Figure 3.11 represent the different dynamic responses of the system for different values of the average STE value. Each point of the curves represents the RMS value of the steady-state forced response in terms of DTE oscillating component in a mesh cycle. It is worth to say that higher values in the STE correspond to lower values of mesh stiffness.The tooth-passing component and the order of the holes are kept fixed to a reference value of 4 and 0, respectively. In particular, the latter value corresponds to a configuration in which no holes are present in the gear blank. The effects of an increasing average value of the STE, shown in Figure 3.11, can be summarized in a shift of the resonant frequency of the system to lower values, an increase in the peak value of the DTE, and a reduction of the frequency range in which teeth lose contact.

3.4.2 Effect of STE Harmonic Component at the Mesh Frequency

The effects of the amplitude of the meshing harmonic component of the STE are shown in Figure 3.12. As above, the simulation parameters are unchanged for all the simulations of the campaign except for the amplitude of the harmonic component at the angular period corresponding to the tooth meshing period. Increasing the amplitude for the meshing harmonic component of the STE does not alter the resonance frequency of the equivalent LTI system; therefore all curves remain centred around the same resonance frequency. Furthermore, higher meshing harmonic amplitudes correspond to a proportional increase in the dynamic response in the linear dynamic region. It is worthy to notice that such increase in the dynamic response makes the gears lose contact at a lower frequency. Similarly, gears regain full contact later at higher frequencies.

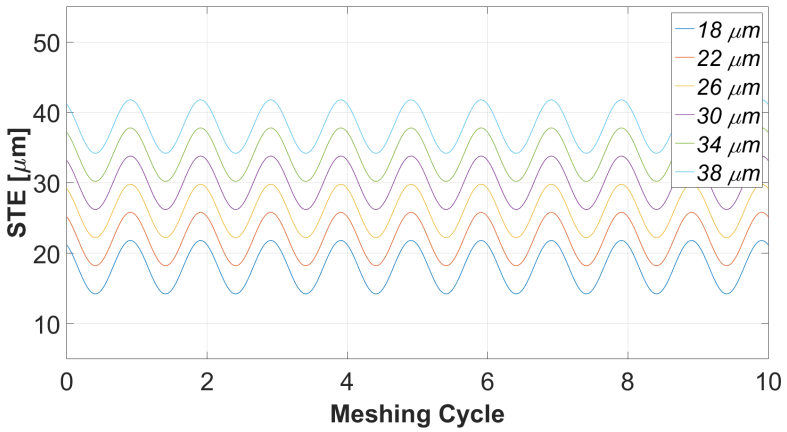

(a)

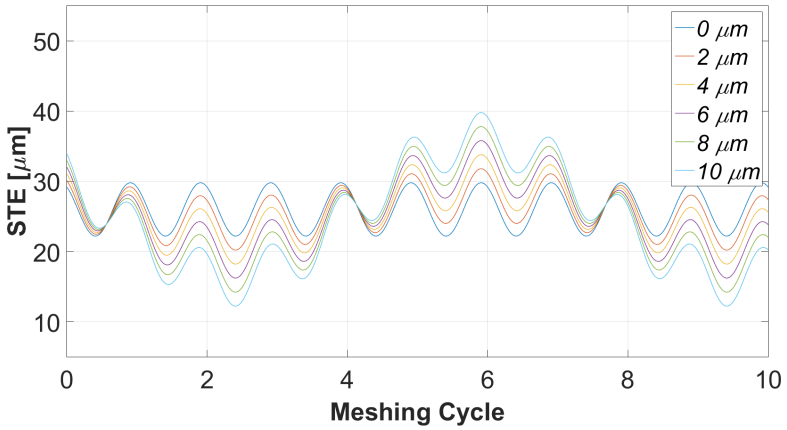

(b)

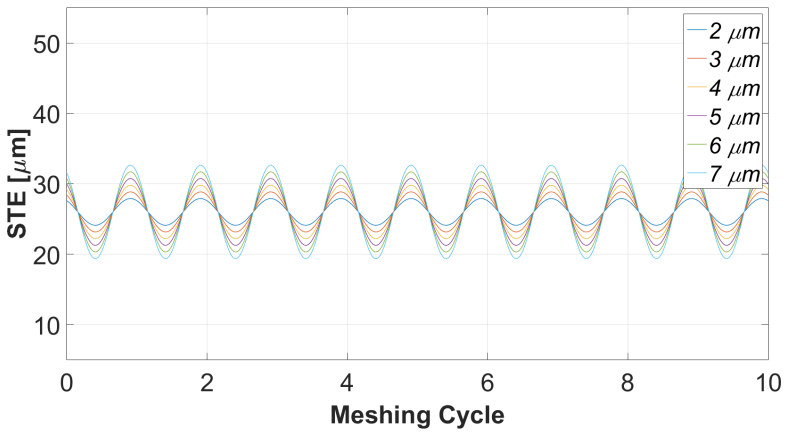

(c)

FIGURE 3.10: Portions of STE curves analytically generated by 3.10(a) varying the average value of the STE, 3.10(b) varying the amplitude of the harmonic component at the angular frequency of the holes, and 3.10(c) varying the amplitude of the harmonic component at the angular frequency of the meshing teeth.

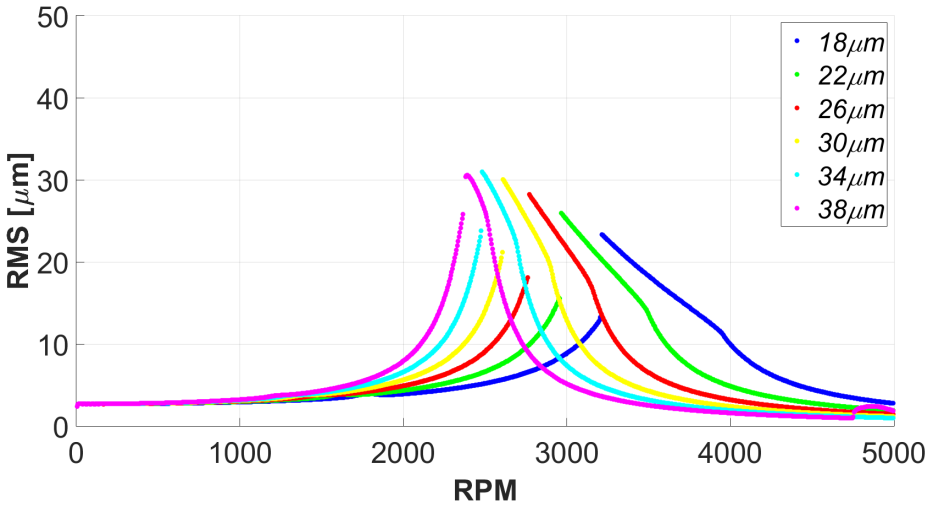

FIGURE 3.11: RMS of the different DTE curves obtained by using different average values of STE.

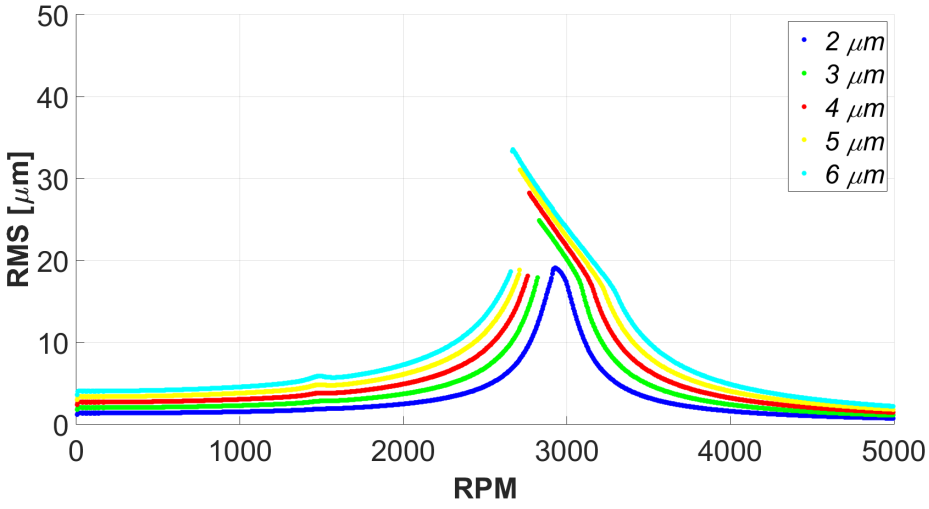

FIGURE 3.12: RMS of the different DTE curves obtained by using different values of the amplitude of the harmonic component at the meshing frequency.

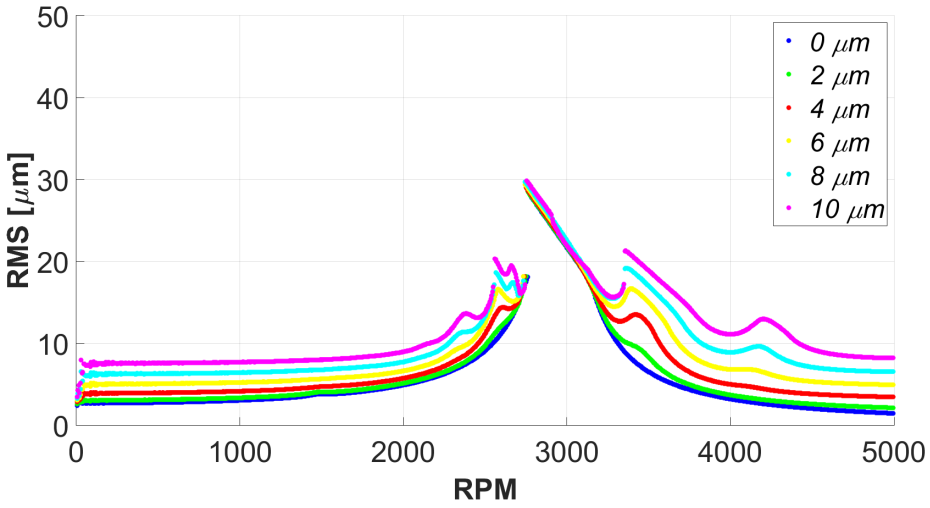

FIGURE 3.13: RMSof the differentDTE curves obtained by using different values of the amplitude of the component due to discontinuities in the gear web.

3.4.3 Effect of STE Harmonic Component due to Discontinuities in the Gear Web

The effects of varying the amplitude of the harmonic component of the STE due to discontinuities in the gear web are shown in Figure 3.13. It is important to highlight that the average value of the STE curve is not affected by the amplitude of the contribution coming from the material discontinuities in the lightweight gear blank. Consistently, the jump phenomenon is not modified in its amplitude by the presence of the holes. From Figure 3.13 it is clearly visible that additional amplifications in the RMS curve are directly dependent on the amplitude of this additional harmonic component. These amplifications have the characteristic of modulation sidebands of the DTE curve. Additional jump phenomena appear when a sideband due to the web discontinuities matches the resonance frequency of the gear pair. Considering Figure 3.14, where an example of STE curve used in the analysis is reported together with its FFT analysis in angle domain, it is possible to notice that no amplitude modulation sidebands are present since the harmonic components shown in Figure 3.14(b) are corresponding, by analytical definition, to the meshing and to the hole components only. Sidebands are instead clearly visible in the FFT analysis of themesh stiffness derived fromthe STE curve according to relation expressed in eq. 3.4 and shown in Figure 3.15. Dynamic sideband amplifications are observed also in the waterfall diagram shown in Figure 3.16.

3.5 Conclusions

In this chapter the effects of blank lightweighting on the static and on the dynamic behaviour of a pair of meshing gears have been investigated by combining nonlinear FE simulations and lumped-parameter modelling. In the first part of the chapter four case

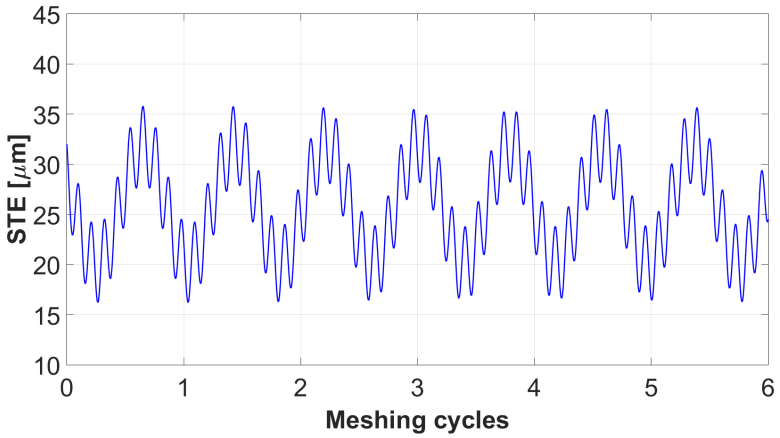

(a)

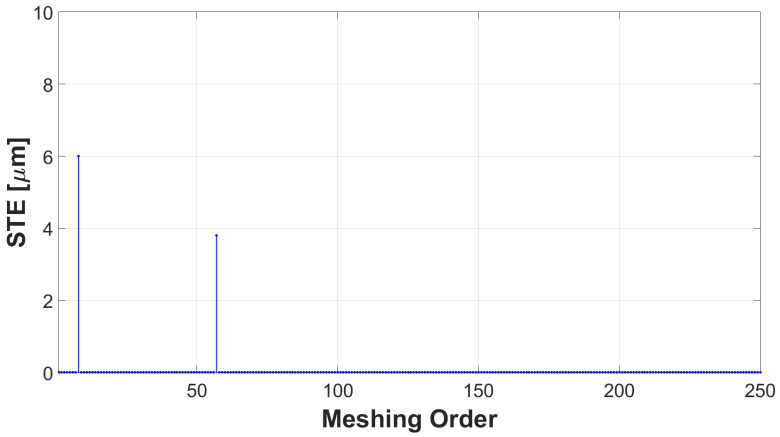

(b)

FIGURE 3.14: Example of STE curve obtained for STEh = 10 μm and STEm = 3.8 μm. STE curve 3.14(a) and the results of an FFT analysis in the angle domain 3.14(b).

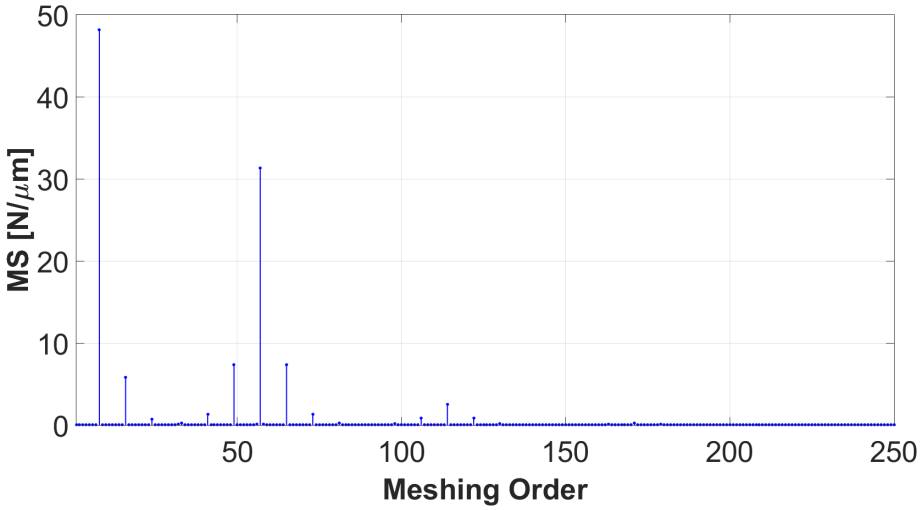

FIGURE 3.15: FFT analysis of the mesh stiffness obtained from STE curves of Figure 3.14.

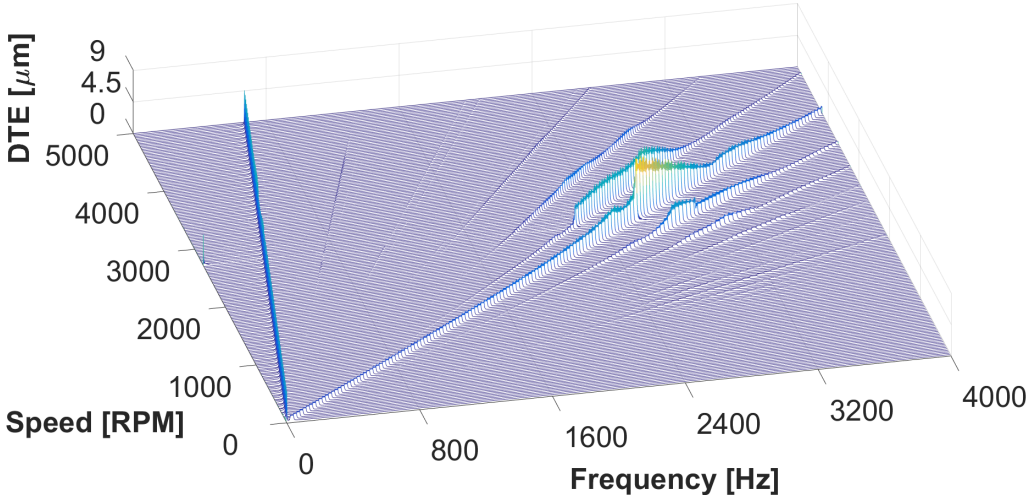

FIGURE 3.16: Waterfall diagram of the DTE of the system obtained using STE curves reported in Figure 3.14.

studies have been analysed, with different lightweight designs: in two cases, an axisymmetric lightweight gear, with reduced blank thickness, engages with a solid gear; in the other cases, weight reduction is achieved in the lightweight gear through holes and slots in the blank achieving the same mass reduction as in the corresponding axisymmetric gear. The STE curves are derived through a series of nonlinear FE simulations, allowing for a detailed description of the impact of gear blank topology on the mesh stiffness. The latter is then used in a lumped parameter formulation for nonlinear dynamic analysis. The simulation results, analysed in both time and frequency domain, show that the dynamic behaviour of the gear pairs with material discontinuities in the web is significantly different from the one of the axisymmetric gear pair. The variability of the average mesh stiffness during gear rotation, in fact, causes additional excitation orders and produces modulation effects in the dynamic response of the transmission analysed in terms of DTE. The frequency and amplitude of these contributions are dependent on the topology of the gear blank and on the harmonic content of the STE, which is well captured by the nonlinear FE simulations. Sideband effects show up in the regions where the meshing order excites the resonance of the system. One of the most interesting phenomena linked to gear dynamics, that is, jumps in the RMS of the DTE due to tooth loss of contact, is significantly affected by blank topology and seems to completely disappear in extremely lightweight design. To provide an insight of the observed phenomena, dynamic simulations with analytically generated STE functions have been performed in order to analyse the effects of the additional STE harmonic component, due to the discontinuities in the gear blanks. The results showed additional amplifications in the RMS curves, due to the modulation effects of the holes on the mesh stiffness.

Chapter 4

Transmission Error and Strain Analysis of Lightweight Gears by using a Hybrid FE-Analytical Gear Contact Model

4.1 Introduction

Geared mechanical transmissions are some of the most common subsystems in many fields of the mechanical industry, from the more established ones, such as heavy equipments, wind turbines and precision machinery to relatively new areas represented by robotics and electric vehicles. Generally in all these applications the transmission is one of the most expensive components and a potential substitution cost or maintenance time can be very high. Taking as reference the wind energy industry according to [105], in a typical wind turbine, the gearbox is recognized to be the component with the second lowest failure rate, but on the other side it is responsible for up to 40% of the total downtime, being the repairing time the longest compared to all the components. The study of gears behaviour, especially for fault prevention and prediction where cracks, pitting, mounting and manufacturing errors cause additional excitations, still involves the attention of the researchers [137], [47] and represents an actual research topic [27], [97] also in condition monitoring applications [111].
Additionally, new and more demanding environmental regulations enforce different design targets focused on the global efficiency of the system in order to reduce greenhouse gas emissions and fuel consumption especially in the automotive and aerospace industries. One of the possible strategies to cope with such constraints is a reduction of the mass of each component of the system. Different approaches to achieve this goal in geared transmissions are currently under research. For instance in [24], the dynamic performance of gear bodies manufactured using composite materials is evaluated. More established approaches to reduce the weight are based on the manufacturing of gears with thin bodies, possibly with holes and slots. These approaches however impact on the dynamic behaviour of the gears [118] increasing the global compliance of the gear pair and generating higher and more complex stress field in sensitive parts of the gear

body. According to [34], excessive load in different regions of the gear causes typical failure modes, such as pitting on the tooth surface or crack propagation on the tooth root. In [56] the importance of the root stress as design parameter is empathised by its inclusion in the constraints of an optimisation strategy for the design of cylindrical involute gears. When lightweight gears are used the complex shape of the gear body adds multiple regions where stress concentrations may occur. The accurate simulation of the meshing process without any limitation on the body shape is therefore fundamental for the evaluation of strength criteria in the gear body and to perform durability analyses in lightweight gears.

Due to the complexity of the gear meshing process, accurate simulation tools are needed to provide the required level of detail. Non linear Finite Element (FE) analyses are able to provide the highest level of accuracy, especially when contact load distribution on the tooth surface is investigated [80]. One of the drawbacks is that the computational time is particularly high, limiting the use of such tools to static analyses or to very short dynamic events at component level. The time required to simulate even short time-domain phenomena of few milliseconds is still prohibitively large with standard FE solutions. In the work of Ziegler and Eberhard [155], FE simulations are used as reference and in one of the case studies reported the time required to simulate 13 impacts between two gears for a total duration of 300 ms is about 194 hours on a standard machine. The reason for the high computational efforts required by FE simulations is in the high number of degrees of freedom required to properly model the contact area. Other approaches different from the full FE discretization are investigated by other authors. In [139] a combination between FE formulation together with an analytical description of the local contact displacement is used to address the problem of simulating the gear under meshing conditions. An extension of the method is used for the analysis of a gear pair [101] and of a planetary gear set [99] under dynamic conditions but this method still has limited applicability for time-domain simulations at system-level. The same approach is used to compare the time-domain strain in external gears [32] and in planetary gear stages [63], but the analysis was not extended to lightweight gears.

Multibody (MB) simulation tools are often used to simulate the behaviour of a complete transmission, under the assumption that the meshing gears can be represented as rigid bodies connected to each other by spring-damper elements. By exploiting the much lower computational cost with respect to FE-based methods, MB approaches allow to simulate longer events. However, accurate results are achievable only if the position-dependent mesh stiffness is properly modelled [71]. Although MB simulation tools are extensively used to investigate the dynamic behaviour of geared transmissions because of the low computational cost, their application in the study of lightweight gear meshing as well as in stress and strain analyses is limited, since the detailed elastic deformation field of the gear body is not available in most of the implementations. Using elastic MB formulations the displacement field is available for the recovery of stress and strain in the components either online during the time integrations or offline in a post-processing

phase [128] with an obvious increase of the simulation time compared to rigid MB simulations. Model order reduction techniques can be used to improve the efficiency of the simulation: in [116] the problem of recovering the stress field in MB gear simulation is analysed using different model reduction techniques.
In this work an elastic MB approach combining FE and analytical representations of the gear stiffness contributions is used to investigate the meshing behaviour of lightweight gears [120] where different blank geometries are designed to reduce the overall mass of the transmission. The advanced elastic MB formulation provides an higher computational efficiency when compared to state-of-the-art elastic MB approaches, allowing at the same time to precisely describe the gear mesh stiffness and to recover the strain field in the gear body of lightweight gears. Section 4.2 describes the hybrid FE-analytical gear contact model used to enable a time-varying representation of the mesh stiffness in the MB simulation environment. The methodology for stress recovery and strain field estimation is illustrated in section 4.3. Several experiments have been conducted in order to evaluate the robustness of the proposed technique. This methodology has been validated using the data obtained from different experimental campaigns, using the in-house gear test rig. In particular the transmission error and stress values have been acquired and compared to the corresponding simulated signals. Two gear sets with different body geometries have been analysed. The detailed analysis of the results is presented in section 4.4.

4.2 Gear Contact Model

This chapter investigates the behaviour of two gear pairs, in which a standard cylindrical gear engages with a ligthweight gear using an elastic MB formulation based on the combination of the FE method and an analytical representation. The main motivation behind the application of the methodology is a reduction of the computational requirements typical of the non linear FE approach used in gear simulations, while ensuring an accurate description of the gear meshing process that is verified by comparing the simulation results with experimental measurements.
The approach used in this work is based on a penalty formulation of the contact problem [148], where in an initial contact detection phase, the unphysical penetration between the meshing teeth is computed according to the relative position of the gears and to the actual working conditions. In a second step the contact loads are computed based on the penetration between the meshing teeth and a contact stiffness. The potential teeth in contact are searched exploiting the kinematics equations of meshing defined by the tooth geometry and spatial position of the gear [131] [132]. The assumption behind the contact detection phase is that the deformation of the gear profile remains small, so that the contact points are considered to lie on a rigid involute profile in the direction defined by the normal to the unmodified tooth flank. No a-priori assumptions are made on the global displacement of the gears in the reference frame, while the deformation under load of different components, such as flexible shafts and cases, bushings and bearings, may change

the relative position of the gears with respect to the initial one.
The above assumption does not represent a limit for most of the industrial applications where metallic gears are used, with a tooth profile that is nearly the theoretical one. When gears with a deviation from the perfect involute geometry (i.e. gears with micro-modifications) are analysed, the amount of deviation is generally very slight and the geometrical definition of the profile normals is only marginally affected by the modifications, so that the difference between the actual and the theoretical position of the normal direction to the tooth surface is negligible. The changes in the contact point position due to the micro-modifications, instead, are taken into account. These assumptions may lose their applicability when extremely low stiffness materials are used for the gears (e.g. rubber-like materials), but this does not represent the focus of this work.
The penetration between the meshing teeth and the relative velocities of the tooth, which represent the output of the contact detection phase, are computed for each active tooth pair (i.e. meshing teeth) using a slicing approach, where the teeth are divided into multiple slices along the width, under the assumption that these quantities remain constant along the width of each segment. The slicing approach used in the contact detection phase improves the accuracy of the solution and is particularly relevant in the case of misaligned gears or profile modifications along the tooth width, where the load distribution along the tooth width may be non-uniform.
As result of the contact detection phase a set of penetration values between the tooth profiles for each segment is available and can be used as input for the subsequent force calculation phase. The tooth stiffness computation reflects the teeth slicing approach where a stiffness vector is computed for each segment of the engaged teeth of the two meshing gears, i.e. gear *1* and gear *2*. The stiffness vector has a dimension which depends on the number of the considered slices, being the coupling terms between the slices included in the formulation.
The mathematical description of the force computation phase is provided by equations 4.1, 4.2 and 4.3 in the form of a non-linear complementarity problem (NLCP) [91], which is solved at each time step of the time domain simulation for each active slice:

$$\begin{aligned} \delta^{12} - f(\mathbf{F_n}^{12}, geom_{12}, E_{12}, \nu_{12}) + \\ +[\boldsymbol{C}^1(geom_1, E_1, \nu_1 + \boldsymbol{C}^2(geom_2, E_2, \nu_2)]\ \mathbf{F_n}^{12} = \\ = \mathbf{g}(\mathbf{F_n}^{12}, geom_{12}, E_{12}, \nu_{12}) \geqslant 0 \end{aligned} \tag{4.1}$$

$$\mathbf{F_n}^{12} \geqslant 0 \tag{4.2}$$

$$\mathbf{g}(\mathbf{F_n}^{12}, geom_{12}, E_{12}, \nu_{12})^{\mathrm{T}} \cdot \mathbf{F_n}^{12} = 0 \tag{4.3}$$

where:

- δ^{12} is the vector of instantaneous penetrations on each active slice for each of the teeth that are simultaneously in contact at a certain time instant. The penetration vector is corrected for the contribution due to the micro geometry in the normal direction;
- $\mathbf{F_n}^{12}$ is the vector of unknown contact forces in the normal direction with respect to the involute profile;
- $\mathbf{f}(\mathbf{F_n}^{12}, geom_{12}, E_{12}, \nu_{12})$ is a vector of non-linear functions of the normal contact forces that accounts for the non-linear Hertzian contact compliance effects. The terms $geom_{12}, E_{12}, \nu_{12}$ represent known input parameters related to the gears geometry and material properties;
- $\boldsymbol{C}^i(geom_{\mathrm{i}}, E_{\mathrm{i}}, \nu_{\mathrm{i}})$ is a full matrix that includes the FE based compliance for gear i;
- $\mathbf{g}(\mathbf{F_n}^{12}, geom_{12}, E_{12}, \nu_{12})$ is the penetration.

From the structure of equation 4.1, it can be noted that the total displacement field of each gear is computed starting from a decomposition of the stiffness data into two contributions, which is the main assumption on which the approach is based. The description of the main concept of the method can be found in [134] where the idea of the decomposition of the gear meshing stiffness is developed, but its application is limited to static analyses. An extension of the method to the study of the dynamic behaviour of helical gear pairs can be found in the work of Andersson [9]. In [22] the approach is exploited in a flexible MB formulation showing an improvement of the computational performances compared to state-of-the-art flexible MB approaches, without showing a relevant reduction in the accuracy. A schematic representation of the decomposition of the gear displacement field is shown in figure 4.1:

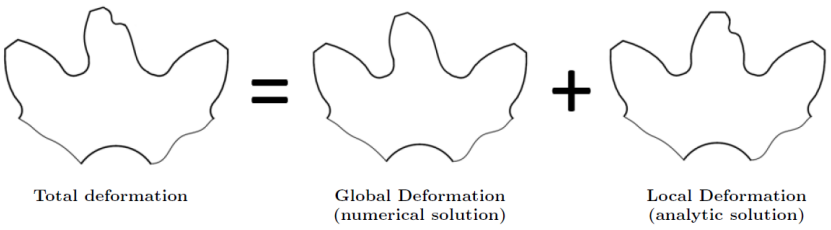

FIGURE 4.1: Decomposition of the gear displacement field in meshing conditions, [22]

Therefore the total deformation of the gear resulting from the meshing process is considered as the superposition of two different contributions:

- **A global linear deformation** caused by the tooth bending and shear as well as by complex effects due to the gear body geometry and coupling between different teeth (e.g. when one tooth is loaded, also adjacent teeth will deform.
- **A local non-linear deformation** represented by the terms caused by locally non-linear Hertzian-like effects;

The first contribution representing the global deformation, is the response of the gear to tooth bending and shear loads originated during the meshing, coupled with the complex effects due to the topology of the gear body and with the coupling between different teeth. The displacement field of gear i (with i=1,2,n), considered as linear, can be modelled using a linear FE approach. The resulting stiffness matrix ${\boldsymbol{K}_{FE}}^{i}$ is build with a relatively coarse mesh compared to the one used in the contact analyses with non-linear FE formulations. This is possible since the non-linear contact phenomena are not taken into account while computing the linear component of the displacement field.
The geometrical proprieties of the problem of two meshing gears allow to exploit the symmetry in order to further increase the computational efficiency of the problem. When two gears engage only a few teeth pairs are loaded simultaneously, while the others are unloaded. This means that a small set of nodes are loaded in the FE stiffness matrix of the gear $\boldsymbol{K}_{\mathrm{FE}} \in \mathbb{R}^{n_{FE} \times n_{FE}}$ (where n_{FE} is the number of degrees of freedom of the FE model of the gear), while all the other nodes belonging to the un-engaged teeth as well as to the gear body are unloaded. The dimension of the problem can be therefore reduced by the use of a reduction space to condense the information contained in the FE stiffness matrix, according to equation 4.4, resulting in a reduced stiffness matrix ${\boldsymbol{K}_{red}}^{i} \in \mathbb{R}^{n_C \times n_C}$:

$$ {\boldsymbol{K}_{red}}^{i} = \boldsymbol{\Psi}^{\mathrm{i}\mathrm{T}} {\boldsymbol{K}_{\mathrm{FE}}}^{\mathrm{i}} \boldsymbol{\Psi}^{\mathrm{i}} \tag{4.4} $$

In this work, the used reduction space $\boldsymbol{\Psi}^{\mathrm{i}} \in \mathbb{R}^{n_{FE} \times n_C}$, is obtained by the concatenation of n_C deformation patterns, each of which is computed based on a procedure similar to the one detailed in [134]. Each mode is the result of a computation for each node belonging to a potential contacting surface, while the reduction space is formed concatenating each of the solutions. As previously explained, the reduced stiffness matrix ${\boldsymbol{K}_{red}}^{i}$ has to model only the global deformation field of the gears. Each of the static modes in the reduction space is therefore computed according to the scheme represented in figure 4.2, where the first two images on the right-side refer to the FE-based calculations. In the same figure, the rightmost image represents the analytical non-linear contact deformation.
The global deformation field of the gear computed using the FE method is performed in two computational steps 4.2. In the first step, the actual static deformation of the gear after the application of a point load in the normal direction to the tooth surface is calculated. This step however includes also the unphysical local effects due to the point load application on the FE mesh. The latter contribution must be removed since it partially

FIGURE 4.2: Computational steps to represent gear total deformation [22].

contains a local effect that, in the proposed approach, is modelled using the analytical representation instead. The effects of the local Hertzian contribution are not included in the global deformation of the gears and hence must be removed. The local effect can be removed by superimposing an additional deformation field obtained applying a point load in the opposite direction on the loaded tooth.
It is noteworthy that the FE formulation allows to represent the global deformation of the gears implicitly considering all the different combinations of tooth and body shapes, including the detailed effects arising from the holes and thinned bodies that are typical in lightweight gears. The formulation used exploits these consideration in order to compute the contact forces in a numerically efficient manner. The numerical results obtained using this methodology are compared with the experimental ones in section 4.4

4.3 Stress recovery

The problem of dynamic stress recovery in gear simulations has already been investigated by other authors using different techniques. In order to obtain a detailed description of the strain or stress fields in the gears under meshing conditions the displacement field in the elastic gear body has to be available. Different formulations are used in literature to model the compliance of gear, making the displacement field of the gear bodies available. In the work of Cooley [29] an analytical representation of the gear body flexibility is used to analyse the gyroscopic effects in the frequency response of high-speed transmissions where the gear body compliance is fundamental in determining its dynamic behaviour. The formulation used is based on the analytical elastic equation of curved beams and rings. However analytical representations have limited applicability to specific applications and provide poor accuracy when gears with complex body shapes are considered, which is the case of gears with a lightweight design. An FE discretization of the gears enables a high level of accuracy of the computed displacement field without any assumption on the geometry of the gear body, but on the other hand the size of the problem is considerably increased.
In the study of [156] a modal reduced model is used, allowing to drastically reduce the computational time compared to non-linear transient FE simulations. In another work [155] the approach is extended to a multibody environment using a floating frame of reference formulation to perform impact analysis on very compliant gear with a lightweight design. The results in terms of strains are also validated with experimental results. The analyses however are limited to impact simulations between a gear and another body

with a total duration of a few milliseconds, while longer events, covering several meshing cycles are not analysed.
The problem of reducing the size of the model is also faced in [126] using a different approach based on a parametric model order reduction scheme. In that work, numerical results are used as reference for the validation of the stress field. The application of this scheme to elastic MB simulation of gear meshing can be found in [16] where a good agreement with the FE results, taken as reference, is shown. The analysis however is still limited to short-time events, and moreover the effects of a lightweight design on the meshing behaviour are not analysed.
The transient elastic MB analysis of lightweight meshing gears in relatively long events (compared to impact analysis) is addressed in this work. The simulation results, including the strain analysis are validated using experimental data.
For this purpose, the strain value at a specific location $\boldsymbol{r}(x,y,z)$ and at a given simulation time t can be computed in a post processing phase once the displacement field $\mathbf{d}^i(\mathbf{r},t) \in \mathbb{R}^{n_{FE}\times 1}$ of gear i is available, using the formulation of eq. 4.5.

$$\epsilon(\mathbf{r},t) = \boldsymbol{B}\ \boldsymbol{dn}^i(\mathbf{r},t) = \begin{bmatrix} \frac{\partial}{\partial x} & 0 & 0 \\ 0 & \frac{\partial}{\partial y} & 0 \\ 0 & 0 & \frac{\partial}{\partial z} \\ \frac{\partial}{\partial y} & \frac{\partial}{\partial x} & 0 \\ \frac{\partial}{\partial z} & 0 & \frac{\partial}{\partial x} \\ 0 & \frac{\partial}{\partial z} & \frac{\partial}{\partial y} \end{bmatrix} \boldsymbol{dn}^i(\mathbf{r},t) \tag{4.5}$$

Where the matrix $\boldsymbol{dn}^i(\mathbf{r},t) \in \mathbb{R}^{3\times n_{nodeFE}}$, being n_{nodeFE} the number of nodes in the FE model, is the matrix form of the nodal displacements contained in $\mathbf{d}^i(\mathbf{r},t)$. Different scenarios are open when the displacement field $\mathbf{d}^i(\mathbf{r},t)$ in the gear body i is recovered from the MB simulation and its mathematical description is related to the elastic MB formulation used to solve the gear meshing process. In this chapter two different techniques, corresponding to two different representations of the displacement field are used to recover the strain field in the post-processing phase.

1. The first method is based on a model order reduction technique used to represent the gear bulk compliance. As result of the simulation a set of modal participation factors are available, from which it is possible to reconstruct the displacement field for any suitable location in the gear $\boldsymbol{r}$, according to equation 4.6.

$$\mathbf{d}^i(\mathbf{r},t) = \mathbf{\Psi}^i(\mathbf{r})\ \mathbf{q}^i(t) \tag{4.6}$$

   Where the matrix $\mathbf{\Psi}^i(\mathbf{r})$ is the column matrix representing the reduction space of eq.

4.4 formed by concatenating the n_C static modes.
It is important to note that the modal participation factors sets $\mathbf{q^i}(t) \in \mathbb{R}^{n_C \times 1}$ of gear i are functions of the simulation time and each of them is the output of a single time step of the multibody simulation, therefore the displacement computation has to be repeated for each time frame of the simulation.

2. The second approach is based on the computation of the displacement field directly from the contact forces computed during the MB simulation according to eq. 4.7, assuming that the full FE stiffness matrix of the gear $\boldsymbol{K}_{\mathrm{FE}}$ is available together with the vectors containing all the meshing forces $\mathbf{F}_e^i \in \mathbb{R}^{3\times 1}$ for gear i and all the e slices. The results given by this method are similar to the ones of the first approach. This is due to the fact that each force $\mathbf{F}_e^i$ is an internal force computed during the time-domain simulation that already includes the inertial and damping contributions. The dynamic effects due to the body flexibility are not taken into account in this work.

$$\mathbf{d}^i(\mathbf{r}, t) = {\boldsymbol{K}_{FE}^i}^{-1} \mathbf{F}_{FE}^i(\mathbf{r}, t) \tag{4.7}$$

where The contact loads computed during the simulation can not be guaranteed to be located exactly in the model nodes location. The vector of nodal loads $\mathbf{F}_{FE}^i(\mathbf{r}, t) \in \mathbb{R}^{n_{FE}\times 1}$ can be retrieved by assembly all the element nodal load vectors $\mathbf{r}_e^i \in \mathbb{R}^{(node_{el}\times 3)\times 1}$ for each element e of the *i-th* gear. In this context $node_{el}$ represents the number of nodes for each element, depending on the chosen formulation. Each vector $\mathbf{r}_e^i$ can be computed from the three-dimensional meshing loads $\mathbf{F}_e^i$ acting on the tooth surfaces exploiting the relation in eq. 4.8 [85], where $\boldsymbol{N}_e^i$ is the shape functions matrix of the *e-th* element computed at the application point of the *e-th* meshing force $\mathbf{F}_e^i$ acting on the surface of the corresponding element of gear i.

$$\mathbf{r}_e^i = {\boldsymbol{N}_e^i}^T \mathbf{F}_e^i \qquad \text{where } \boldsymbol{N}_e^i \in \mathbb{R}^{3\times(node_{el}\times 3)} \tag{4.8}$$

Each shape functions depends on the natural coordinates of the meshing force application point $\mathbf{x}_e^i \in \mathbb{R}^{3\times 1}$ on the external face of the element. The shape function matrix is therefore a non-linear function of the natural coordinates. Once the application point of the meshing force $\mathbf{F}_e^i$ in the global reference frame at a given timestep is known from the time-domain simulation, its value can be used to find the shape functions contained in $\boldsymbol{N}_e^i$ by solving equations 4.9:

$$\mathbf{x}_e^i - \mathbf{P}_e^i = 0 \qquad \mathbf{P}_e^i = \boldsymbol{N}_e^i \, \mathbf{x}_{ne}^i \tag{4.9}$$

Where $\mathbf{P}_e^i \in \mathbb{R}^{3\times1}$ is the position of the *e-th* contact point of gear *i* defined using the isoparametric formulation. The vector $\mathbf{x}_{ne}^i \in \mathbb{R}^{(node_{el}\times3)\times1}$ represents the spatial coordinates of the *e-th* element nodes in the deformed state defined in the same reference frame as $\mathbf{x}_e^i$.

4.4 Experimental Validation

The numerical results obtained by applying the methodology presented in this work to the analysis of lightweight gears have been validated using multiple experimental results in terms of strain at the tooth root as well as of TE, which is an important quantity when the performance of a geared transmission are considered.
The importance of the TE arises from its consideration as one of the main excitation sources in a system where meshing gears are present [123]. It can be defined as the difference between the actual position of the driven gear and the position it would occupy if the gears were infinitely rigid and the tooth profiles perfectly conjugate.
Clearly a relative displacement is present if two meshing gears are not perfectly rigid or if their flanks are not perfectly conjugate (e.g. with ideal involute profiles). This relative displacement overlaps the pure kinematical one, and its amplitude is determined by different phenomena:

1. The geometrical contribution is present when two micro-modified gears are meshing. Their relative rotation is not anymore the pure kinematical motion resulting from a couple of perfect involute gears. The micro modifications result in a geometrical effect that can be determined based on the teeth surface geometry.

2. The tooth and gear body contribution arises from the deformations due to the applied load and is highly dependent on the geometry of the gear teeth, and gear body and the actual working conditions of the gears.

3. The local non-linear contact deformation is a contribution arising from the contacting tooth surfaces. The contact pressure distribution generates a Hertzian type displacement field, which is non-linear with the applied load. It is mostly independent on the gear body geometry, but depends on tooth shape and material;

In conventional, non-lightweight gears, the TE curves are typically dominated by the harmonic content at the meshing frequency originated mainly from the gear deformation in the tooth region. One of the effects of gear lightweighting is the occurrence of additional harmonic components at lower frequencies, originating from the nonuniform distribution of material along the gear blank caused by the holes, which generates an additional nonuniform deformation in the gear body. In this work the TE is computed according to the following expression 3.1 where θ_{G} and θ_{P} represent the rotation of the gear and of the pinion, respectively, while r_{bG} and r_{bP} are their base radii. Therefore the angular relative displacement of the gears is converted into a linear motion along the line of action.

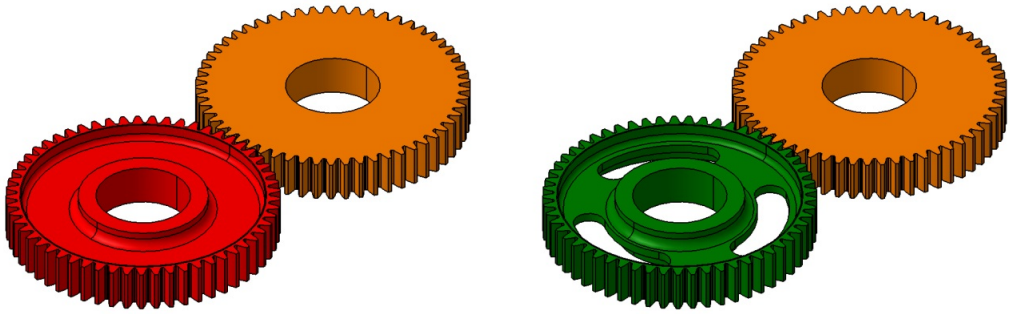

(a) (b)

FIGURE 4.3: CAD representation of the two gear pairs analysed.
Reproduced from [119]

4.4.1 Numerical models and test-cases

In this chapter, three spur gears are tested arranged into two gear pairs, each of them consisting of one standard gear and one gear in which a lightweight design is machined. The standard gear presents also a profile modification of 10 microns. The latter is intentionally applied on the gear with the two goals of making the meshing process smoother by reducing the edge contact effects at higher loads and also to validate the capabilities of the methodology to properly model the geometrical contribution of tooth micro-modifications to the TE. The gear pairs used in this chapter have already been described in Chapter 3, and the geometrical specifications and the micro-modifications of the gears are reported here and summarized in Table 4.1 for convenience.

Parameter	**Units**	**Gear 1**	**Gear 2**	**Gear 3**
Tooth number	[-]	57	57	57
Pressure angle	[deg]	20	20	20
Module	[mm]	2.6	2.6	2.6
Face width	[mm]	23	23	23
Micromodifications	[μm]	10 (profile crowning)	-	-
Lightweighting	[-]	-	thin rimmed	thin rimmed & 3 slots

TABLE 4.1: Main design parameters of the analysed gears

A CAD representation of the analysed gear pairs is reported in figure 4.3, where the different body topology of the gears can be observed. In the gear pair of figure 4.3(a) gear 1 and gear 2 are meshing. Gear 2 presents a lightweight design in which the mass reduction is obtained by an axis symmetrical material removal, resulting in a thin-rimmed gear. In this case, the TE is dominated by the tooth bending under load and by the high body compliance of the gear. A second case-study, consisting of the gear pair B represented in

figure 4.3(b), is also analysed. In such a case, the solid gear 1 engages with gear 3. The latter has an extremely lightweight design, achieved by three slots machined in the thin body of the gear.

4.4.2 Experimental setup

The experimental activities were performed using the high precision gear testrig [96], that is shown in Figure 4.4.2. The test-rig allows to measure different physical quantities in meshing gears, in both static and dynamic range, for different working conditions in terms of applied load, relative displacements of the gears and shaft compliance. In this work the focus is on the TE and on the strain levels measured in different location of the gear under multiple load conditions.

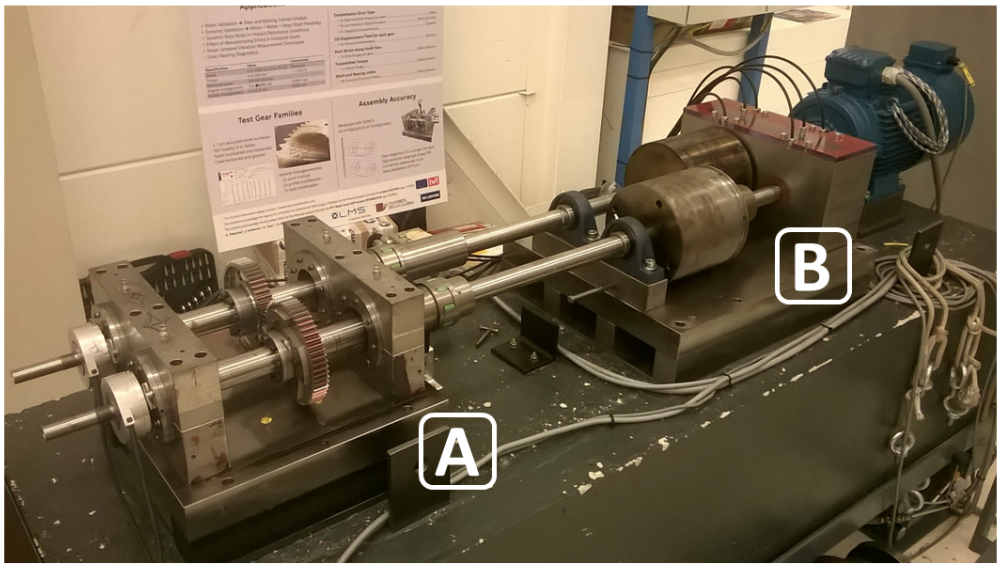

FIGURE 4.4: A picture of the test rig. It is possible to distinguish the test side on the left (A), where the test gears are placed. The reaction side is located on the right (B). The safety protection were removed in order to display the internal components. Reproduced from [119]

Test Rig Design

The test-rig has a power circulation arrangement, in which two main subsystems can be identified: the test side and the reaction side. These parts are dynamically separated from each other by using flexible couplings. The tested gears are mounted at the test side, while the other gear pair is not intended to be instrumented and its utility lies in reacting the applied torque on test gears. One of the advantages of this arrangement is that the torque required to spin the shaft is relatively low, being just the torque needed to overcome the friction forces acting between the meshing teeth and inside the bearings. This simplifies the application of smooth speed and constant torque pre-loads and facilitates

the measurement of rotational and linear vibrations in the system.
The testrig described here allows to impose parallel and angular misalignments exploiting the five degrees of freedom available for the relative positioning of the gears. The possibility to adjust the shaft compliance allows to set the ration between the mesh and the shaft stiffnesses, resulting in a different response of the testrig. This can be appreciated more in the dynamic range, where depending on whatever is the dominant stiffness, the resulting dynamic behaviour differs. All the measurable quantities can be measured in a range of rotating speed and for a discrete range of applied torque, according to the main features reported in Table 4.2.

Parameter	Range	Uncertainty
Speed	0 to 4500 rpm (0 to 75 Hz)	Measured
Torque	0 to 500 Nm	$\pm$ 0.05 %
Angular misalignment	0 to 2 mrad	0.1 mrad
Parallel misalignment	0 to 0.3 mm	0.020 mm

TABLE 4.2: Test rig specifications

The main layout of the test rig sees a concrete base which fulfils the main functions of providing a reliable aligned position for the test and the reaction sides and to isolate the system from the vibrations coming from the external environment. The damping proprieties of the concrete help, moreover, to avoid any propagation of the vibration from the reaction side to the test side.
A proper lubrication is ensured by a temperature-controlled system that provide the required oil to the gears and to the bearings. A groove in the external race of the bearings fed by dedicated oil lines allows to the oil to lubricate the rolling elements. Both the test and the reaction gears are lubricated by dedicated nozzles which are placed in the correspondence of the meshing teeth. The closed-loop layout of the oil circuit is ensured by an enclosure that collect the oil through the reservoir. Safety grids (not shown in the picture) cover the rotating elements which are potentially dangerous.
The rotation is imposed by a 9 kW asynchronous motor driven by a frequency inverter, which controls the set speed. The torque is inserted in the system using different precalibrated weights and an arm. The procedure to apply the preload consists in fixing a flywheel, releasing the clutch, fitting the torque arm and by inserting the selecting calibrated weights a twist in the shaft is imposed which is equivalent to the desired torque preload.
The maximum preload allowed is 500 Nm, which generate a safety factor of 4 to the yelding point in the most critical regions, computed according to the von Mises criterion. The chosen material is a ductile medium-carbon C45 steel (360 MPa yield stress) for the supporting structures, while the shafts are made out of a low-alloy 1.2312 steel (820 MPa yield stress).
The chosen bearings are reported in Figure 4.5, and the criterion behind the choice was to

provide the highest stiffness while still ensuring infinite service life when the maximum preload is applied.

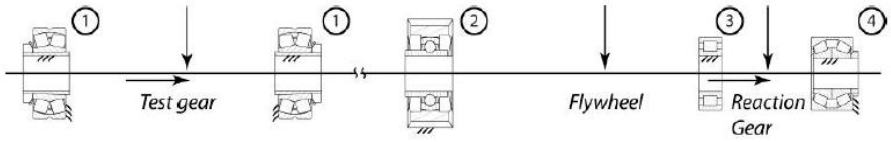

FIGURE 4.5: Bearings arrangement for one shaft branch of the test rig and average bearing stiffness in the loading range. 1. High-precision spherical roller bearing (1x109 N/m); 2. Y-bearing unit; 3. Wide-face single-row cylindrical roller bearing (6x108 N/m); 4. Double-row tapered roller bearing (1x109 N/m radial, 3x108 N/m axial). Reproduced from [1]

The configuration consists in precision spherical roller bearings to support the shafts on the test side. A conical adapter sleeve allows to adjust the radial preload of the bearing over the shaft by varying the radial interference. The coupling between the external race and the supporting structure (i.e. bearing caps) is chosen to have light interference to achieve a good accuracy when the bearing caps are turned, to set the relative position of the gears. The reaction side including the flywheels and the helical reaction gears uses Y-bearing units and wide-face single-row cylindrical roller bearings. The first are selected because they do not require an accurate location of the supporting structure on the base, since the supporting structure and the bearing itself is built in a single unit. The cylindrical roller bearings are chosen to contrast the radial loads generated by the reaction gears and by the flywheels weight. The axial trust generated by the helical reaction gears impose, instead, the choice of double-row tapered roller bearings in a locating configuration. The location is created by machining a shoulder in the bearing housing and by inserting laminated shim on the opposite side through the base .
One of the main goals of the overall design is to isolate the test side from the vibration coming from the reaction side. This is achieved by lowering the natural frequency of the modes involving the mesh deflection in the reaction side, by moving them in a frequency range different from the one measured for the test gears. The practical implementations are the increased rotary inertia guaranteed by the flywheels and the low torsional stiffness of the shaft and of the couplings elements.
Low values of the torsional stiffness of the shafts have also the advantage of making the system less sensitive to the rotational vibration caused by the transmission error. An imposed preload of 500 Nm corresponds to a twist angle of 1.5°, and the vibrations originated from the teeth deflection do not produce significant variation in the preload value. The compliant elastomeric couplings further isolate the two sides from the non-torsional loads generated when the shafts are subjected to bending loads, the eccentricity limit is set up to 0.28 mm and angular misalignment up to 35 mrad.
In a work by Palermo [1] an analytical 4 DOF model of the test rig is built to perform

a qualitative dynamic analysis, where only the rotation of all the gears are included. A reproduction of the model is reported in Figure 4.6.

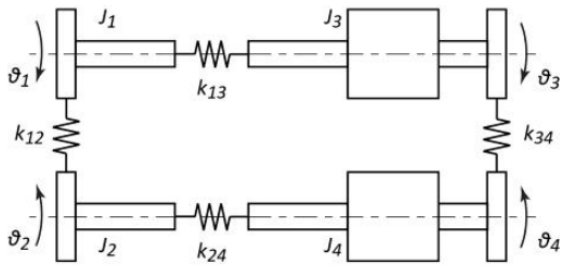

FIGURE 4.6: Illustration of the 4-DOF rotational model of the test rig. Reproduced from [1]

The term k_{12} represents the equivalent stiffness corresponding to the mesh stiffness and the shaft torsional and bending stiffness. The value of the mesh stiffness chosen in the work is equal to $1.6 * 10^6 Nm/rad$. The value of the mesh stiffness for the reaction gears indicated by the term k_{34} is chosen to be equal to $1.8 * 10^6 Nm/rad$. The torsional stiffness of the elastic couplings are indicated with the terms k_{13} and k_{24}. The rotary inertia of the gears, the shaft and the flywheel are lumped in the four inertia moments expressed by the constant J_i. It can be noticed that the computed inertia moments for the test side equal respectively to $J_1 = 0.0218 kg \cdot m^2$ and to $J_2 = 0.0118 kg \cdot m^2$ are one order of magnitude lower than the ones computed for the shafts of the reaction side, equal to $J_3 = J_4 = 0.2 kg \cdot m^2$. In Figure 4.7 the obtained mode shapes and natural frequencies for the analysed model are reported.

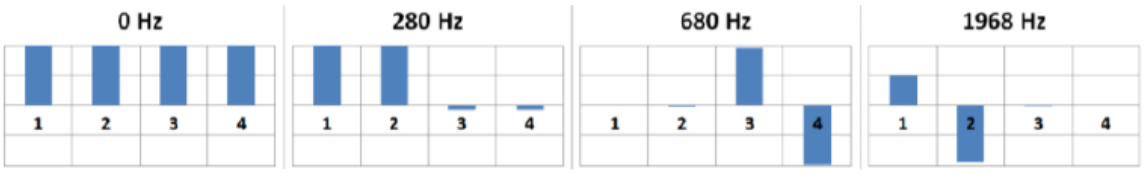

FIGURE 4.7: Histogram representation of mode shapes for the 4-DOF rotational model of the test rig. Reproduced from [1]

By its observation it is evident that the first 0 Hz mode is related to the unconstrained rotational DOF of the model and does not involve any tooth deformation. A second mode corresponds to a natural frequency of 280 Hz and involves an in-phase rotation of the test side and of the reaction side as well. This mode therefore does not imply a relative motion of the gears meaning that the teeth deflection is only marginally excited, while the most of the deformation is carried out by the elastic couplings. The mode at 680 Hz mainly involves a out-of-phase motion of the reaction gears characterized by a deflection of the meshing teeth. This is therefore a mode shape that is excited by the

fluctuations present in the TE of the reaction gears. The test gears on the other side see a very limited motion corresponding to 3% of the modal amplitude of the reaction gears. The highest frequency mode occurs at 1968 Hz and is similar to the one at 680 Hz but this time the reaction gears are marginally involved since the amplitude corresponds only to the 0.2% of the test gears modal amplitude. The third and the fourth modes are the ones corresponding to a resonance of the test gear pair and of the reaction gear pair respectively, where the dynamic behaviour is mainly condensed. For these two modes a good decoupling between the motion of the test side and of the reaction side is highlined by the low percentage of the modal amplitude of the reaction side when the test side is mainly involved and vice-versa.
In order to better estimate the percentage of the meshing force generated at the reaction side which is transmitted to the test side, a forced response analysis was performed. The input in the model was a variable contact force, whose amplitude was chosen to be the double of the estimated one, while the output parameter was chosen to be the transmission error at the test side. The modal damping ration was set to 5% according to the typical values.

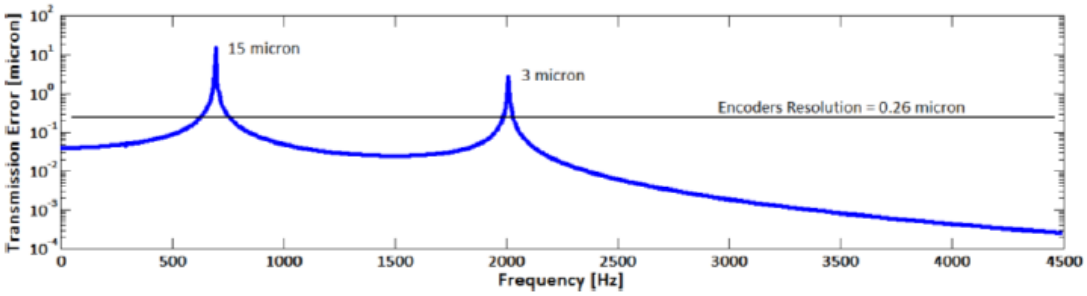

FIGURE 4.8: Forced-response Transmission Error for the test gear pair when exciting the reaction gears with twice the maximum expected dynamic contact force. Reproduced from [1]

The results reported in Figure 4.8 confirm that the excitation coming from the reaction side is higher than the encoders accuracy only in correspondence of the reaction gears resonance, which should be avoided.

During the tests performed in this work the gears were rotated at a low rotational speed of about 10 rpm, in order to properly measure the static contribution to the mesh stiffness fluctuation to the TE.
Due to the small amplitude of the quantities measured in the campaign, the gears were manufactured with tight tolerances and measured tooth by tooth in the profile and lead directions. Tooth surfaces have been hardened and precision ground to ISO quality 3

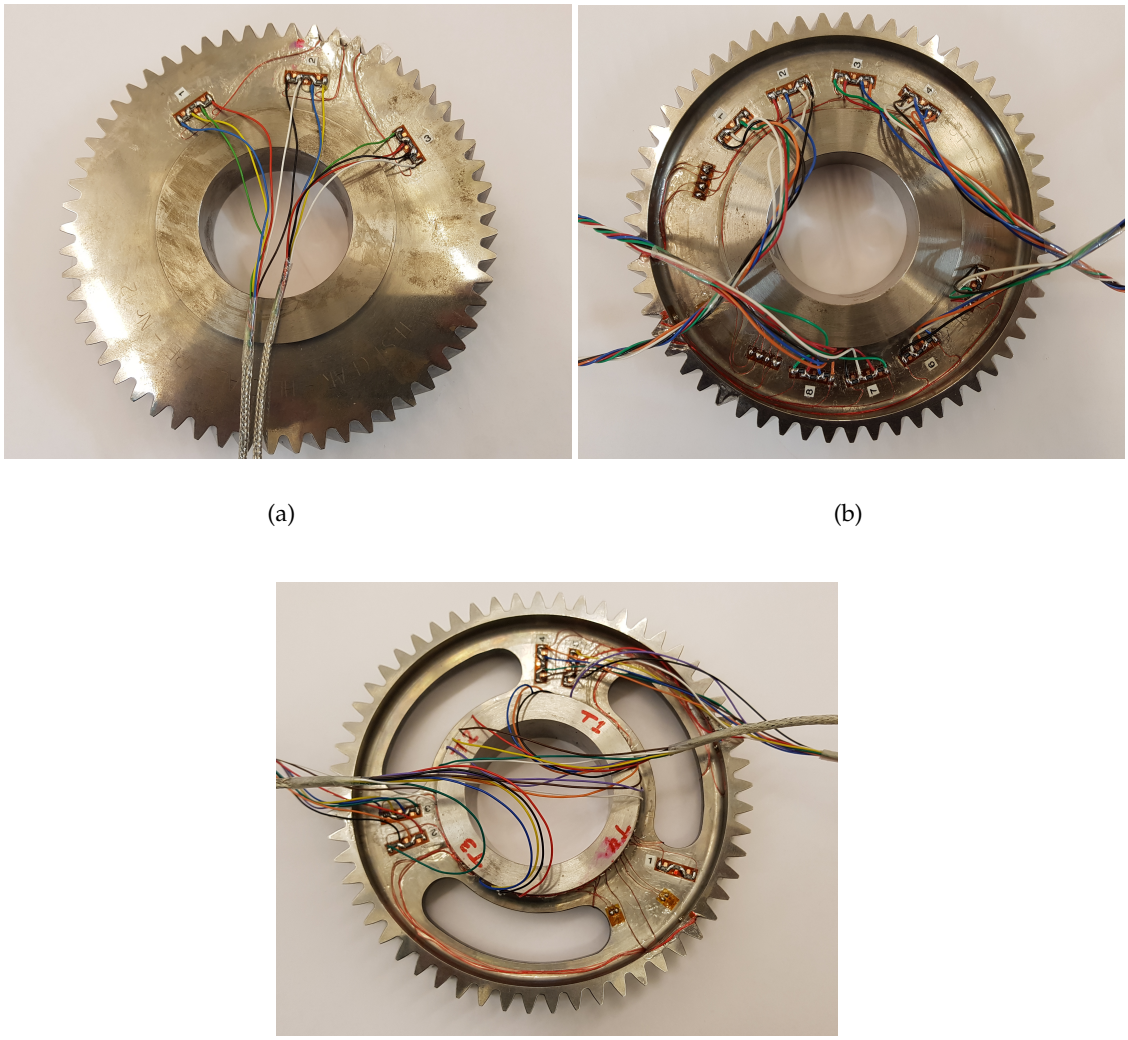

(a) (b)

(c)

FIGURE 4.9: Picture of the gears used in the experimental campaign.
Reproduced from [119]

(equivalent to AGMA 15). The relatively uncommon geometrical parameters of the gears were chosen in order to decrease the tooth stiffness, as to emphasize the signal-to-noise ratio of the measured TE and of strain values. The resulting teeth geometry allows also the mounting of strain gauges at the tooth root. A figure of the gears used in the experimental campaign is shown in 4.9, where it is possible to notice the different lightweight designs of the gear body.

Test Rig Instrumentation

The TE of the test gear pair is computed as the difference between the measured angle of the two gears, using two digital incremental encoders. The used encoders are Heidenhain ERN 120 with 5000 ppr. Each of the encoders is mounted directly on the corresponding test shaft, allowing in this way to reach a high level of accuracy in the angle

measurements. High levels of accuracy are reached also thanks the small radial run-out between the the encoder location and the supporting bearings, equal to $10\mu m$. The selected encoders are also equipped with high precision radial bearings that allow a perfect alignment between the stator and rotor units. The strength levels inside the gears at specific locations can be evaluated by measuring the strain fields. Strain gauges in different position on the two gears in the test gear pair are applied. The selected strain gauges for the tooth root measurements are Vishay Micro-Measurement EA-06-031PJ-120. The are arranged in strip gauges, where each strip is arranged in a pattern of 10 micro strain gauges aligned on the same line as can be seen in Figure 4.10 and in Figure 4.11.

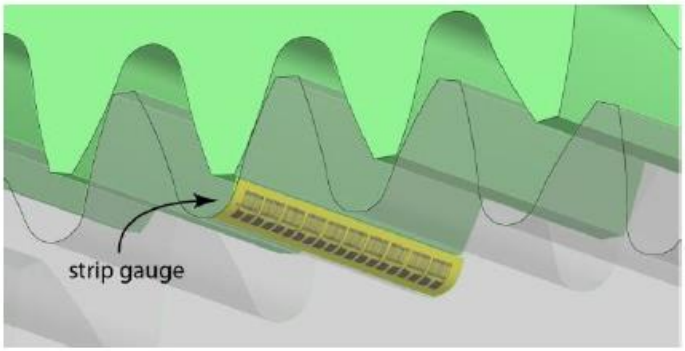

FIGURE 4.10: Strip gauge positioning at the root of a test gear tooth.
Reproduced from [1]

Each strain gauge in the strip has dimensions equal to 0.79 mm by 1.78 mm. The small area of the strain gauges is required due to the step strain gradient in the tooth root area. As the strain gauges are located on the rotating components, a slip-ring is necessary to transfer the measured strain signals to the data acquisition device. Two models are selected depending on the shaft they are mounted on: a 12-channels HBM SK-12 and a 20-channels Michigan Scientific SR-20. According to the manufacturer specifications the resistance fluctuation are lower than 0.002 Ω and 0.1 Ω respectively. The different channel number of the two slip rings is chosen depending the gear on which it is mounted. The standard design gear dos not require multiple measuring locations due to it angular symmetry, while multiple locations are analysed on the lightweight gears.
Every strain gauge has been connected to an independent full bridge circuit, also attached to the gear body. Preliminary experimental results showed that the signal-to-noise ratio of the measured strain signals are improved in comparison to the case where quarter bridge is applied. The slip rings mounted on both rotating shafts allow to accurately measure the dynamic strain signals in different speed conditions.

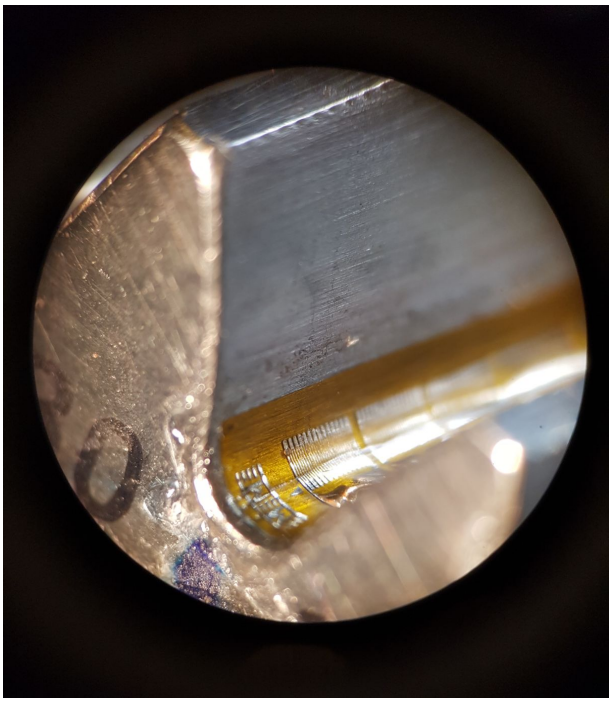

FIGURE 4.11: Detail of one of the strain gauges applied on the toot root. Ten different strain gauges are present on a single strip. Reproduced from [119]

The entire sensor data is acquired using a Simcenter SCADAS frontend, allowing the simultaneous measurements of multiple sensor data (strain, angles, etc.). In a post processing phase, the raw experimental time-data is converted to angle and order domains.

4.4.3 Transmission Error Validation

In this section the results in terms of TE are reported for both the analysed gear pairs. The comparison between the measured and the simulated transmission error for gear pair A is shown in figure 4.12, where the different curves are reported in angle domain to remove the effect of speed fluctuations intrinsically present in the experimental data sets. The experiments were conducted for different torque levels, ranging from 50 to 300Nm, while the rotational speed was kept low at around 10 rpm in order to exclude any dynamic effects from this validation process. Due to the low rotational speed, a relatively high friction coefficient equal to 0.3 was chosen for the simulations. Such a choice can be justified by the consideration that for low rotational speed a consistent lubricant film can not be developed between the flanks of the meshing teeth.
The comparison between the measurements and the simulated results for all the applied torque values shows that the proposed method is capable to properly model the geometrical non-linearities present due to the contact loads. The coupling between the increased compliance coming from the lightweight design and the stiffness variations due to the changes in the instantaneous number of meshing tooth pair at high loads is also well represented.

At low loads the mesh stiffness fluctuation is smoother and the good correlation achieved proves that the contact detection algorithm is capable of modelling the geometrical components of the TE generated by the microgeometry modifications with a high level of accuracy.

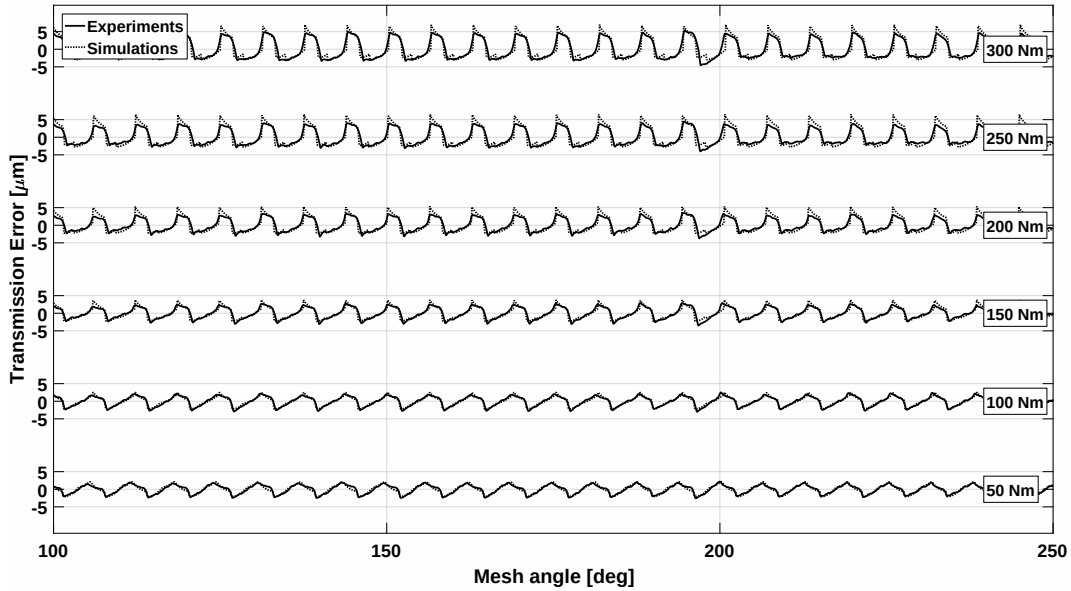

FIGURE 4.12: Transmission error in angle domain for different torque for gear pair A. Reproduced from [119]

In Figure 4.12, it is interesting to see how both measurements and simulations show the same particular shape of TE, which is dominated by the microgeometry in the first case (Figure 4.13(a)) and by the high friction forces in the second case (Figure 4.13(b)). In the latter case, sharp TE variations can be appreciated, due to the friction reversal phenomena occurring after each angular pitch in the position along the meshing cycle where, the relative speed between the tooth profiles changes sign.

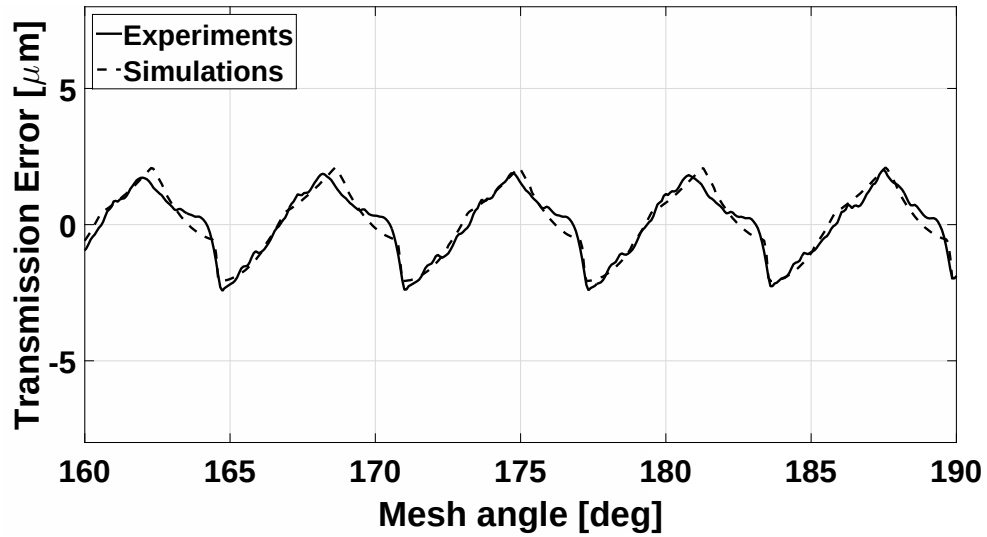

(a)

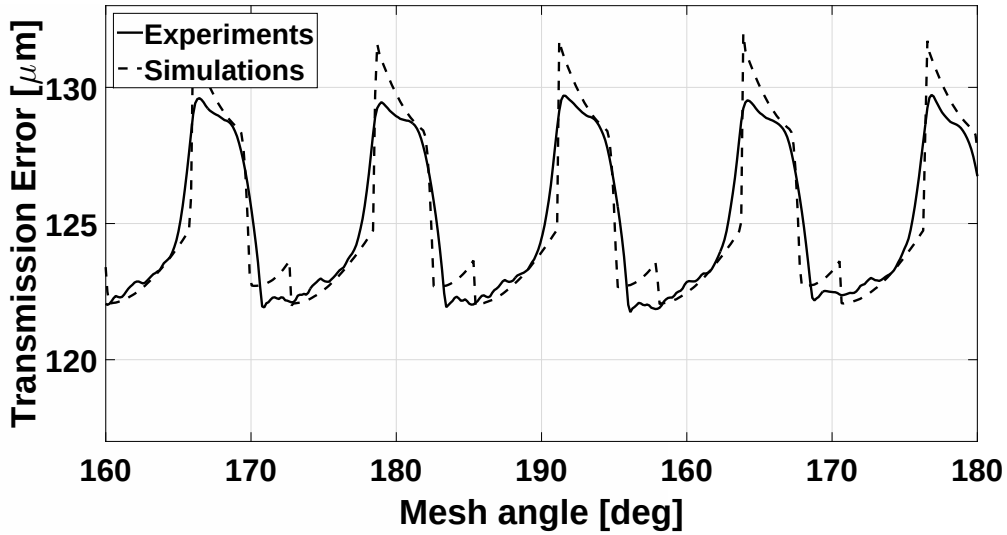

(b)

FIGURE 4.13: Detail of the transmission error in angle domain for gear pair A for 50 Nm 4.13(a) and 300 Nm 4.13(b). Reproduced from [119]

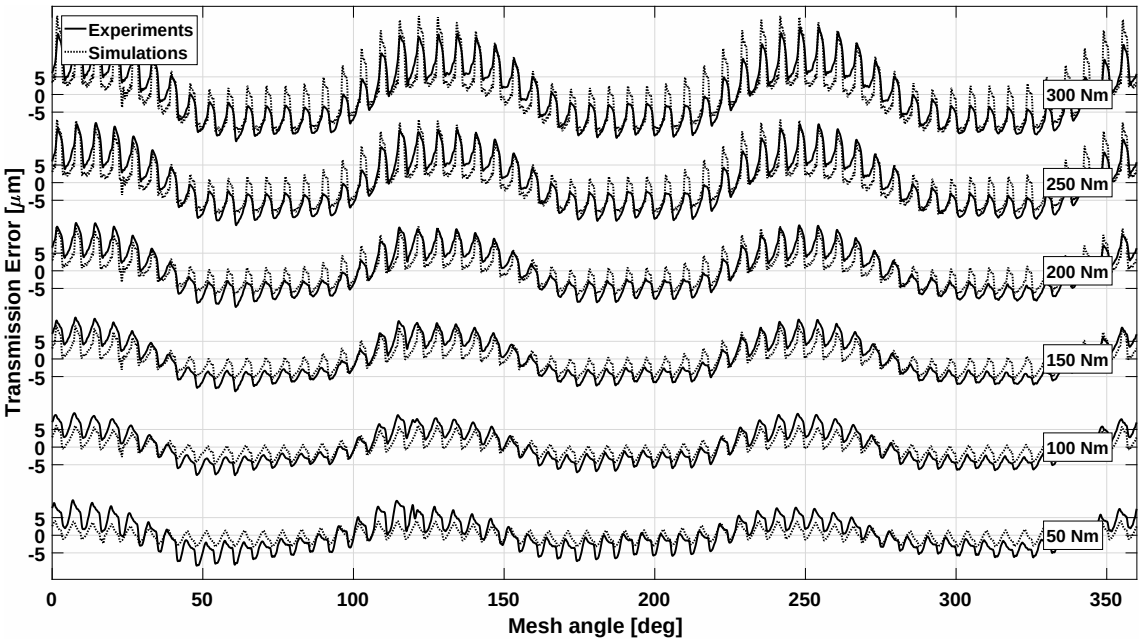

FIGURE 4.14: Transmission error in angle domain for different torque for gear pair B. Reproduced from [119]

The results for gear pair B are reported in Figure 4.14, in the same working conditions as described for gear pair A. In this second case study, the TE curves show a more complex behaviour due to the non-uniform material distribution along the gear body. A low frequency contribution in angular domain is clearly visible in all the curves, with an angular frequency equal to the number of holes present in the lightweight gear, which corresponds to the third order of the gear pair rotation. The level of matching with the experiments is similar to the one obtained for the first case study even if the particular displacement field is more difficult to be captured by the numerical model. The curves corresponding to the higher torques in the result show that the FE-based representation of the body stiffness can model this additional contribution in an accurate way. Still the coupling with other effects such as microgeometry modifications and Hertzian contact loads are properly represented in the simulation environment.

4.4.4 Root Strain Validation

In this section, the results in terms of strain at the root of the teeth are presented for the two gear pairs analysed (Gear pair A and B). All of the presented plots in this chapter refer to the strain in the direction tangential to the surface of the tooth in that section. This is done in order to properly compare the experimental and the numerical results. The strain gauges are attached to the surface of the tooth and follow the curvature in that specific region, as shown in figure 4.11. This particular configuration is replicated in the simulation environment by computing the strain tensor for each chosen element, and rotating it in the direction determined by the two external nodes of the same element edge. The considered elements are 8-nodes linear hexahedral elements, so the straight segment

connecting the nodes defines the direction tangential to the element surface.
The strain tensor in the global reference frame is therefore rotated according to the local tangential direction at the element surface. The x direction refers to the direction tangential to the element edge and the corresponding component ϵ_x of the strain tensor is considered. Due to the non uniform strain field inside the elements, the choice of the strain computation points reflects the physical gauge location in the selected region of the gear, meaning that the strain field is computed at the centre of the external face of the considered elements on the root fillet. Due to the FE discretization of the gear geometry several elements are present in the analysed portion of the gear, and their dimension is smaller than the selected strain gauges used in the experimental campaign. In such a way, different elements belong to the region covered by a single strain gauge. For this reason an average of the strain values estimated for the different elements is performed, after the strain tensor in each element is rotated in the proper direction.
The gear contact model used in this work allows to recover the displacement field from the global deformation of the gear body, excluding the non-linear displacement field that originates locally in the contact area. Following the analytical description of the contact loads in the method, the inclusion of the local contributions to the displacement in the stress recovery phase is theoretically possible using the well known laws that describe the Hertzian phenomena [60]. The analysis of the tooth root strain involves a region where the distance from the contact zone is sufficiently large to neglect the contribution from the geometrical non-linearities due to the local phenomena, being their extension limited to a small portion of the tooth.
The extension of the load distribution $2L$ due to the local contact deformation, which is the deformation between the tooth surface and the border due to the Hertzian contact pressure, can be calculated using the formula derived by Weber and Banaschek [144]:

$$L = \sqrt{\frac{4}{\pi}((1-\nu_p^2)/E_p + (1-\nu_g^2)/E_g)q\rho} \qquad \rho = \frac{\rho_p \rho_g}{\rho_p + \rho_g} \tag{4.10}$$

where the load intensity $q = F/b$ is defined as the ratio between the normal load F and the gear tickness b, while ρ is the equivalent radius.
The constants E and ν are respectively the Young modulus and the Poisson ratio of the material and is the width of the gears. The subscripts p and g refer to the pinion and to the gear respectively. According to equations 4.10, for the gear pairs analysed in this work and with the material and geometrical properties reported in Table 4.3, the obtained extension of half of the contact area is $L = 0.190$ mm for an applied load of 300 Nm.

	Units	Pinion	Gear
E	[GPa]	210	210
ν	[-]	0.3	0.3
b	[mm]	23	23
ρ	[m]	0.0308	0.0308

TABLE 4.3: Geometrical characteristics of the analysed teeth

The extent of the contact area is small compared to the tooth dimension and the stress field at the tooth root can be therefore considered as non affected by the Hertzian stress field occurring in the contact region. Its limited extension, indeed, does not generate significant effects in a region distant from the contact forces application point according to the principle of Saint-Venant. In the present work the strain recovery is focused mainly on portions of the gear sufficiently distant from the load application, i.e. the tooth root region.
As explained in section 4.2 the static modes used for the reduction of the FE stiffness matrix of the gear are computed following the approach originally developed by Vedmar [134].
In order to asses the approximation introduced by using the reduced stiffness matrix $\mathbf{K}_{\text{red}}$ with respect to the full FE stiffness matrix $\mathbf{K}_{\text{FE}}$ on the stress field at the tooth root, the von Mises stress estimated by using both matrices at the centre of some elements belonging to the tooth root region have been compared to each other. The results reported in Table 4.4 represent the von Mises stresses predicted for three elements along the tooth root for the gear shown in Figure 4.9(c), while the von Mises stress field due a line load applied on one tooth of the same gear is shown in Figure 4.15.

Element	**1**	**2**	**3**
$\mathbf{K_{FE}}$	45.9	44.5	38.9
$\mathbf{K_{red}}$	49.0	46.0	40.6
Difference	6.9%	3.2%	4.5%

TABLE 4.4: Tooth root von Mises element stresses [MPa] using the full stiffness matrix $\mathbf{K}_{\text{FE}}$ obtained from the FE discretisation and the reduced one $\mathbf{K}_{\text{red}}$.

From the numerical results it is possible to conclude that the reduced stiffness matrix approximates the stress field at the tooth root with a maximum error lower than 7%. This observation leds to conclude that the influence due to the reduction of the stiffness matrix is limited.

Friction effects

As explained in section 4.3, two methods were used in this work to recover the strain due to the meshing loads. The first method is based on a reduced stiffness matrix of the gear trough a series of static modes generated by a normal load with respect to the teeth surface. This means that the reduction space is not rich enough to capture the friction influence and therefore such effects can not be taken into account in the strain recovery phase, but the methodology can be easily extended. In most of the applications where gears rotate at a relatively large rotational speed this does not represent a limitation since

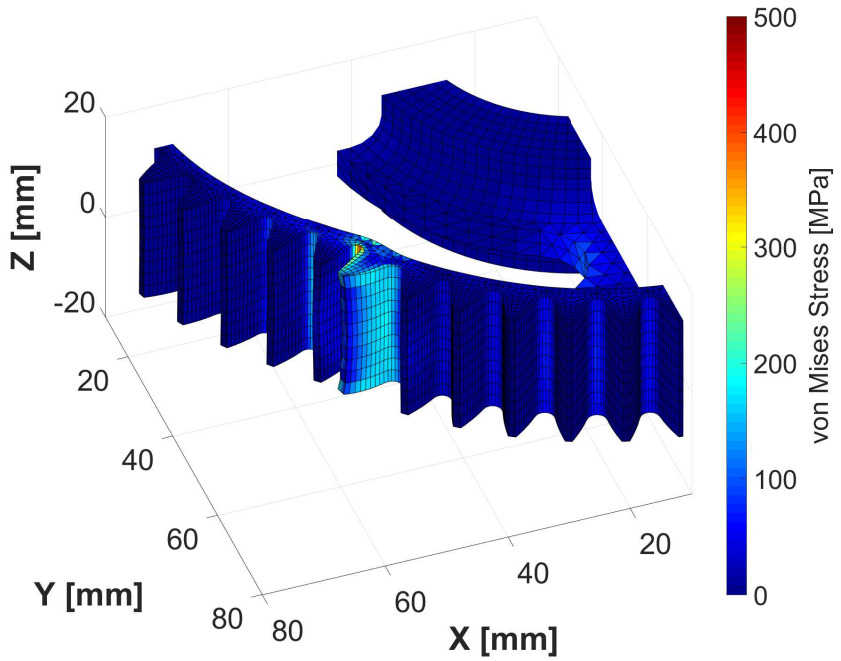

(a) Condensed stiffness matrix.

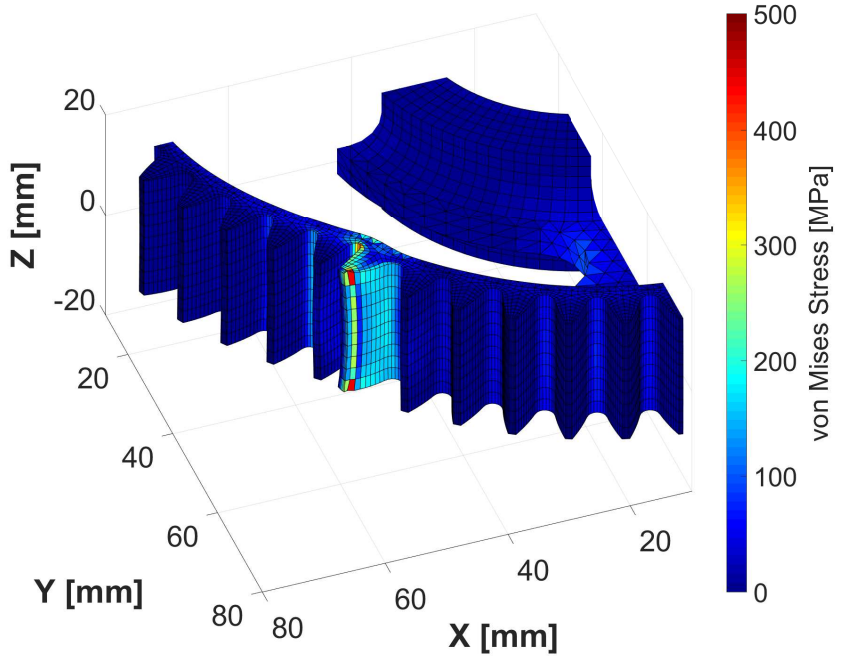

(b) Full FEM stiffness matrix.

FIGURE 4.15: Detail of the von Mises stress field due to a line load applied on a tooth of a lightweight gear, for the reduced stiffness matrix and the full one respectively. The colour scale represents the stress value at the centre of the elements. The nodal displacements are magnified 100 time. Reproduced from [119]

the relative speed between the tooth profiles is sufficiently high to generate an appropriate lubrication condition, where the friction coefficient is significantly lower.
In this work low speed analysis were performed, where the rotational speed is not high enough to generate the appropriate lubrication regime. For this reason, the influence of the friction forces on the global deformation of the tooth was investigated. In order to include the friction effects in the analysis, the second approach described in section 4.3 was used. It is based on the application of the meshing loads, computed during the MB simulation, directly on the full FE mesh of the gear. The meshing loads consist of a normal force vector $\mathbf{F_n}$ which is an output of the dynamic simulation, and a tangential friction force $\mathbf{F_t}$ proportional by the friction coefficient to the amplitude of the normal force, $\mathbf{F_t}$=$\mu\mathbf{F_n}$.
Since the direction of the friction force is determined according to the direction of the relative velocity between the tooth profiles in the contact point, an additional routine is included in order to properly check when a change of the direction of the relative velocity occurs. Exploiting the kinematic laws of meshing [81], the moment when the friction force changes direction can be individuated in the instant when the contact point crosses the pitch circle.
The influence of a tangential force on the tooth root stress field is analysed quantitatively in an illustrative example. One of the gears examined in this work was loaded with a normal force corresponding to a torque of 250 Nm applied on the nodes at the highest distance from the pitch point, where the friction effects are supposed to have the highest relevance. Two loading scenarios were analysed: in the first scenario, only a normal load was applied, while in the second condition an additional tangential force corresponding to a friction coefficient of 0.3 is applied. The results are reported in terms of von Mises elemental stress computed at the centre of the element for different locations along the tooth root at a given axial position.
By looking at the Figure 4.16, which shows the colour map of the stress distribution on the loaded tooth in the two different load cases, it is evident that the friction is responsible for a reduction of the stress on the loaded flank. Indeed, due to the bending components on the tooth, the flank is loaded with traction stress. On the other hand when the friction is included, it acts as an additional compression component that lowers the stress field generated by the normal force. This consideration is valid when the force application point has a radius which is bigger than the pitch radius. The consideration is exactly the opposite when the radius at the contact point is smaller than the pitch radius. In this case the friction component acts as an additional traction stress field on the tooth root, and therefore increases the stress levels. The element von Mises stresses reported in Table 4.5 for the two cases, are compared for five different elements belonging to the root region of the tooth. The difference is up to 38% for the element with the biggest distance from the root among the five analysed. Similar considerations are expected when the friction force has the opposite direction.

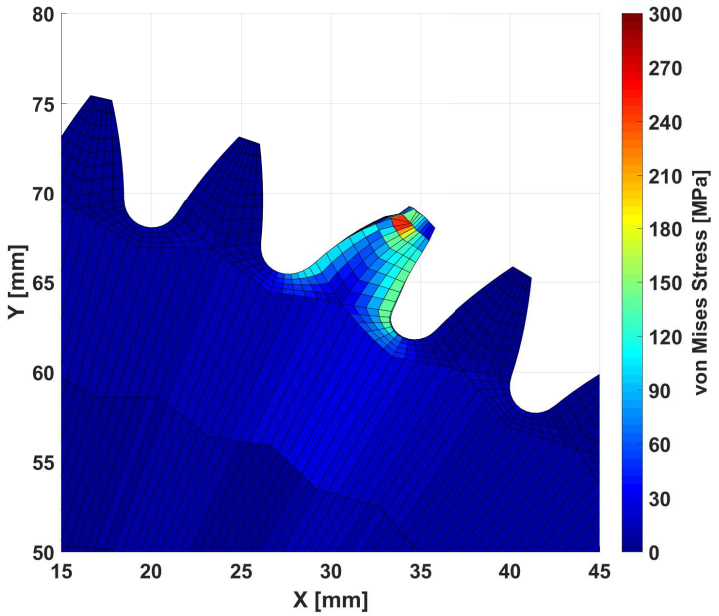

(a) μ=0

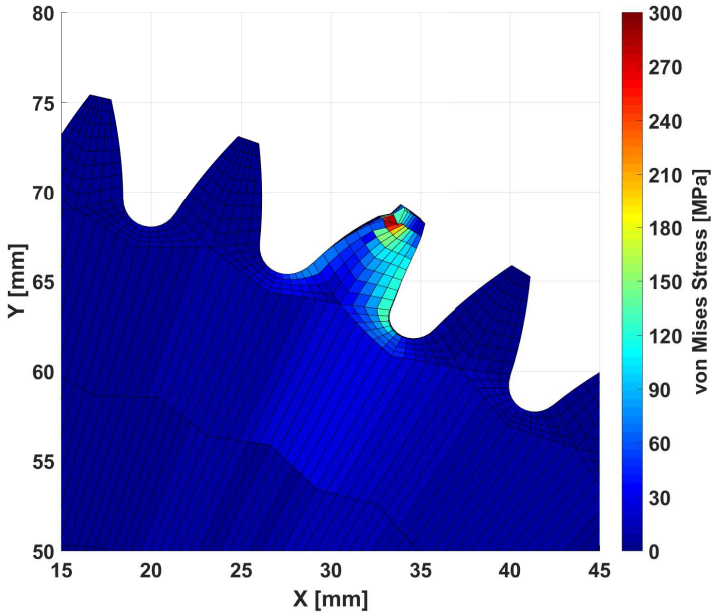

(b) μ=0.3

FIGURE 4.16: Detail of the von Mises stress field due to a line load applied on a tooth of gear 1, for two different values of the friction coefficient. The nodal displacements are magnified 200 times. Reproduced from [119]

Element	**1**	**2**	**3**	**4**	**5**
$\mu = 0$	64.75	87.83	100.43	98.62	86.97
$\mu = 0.3$	49.01	65.40	73.94	71.99	63.06
Difference	32.12%	34.30%	35.83%	37.00%	37.92%

TABLE 4.5: Tooth root von Mises element stresses [MPa]

Comparison between numerical results and measurements

In figure 4.17, the ϵ_x component of the strain tensor is presented over the rotation angle at the tooth root for gear 2 of gear pair A. The numerical results, obtained with an applied torque of 50 Nm for the two methods proposed in this work, are presented together with the corresponding experimental results. For this case, the strain field is well predicted by both methods, showing that the friction effects are small in absolute terms at such a low level of applied load.

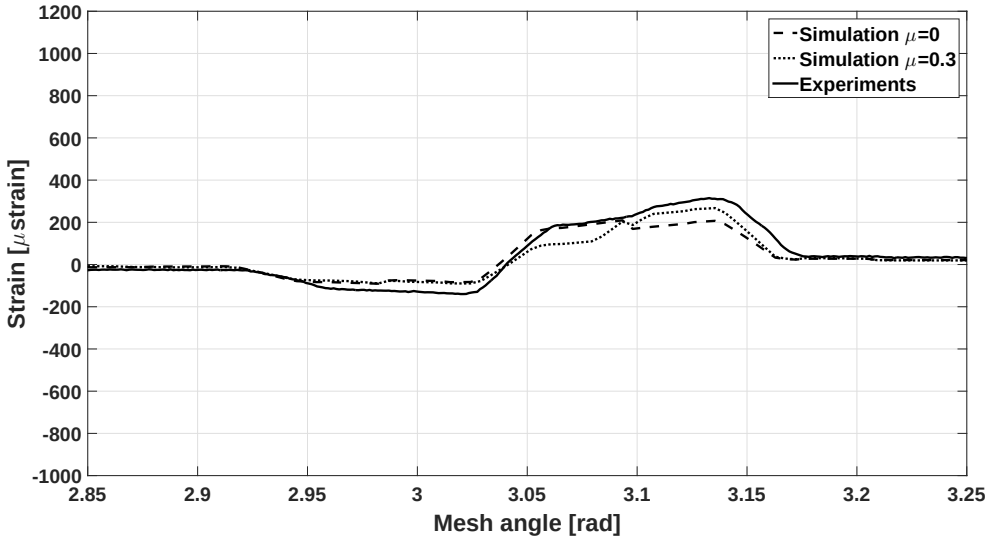

FIGURE 4.17: Root strain versus rotational angle for gear 2 at 50 Nm.
Reproduced from [119]

The results shown in figure 4.18 represent the strain field for a transmitted torque of 300 Nm in the same configuration. As expected, the impact of the friction effects on the predicted strain values is no longer negligible and the global peak to peak amplitude is caught in a more accurate way by the method that takes the friction forces into account. The first method, instead, based on the reduced FE stiffness matrix, shows a good representation of the shape of the curve but it is not capable to show the increase of the strain value due to the additional tangential component of the meshing force.

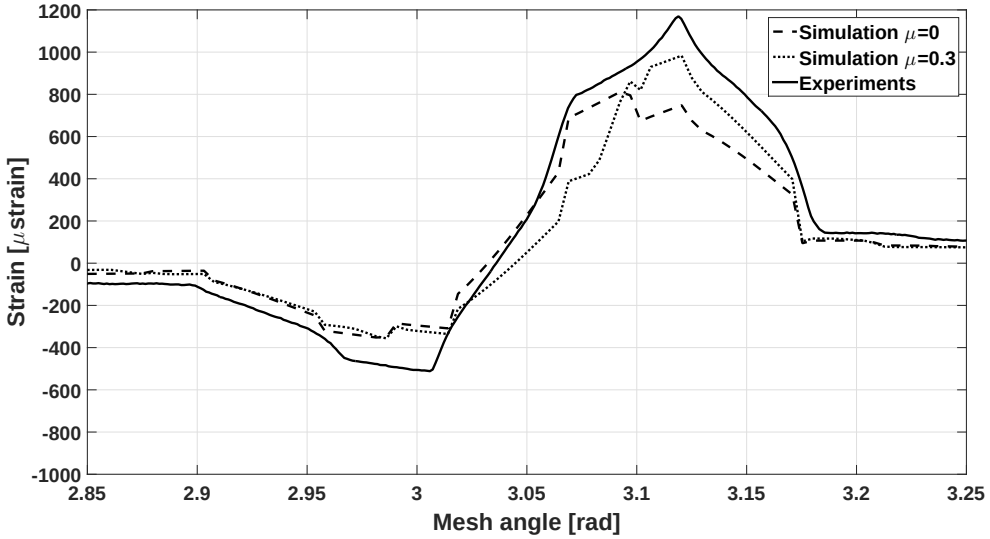

FIGURE 4.18: Root strain versus rotational angle for gear 2 at 300 Nm.
Reproduced from [119]

As discussed in the previous section the two methods provide the same strain prediction for a single point corresponding to the instant when the contact point radius coincides with the pitch radius. Under this condition, the sliding speed between the two profiles is equal to zero, meaning that no friction forces are acting on the gears. For all the other points of the predicted strain curves, the two methods provide different results. By looking at stress plots in Figure 4.19, where the normal loads acting on the FE mesh are also shown it is possible to see that for two different meshing positions of the gears, before and after the contact point crosses the pitch circle, the normal nodal load direction (indicated by the green arrows) with respect to the element edges remains constant, neglecting the small displacement of the nodes due to the deformation. In addition, by observing the blue arrows representing the meshing loads including the normal and the tangential components, it is possible to notice a change in the relative direction with respect to the tooth profile. This change in the direction of the nodal meshing forces causes a sharp change in the strain field in the tooth root.

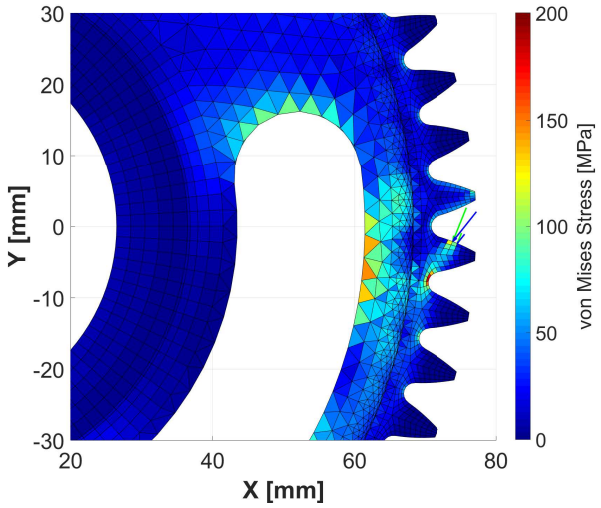

(a)

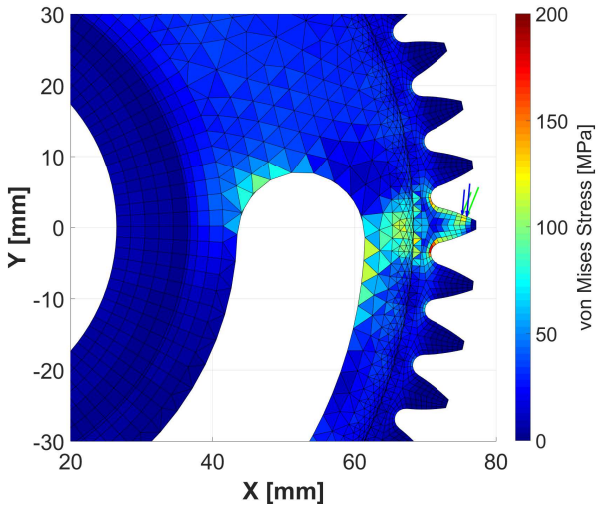

(b)

FIGURE 4.19: Detail of the von Mises stress field with the nodal loads for a given tooth, in two different timesteps. Normal loads are indicated in green, while the nodal loads including friction are represented in blue. Reproduced from [119]

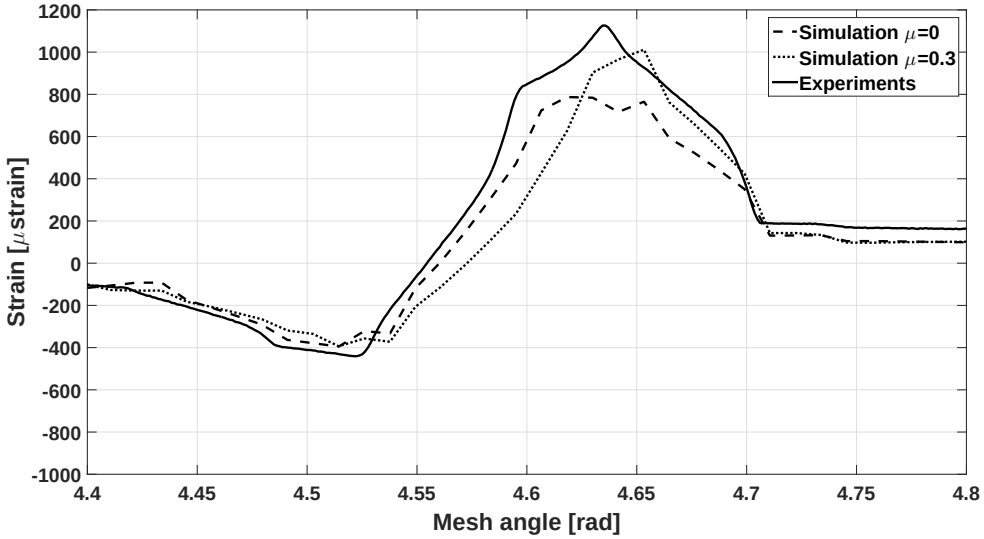

FIGURE 4.20: Root strain over rotational angle for gear 3 at 300 Nm for a tooth close to the bulky region. Reproduced from [119]

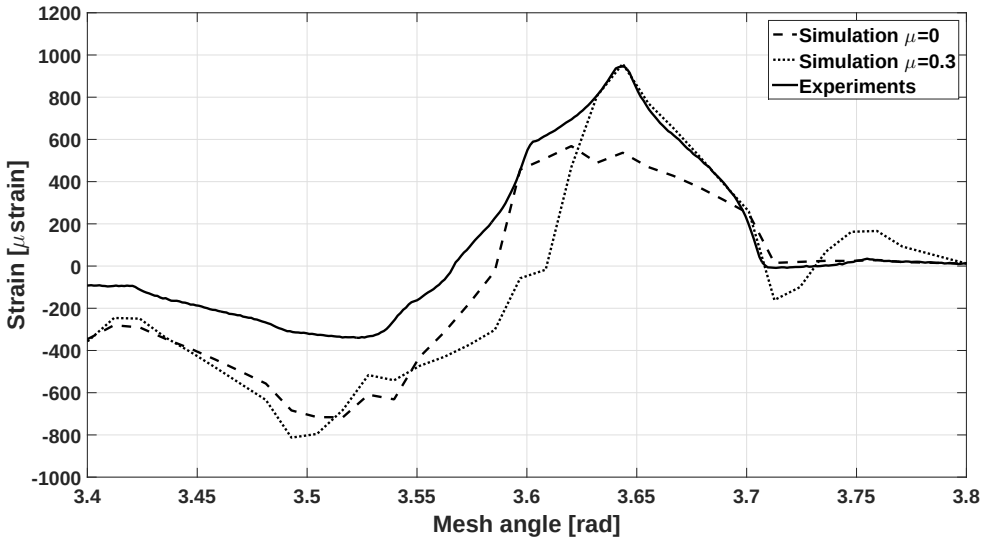

FIGURE 4.21: Root strain over rotational angle for gear 3 at 300 Nm for a tooth close to a slot. Reproduced from [119]

The results for gear 3 of of gear pair B are shown in figures 4.20 and 4.21 for two different meshing cycles of the gear pair under an applied torque of 300Nm. In figure 4.20 the root strain curves refer to a meshing tooth close to the bulky portion of the gear body, while in figure 4.21, the same curves are presented for a meshing tooth close to a slotted region. The shape of the experimental strain curves in angle domain is overall caught by the method. Some discrepancies can be observed in the compression region of figure

4.21, and the phenomena under these effects are under investigation. The fluctuations in the numerical curves visible in picture 4.21 can be explain by the low level of damping used in the simulation. The effects of system resonances, damping, and interaction with other components will be investigated in future works.

4.5 Conclusions

In this chapter, the application of a hybrid analytical-FE approach to solve gear contact problem for detailed multibody analysis in lightweight gears was shown. The method allows to retrieve quantitative results describing the body deformation and stress field with an accuracy similar to non-linear FE methods, but with a much lower computational cost, which allows to simulate long events such as multiple meshing cycles. Moreover, the hybrid formulation offers the possibility to analyse complex systems including lightweight gears with a great level of accuracy. An accurate validation of the method against experimental results shows a very good match of the numerical results in terms of transmission error, even when gears with a particular body topology are analysed. The fidelity of the method in capturing the displacement of the gear body and the deformation field is also demonstrated by comparison against strain levels measured at the tooth root.
The results illustrated in this chapter show a great potential of the method for dynamic system level analysis as well, as it will be shown in Chapter 5.

Chapter 5

System Level Dynamic Simulation

5.1 Introduction

The complexity of the dynamic phenomena occurring in mechanical transmissions are interesting from the academic point of view. One of the most challenging goals is to efficiently simulate all the phenomena occurring in the transmissions. The coupling between the behaviour of the different components can not be neglected in order to obtain sufficiently accurate results and represents the main challenge. The interest is additionally motivated by the industrial demand in a context of increased competition among the different producers of transmissions in the global market, that pushes the engineers to design more reliable products in shorter time. Extra design constraints are included in the design process such as the environmental regulations and costs reduction, make the process even more complex.
Being used in many industrial fields, mechanical transmissions deserve the interest of the researchers. In this context, due to more and more powerful resources available to the engineers the interest has moved to system level dynamic simulations of the mechanical transmission that provide a deeper understanding of the behaviour together with more accuracy in the results compared to gear pair models, at the price of higher preprocessing time and higher computational cost. In this way the designer can address multiple, and sometimes even conflicting, performance attributes.
The success of a product in the market is determined by its performances that in the high-technology sectors of transportation, energy production and industrial automation are evaluated through different key factors. The latter are generally represented by product and process sustainability, where a huge importance is given to the impact on the environment.
The more demanding regulations are the ones set to impose higher standards in terms of fuel consumption and emissions of greenhouse gases, and this is particularly evident in the automotive sector. The designers are asked therefore to move closer to the limits of the design, being pushed by conflict requirements which are the performance targets set by customer side and the emissions requirements established by the regulatory entities. The importance given to the efficiency of mechanical transmissions arises from the consideration that the transmissions themselves waste around 6-8 % of the total input energy (in automotive and wind energy applications). Sstudies [59] [46] showed that

there is room for improving the transmissions efficiency of up to 50 % that corresponds to a reduction of 9.3 tons per year in the emission of CO2 only in the automotive field. The obstacle that still prevents this achievement from being reached is the difficulty to determine the interactions between the efficiency improvements and other performance features of the transmission, such as durability or noise emissions. This gap can be filled by developing simulations tool able to predict the behaviour of the system containing the transmission at a system level in the dynamic range with the proper level of accuracy and with an affordable computational time. The dynamic simulation of the complete transmission imposes different challenges to the simulation engineer, which are dependent on the singular application (ranging from low speed heavy duty industrial gearboxes to the extremely fast and lightweight gearboxes used in helicopter transmissions).
The basic components of a gearbox represented by the gears, shafts and bearings are statically and dynamically connected. This coupling is even stronger when a flexible supporting structure is used in the transmission. The supporting structure affects the bearing locations and the gear meshing when deformations under load occur making the gears to operate in a misaligned position with respect to the nominal one. The result of this interaction is in many cases a poor dynamic and NVH behaviour of the transmission. The situation is even more complex when, due to the pursuit for lower fuel consumption and emissions, the weight of the gears is reduced by developing a lightweight design consisting in holes and slots in the bodies. This complex geometry results in a different dynamic behaviour which may led to an important degradation of the system performances if not properly addressed during the design phase.
The efforts of the engineers and of the researchers is directed towards system level simulations of the transmission in order to be able to evaluate the complete set of system performances directly during the design stage. The reason why this approach still has a limited diffusion is the lack of simulation tools able to efficiently and accurately simulate the gear meshing process in a detailed way including the coupling with the surrounding flexible components. Skipping directly the analytical tools intended for the first conceptual design phase, the choice of the engineers is between FE simulations and general purpose MB tools. As already explained in Chapter 2, the advantage of non-linear FE transient simulations is the great accuracy that such techniques can provide. The fine discretization of the physical domain allows to model in detail even the contact deformation occurring in a small region on the tooth flank, implicitly including all of the coupling effects, such as the complex additional deformation field happening due to the holes in lightweight gears, or the misalignment due to the gearbox case deformation under load. But such discretization leads to a model size which is un-practical for many applications where transient simulation are performed. The result is that these tools are not usable when large problems in terms of model size or simulation time are considered. Practically these tools can not go much further than static analysis at gear pair level. The more promising simulation approaches represented by general purpose MB solvers can be used to include the static and dynamic flexibility of the different components. In most of the applications, however, the gear contact model lacks accuracy compared to FE tools,

being based on analytical formulations in most of the applications.
In this chapter the hybrid FE-MB simulation approach already described in Chapter 4 for quasi-static analyses is used to simulate the transient behaviour of a gearbox with a layout that is inspired by the one of the manual transmissions used in front wheel driven cars. The analysis is limited to the layout where the first gear is engaged. In order to increase the accuracy of the simulation, bearing stiffness is included in the model, as well as a flexible formulation of the gearbox case using a modal order reduction technique. The method is used to investigate the influence of the lightweight design of the gears on the dynamic behaviour of the transmission.
In the last part of the chapter the impact of the lightweight design is evaluated also through a series of acoustic analysis, where the acoustic pressure generated by the radiating flexible case is computed for one point in the space surrounding the gearbox.

5.2 Model Description

In this chapter a complete gearbox including gears, rigid shafts, bearings and flexible housing is analysed to show the effects of the gear lightweighting on the response of the entire system. The chosen application belongs to the family of manual transmissions used in the standard non-electric, non-hybrid cars.
The layout reflects the packaging constraints of a typical front-wheel driven car, where the engine is mounted in a transverse configuration. The gearbox, therefore, is mounted beside the engine and connected to it through the clutch. Due to the shortage of available space in the engine compartment, the differential is mounted directly inside the gearbox housing, increasing the load that the case has to withstand. The most diffused configuration of manual transmissions have the different gears mounted on two shafts with an extra shaft represented by the differential. The engagement of a selected gear ratio corresponds to the constrain of the gear to the shaft.
The selected configuration consists of a two stage transmission with three shafts. The first shaft is the input shaft, while the last shaft is the output one and corresponds to the differential axis. The model is analysed only considering the first gear engaged. The contribution due to the other gears is neglected in this analysis. Their contribution is important in terms of rattle, being the non-engaged gears lightly loaded only by the friction and inertia forces, and therefore more prominent to lose contact, but this is not considered here. A representation of the gearbox is reported in Figure 5.1. The different shafts are indicated by the letters A, B and C. The transparent representation allows to appreciate the internal components layout. The input shaft A, virtually connected to the clutch, receives an input torque, while a corresponding resisting torque is applied on the output shaft C. In this representation the output shaft is identified directly with the differential body. The orange bodies represent the outer tracks of the bearings. Each shaft is supported by tapered roller bearing, supporting the radial and axial trusts generated by the helical gears. Their contribution in the MB simulation is lumped in a stiffness and a corresponding damping matrix, populated with stiffness values corresponding to $1.63 * 10^5 N/mm$ in

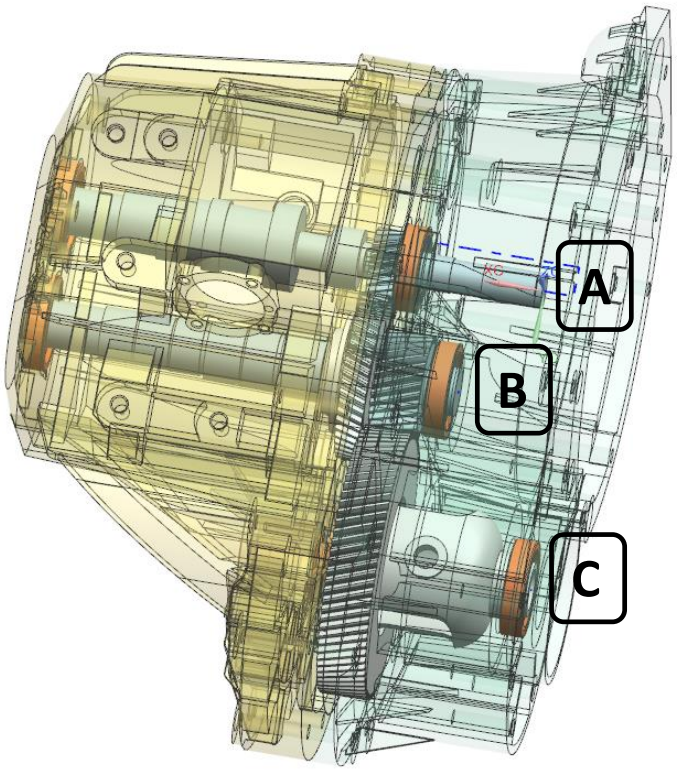

FIGURE 5.1: Translucent CAD representation of the analysed gearbox, highligthing the internal components. The input, intermediate and output shafts are indicated respectively with A, B and C.

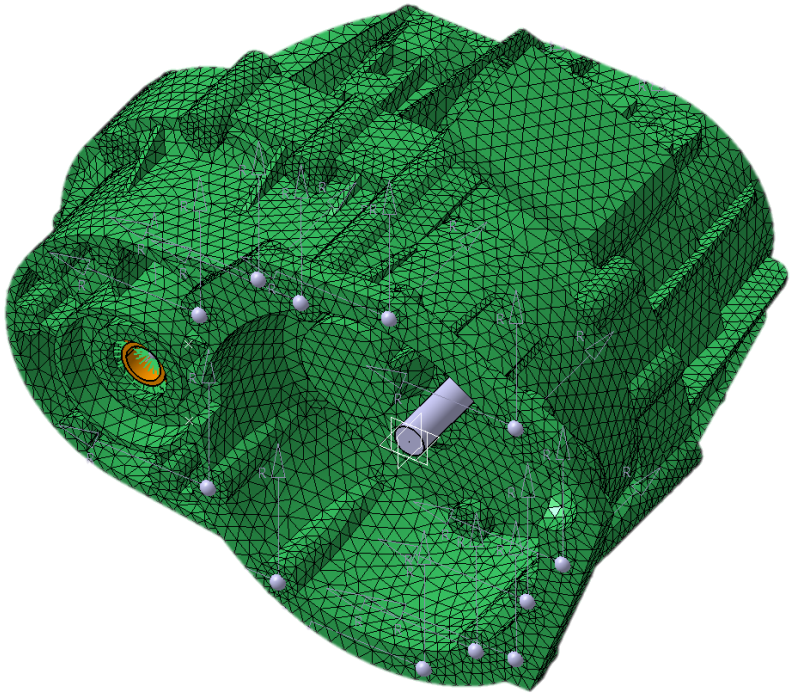

FIGURE 5.2: Finite Elements representation of the flexible case. The constraint points on the connection interface are highlined with the grey dots.

the radial direction and $5.05 * 10^4 N/mm$ in the axial direction. Since the main goal of this study is to analyse the dynamic effects of the gear body topology, no load dependencies of the bearing stiffness is considered. The previous assumption is additionally justified by the constant load chosen for the analysis, which dictates the value of bearing stiffness to choose.

As previously explained the gearbox case is considered as a flexible component, and a FE discretization is used. In Figure 5.2 the FE mesh used during the analyses is reported. The two halves of the case are modelled as a single component in order to keep the model as simple as possible. The carter structure is constrained to the ground in twelve locations, corresponding to the mounting bolts used to connect the gearbox to the engine block. In the FE model the nodes corresponding to the inner surfaces of the bolts holes are identified and connected to a central fixed node for each location by means of Rigid Body Elements (RBE2). A similar approach is used to connect the rotating shafts to the case in the bearing location. This step is particularly relevant since these are the locations where the force generated during the gear meshing are transmitted to the flexible case. A series of RB2 elements connect the nodes on the inner surface of the bearing seats in the carter. The RBE2 elements are connected to a reference frame on the rigid shafts, in the corresponding bearings location. Obviously in this case only the relative translations are constrained, in order to leave the rotating degrees of freedom to the shafts.

The model consists of four gears, the kinematic parameters of which are reported in Table 5.1 for a given transmission ratio $\tau = 0.1463$. In the considered configuration gear 1

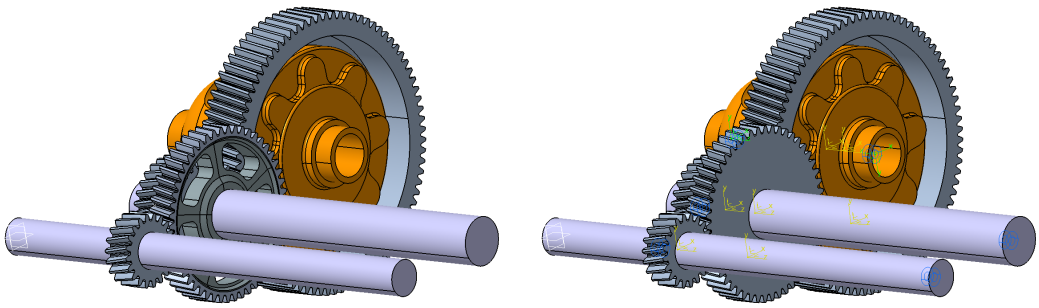

(a) (b)

FIGURE 5.3: CAD representation of the two configurations of the gearbox gears analysed.

is mounted on the input shaft A and engages with gear 2. The second stage is formed by gear 3 and 4. The first one is mounted on the intermediate shaft B together with gear 2, while gear 4 is solidal to the output shaft C.
In the current analysis the dynamic response is evaluated for a run-up simulation with a linearly increasing speed from 0 to 2500 rpm reached in 20 seconds. In order to not over constrain the model the run-up condition is achieved by imposing an input torque and an unbalanced output torque on the differential shaft. The unbalanced torque generates a constant acceleration of the system, whose value depends on the system inertia. Using this configuration there is no need to impose a speed law to the model.

Parameter	**Units**	**Gear 1**	**Gear 2**	**Gear 3**	**Gear 4**
Tooth number	[-]	20	50	30	82
Pressure angle	[deg]	20	20	20	20
Helix angle	[deg]	10	10	10	10
Module	[mm]	2.7	2.7	2.68	2.68
Face width	[mm]	22	22	40	40
Dedendum coeff.	[-]	1.25	1.25	1.25	1.25
Addendum coeff.	[-]	1	1	1	1

TABLE 5.1: Main design parameters of the gearbox gears

In this study two configurations of the system are analysed, reported in Figure 5.3, differing for the topology of gear 2. In the configuration reported in Figure 5.3(a) the gear exhibits a lightweight design with 5 slots made in the gear body, with the aim of reducing the overall mass and inertia of the gear. The configuration of Figure 5.3(b) has a standard design and is used as reference case. In order to properly consider the static contribution of the lightweighting and its influence on the dynamic behaviour of the transmission the simulation technique described in Section 4.2 is used.
The advantage of the hybrid formulation over the analytical ones is the possibility to

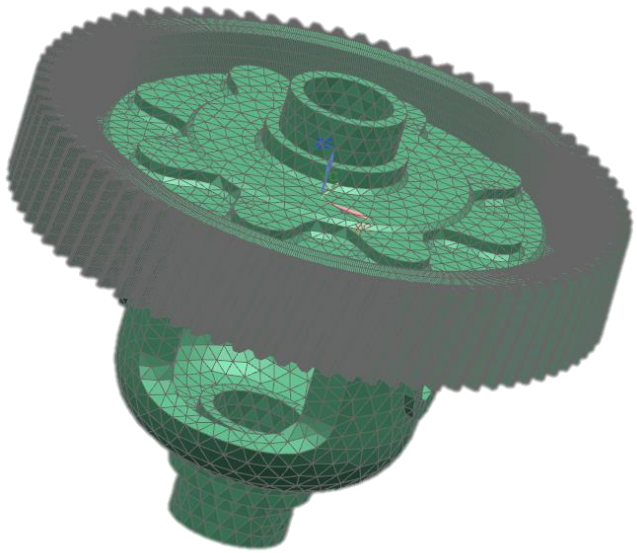

FIGURE 5.4: Finite Elements representation of the differential unit used in the simulations. The FE discretization is used both for the gear itself and for the differential body.

replicate the deformation of gears with complex geometry. Beside lightweight gear, this is relevant also in all the applications where the gears have not the standard configuration such as the helical gear mounted on the differential body. In order to show the influence of the contribution due to the body topology the differential unit is considered together with the gear itself. The FE model is shown in Figure 5.4.

5.3 Simulation Results

The dynamic behaviour of the complete transmission was analysed by means of the methodology illustrated in Section 4.2 and implemented in the commercial multibody software Siemens LMS Virtual.Lab [120]. Simulations were performed by applying a constant torque value of 250 Nm and 1708 Nm on the input and output shafts of the gearbox respectively. A run-up in velocity from 0 to 2500 rpm was thus achieved for the carrier in 25 s thanks to the torque unbalance of 0.04Nm applied on the input shaft.
Figure 5.5 shows the TE curves computed for the gear pair including gear 1 and 2 for the two configurations considered in this study. In this case only the first instants of the simulations are considered here, where the speed is low. The two curves in the plot, belonging to configurations shown in Figures 5.3(a) and 5.3(b), show a different contribution due to the static behaviour of the two gear bodies. The lightweight design exhibits

the fluctuations in the TE typical of the gears with a lightweight topology, already shown in Chapter 4 but for different design.

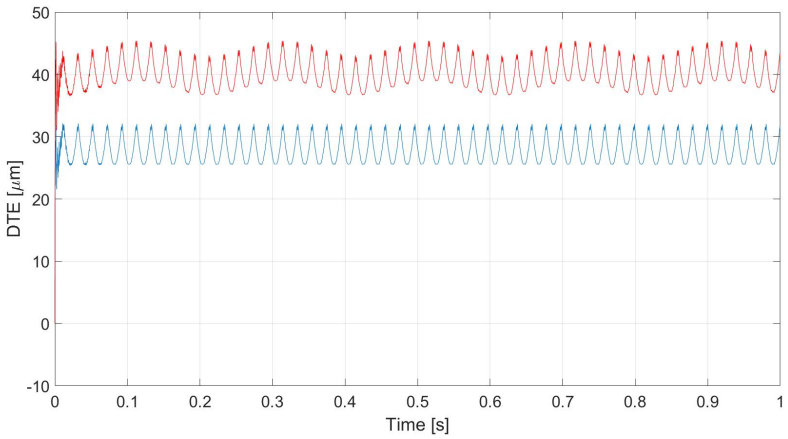

FIGURE 5.5: Low speed transmission error computed along the line of action between shaft A and shaft B. The curves reported refer to the two different configuration of Figure 5.3. The red line corresponds to the TE computed for the configuration of Figure 5.3(a), while in blue are reported the results of the configuration illustrated in 5.3(b).

In Figure 5.6 the low-speed transmission error for the second gear pair in the gearbox is shown. Fluctuations in the value of the TE are evident also here, and obviously generated by the topology of the differential unit. In this case, therefore the variation in the mean value of the TE, are present since the whole body is included in the analysis, while the gear crown itself, constrained to the differential unit keeps a standard design. It is possible to conclude here that the fluctuation are not generated by a lightweight design, but are evident thanks a more accurate modelling of the static behaviour of the transmission components, made available thanks to the hybrid FE approach used.

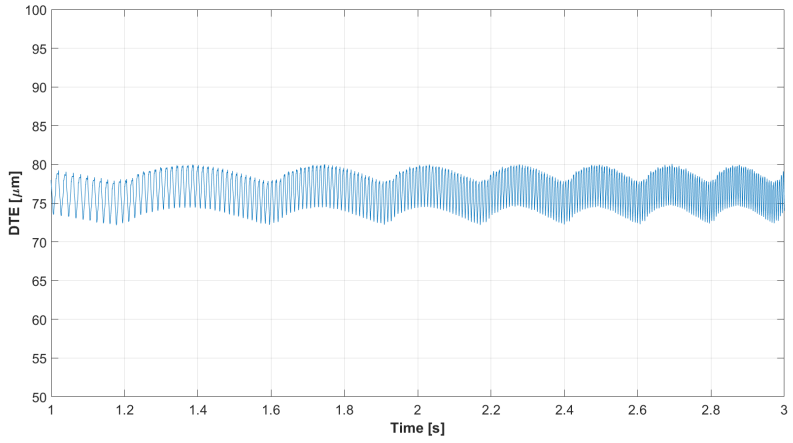

FIGURE 5.6: Low speed transmission error computed along the line of action between shaft B and shaft C. The fluctuation here are due to the geometry of the differential body shown in Figure 5.4

Moving to the dynamic analyses of the gearbox, the influence of the quasi-static behaviour becomes evident in the dynamic response as well. This effect can be recognized by observing the waterfall plots of Figures 5.7 and 5.8. Besides the orders generated by the tooth-passing contribution to the transmission error which are common to both plots, modulation sidebands appear due to a variation in the peak-to-peak amplitude, generated by a different topology of the foundation below the loaded teeth. The orders corresponding to the holes as well as the ones due to the differential geometry are recognizable in the plot of Figure 5.8.

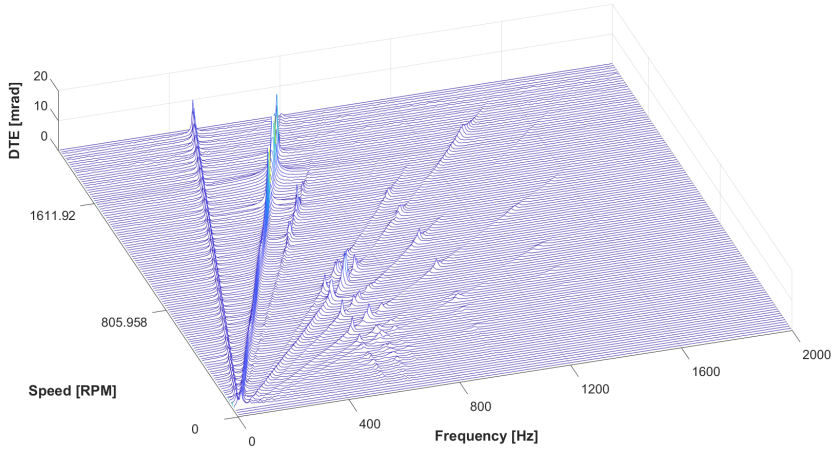

FIGURE 5.7: Waterfall plot of the angular transmission error computed between shaft A and shaft C. The results reported here correspond to the configuration shown in Figure 5.3(b)

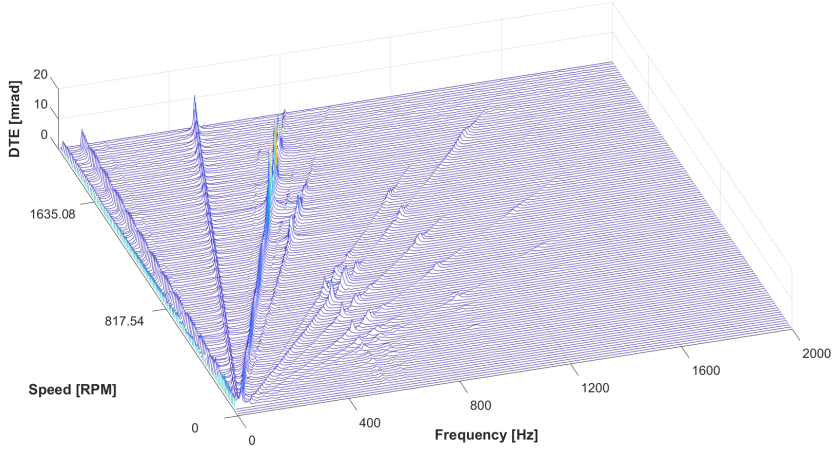

FIGURE 5.8: Waterfall plot of the angular transmission error computed between shaft A and shaft C. The results reported here correspond to the configuration shown in Figure 5.3(a)

5.4 Acoustic Simulation

The acoustic performance of the transmission can be evaluated exploiting the flexible multibody approach used to represent the gearbox cases. An acoustic simulation is performed by extracting the time-histories of the forces on the bearing units and using them as excitation source for a forced-response acoustic simulation. The assumption behind this approach is that the response of the gearbox case under the meshing load in the MB is equivalent to the one computed during the acoustic simulation.
The approach used here consists of a frequency response meaning that the time-histories of the bearing forces computed during the MB simulations have been converted to the frequency domain.
In this chapter the Acoustic Transfer Vectors (ATV) methodology is used to compute the pressure levels in a spatial location near the gearbox. The advantage of this formulation compared to the classical acoustic Boundary Elements Method (BEM) is a reduction of the computational cost. In a typical BEM problem the system equation are made of full matrices that have to be assembled for each desired frequency in the output response, and used in the solution process of the system equations. The concept behind the ATV approach, already described in [45], is a better exploitation of the nominal Acoustic Transfer Functions by reusing them. The ATVs can be considered as the link between the sound pressure level at a specific location in the domain and the velocity in the normal direction to the surface of the flexible structure. This relation can be seen as a space formed by the different acoustic transfer functions from the nodes of the surface to the location on the output domain.
Exploiting the linearity properties of the system, these functions can be considered as independent from the loading conditions, being functions of the acoustic domain, fluid and body properties. The independence from the applied load on the structure impose the assumption of a one-way coupling between the structure and the acoustic field. In the case-study analysed here the vibrating gearbox case creates a pressure field in the surrounding space. The opposite effect (i.e. the influence of the air on the structure) can be considered negligible satisfying in this way the approach hypothesis. The ATVs for a given configuration are computed for a given set of frequencies spreading the interval of interest for the analysis, with a fixed frequency step.
The frequency response of the system in terms of acoustic pressure in the chosen location $p(\omega)$ is computed using the pre-computed ATVs $atv(\omega)$ and the normal structural velocity $v_n(\omega)$ boundary condition vector for the desired output frequency. This process involves a multiplication between two vectors, as shown in equation 5.1 and requires a low computational time with respect to the solution of the system equations for that given condition.

$$p(\omega) = atv(\omega)^T v_n(\omega) \tag{5.1}$$

The convenience of this approach is further supported by the consideration that the fluid domain that surrounds the gearbox case hardly shows the presence of resonances, therefore the ATVs can be considered as smooth functions of the frequency.
The coefficient values for the intermediate frequencies can be evaluated using interpolation schemes exploiting the master frequencies, for which the ATVs are computed. On the other side an interpolation of the normal velocities on the structure surface cannot be interpolated due to the dynamic behaviour of the system, where the resonances prevent the normal velocities from being a smooth function of the frequency.
The starting point for the approach described here is the determination of the normal velocities on the gearbox external surface. In this case the structural response is obtained starting from the MB computed forces in the specific locations. These forces, converted in the frequency domain, are used to excite the FE model of the case and to obtain the normal velocities.

5.4.1 Acoustic Behaviour

The results of the acoustic simulations are reported in Figures 5.9 and 5.10 in terms of acoustic pressure in the chosen location close to the gearbox. In this case a constant speed simulation was performed for the two configurations considered in this chapter.
By looking at the results in the frequency domain reported in Figure 5.9 it is clearly visible that the presence of the holes causes to have extra peaks also in the acoustic response of the gearbox. These peaks correspond to different orders in the waterfall plots reported in Figures 5.7 and 5.8. The excitation generated by the topology of the gears has an influence on the acoustic response of the system as expected.

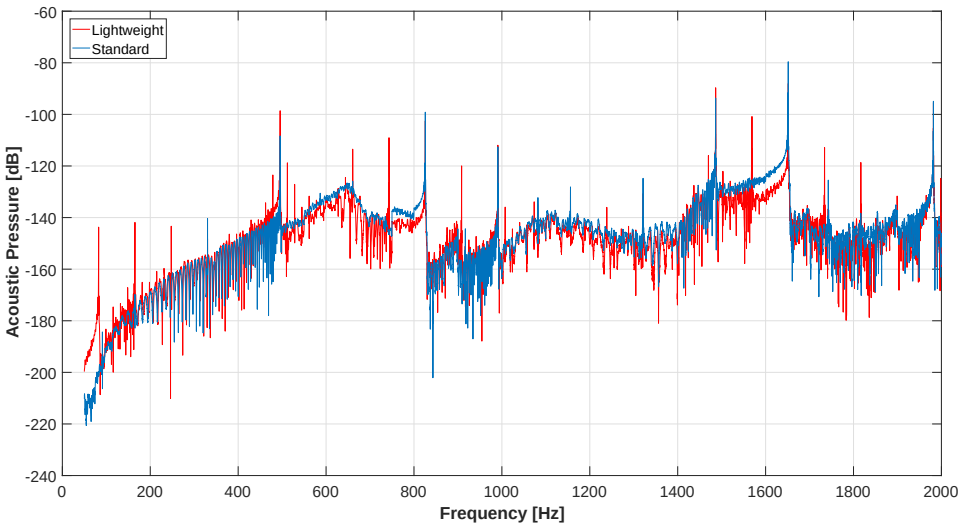

FIGURE 5.9: Acoustic pressure in frequency domain, for the standard configuration (blue) and for the configuration with the lightweight gear (red).

The acoustic signature of the gearbox in terms of time domain pressure curves is reported in Figure 5.10 instead. While it is difficult to spot the different contributions directly form the time histories, the reader can distinguish a different amplitude of the peak-to-peak response.

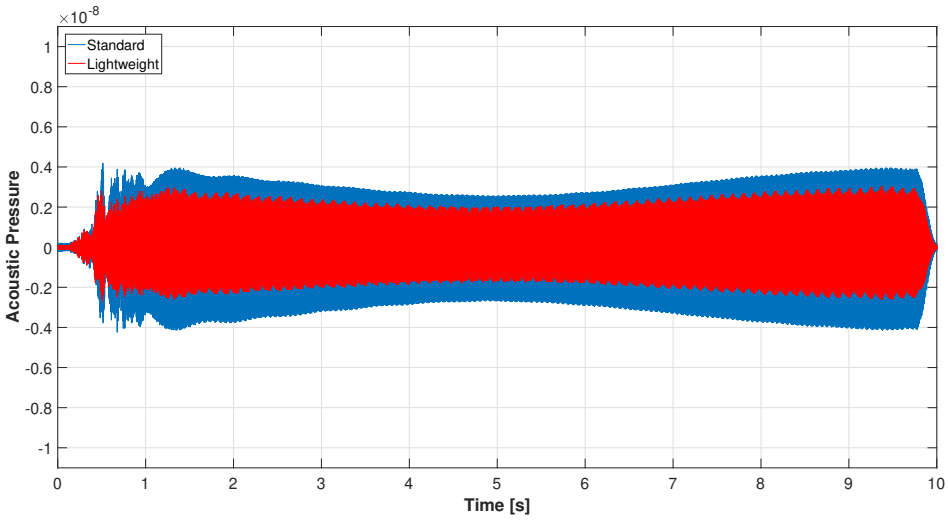

FIGURE 5.10: Time histories of acoustic pressure, for the standard configuration (blue) and for the configuration with the lightweight gear (red).

This effect can be explained by a different mesh stiffness of the lightweight gears, that being more compliant tend to have a deformation field that involves a bigger portion of the gear. This is opposed to the behaviour of a solid gear, where the high stiffness of the gear body tends to localize the deformation in an area close to the tooth root, where the (bending) stiffness is much lower compared to the gear body.
It is interesting to notice how the gear body topology, beside the obvious effects on the weight and inertia of the transmission, can result in different acoustic performances of the system. The designer can use therefore the shape of the gear body to tune the acoustic signature of the system.
Another consideration arising from this analysis is that an accurate modelling of the meshing process is required in order to be able to catch such phenomena. Standard FE methods are not feasible when relative long transient analysis have to be performed. In the simulations reported here where simulations 10s and 20s long have been performed, the used of FE method is not feasible.

Chapter 6

Conclusions

In this PhD thesis the static and dynamic behaviour of lightweight gears was analysed using different approaches. Lightweight gears, unlike standard gears, have the geometry of the body that increases the overall meshing compliance. In many cases, additional holes are machined, adding extra fluctuations in the mesh stiffness function along an entire rotation of the gear. When a hole is drilled in the gear blank, beside the extra fluctuations, the peak-to-peak amplitude of the TE is affected at the same time. By simplifying the problem, one may think that the local material removal results in a lower bending stiffness of the meshing tooth, that will have a higher deformation for a given load, when the considered tooth is close to a hole. The variation in the peak-to-peak amplitude can be identified as an amplitude modulation whose order depends on the number of holes or slots in the gear body.
When these effects are translated in the dynamic response of a transmission, the fluctuations are reported as additional orders in the TE of the transmission in case of speed sweep response. The importance of modelling such effect is in the possibility that, under specific working conditions, the additional orders excite one or more of the system resonances, increasing the vibration response or causing a degradation of the noise comfort. In the worst scenario, if the vibration level is too high, the system may undergo a catastrophic failure. These considerations testify the importance of a proper modelling of the components of the mesh stiffness due to the particular shape of the gear body.
The task of simulating the gear train response under realistic working conditions is a crucial task. The motivations for such type of analysis are clearly in the dominant role of the excitation coming from the meshing gears on the overall NVH performance of the system. The latter is paired with the decreased durability characteristics of the components affected by the dynamic loads generated by the gears. The simulation tools have the fundamental task to replicate the working condition of the system in the most accurate way, before expensive physical prototypes are built. The identification and resolution of potential issues in the design stage is, indeed, much cheaper than in the stages close to the production phase. On the other side the simulation of rotating gears is a difficult task due to the complexity and the mutual coupling of the physical phenomena involved in the meshing process.
Among the different modelling techniques available to represent the transmission behaviour, two of the most representative are considered in this thesis. A first approach

consists of an analytical model, where only the rotational degree-of-freedom of the gear is represented. The second approach included in this dissertation is based on the formulation available in the commercial MB software Siemens Simcenter 3D Motion. The formulation is extended to the analysis of gear with arbitrary body geometry. A dedicated tool was developed in order to recovery the stress and strain field in the gear body, allowing to perform strength analysis on the meshing gears.
The first approach analysed in this dissertation work consists of an analytical model, based on the approach developed by Palermo [95]. A single DOF model representing the torsional motion of the gears, including the nonlinear behaviour due to backlash, is developed.
The main idea motivating this analysis is that despite the simplicity of the model, it can still accurately represent the dynamic behaviour of the gear pair. This is ensured by a detailed representation of the meshing stiffness which is computed using non-linear FE simulations. The stiffness curve over the considered meshing cycle are stored in look-up tables, which are interpolated during the time integration of the motion equations. The FE-based computation of the mesh stiffness allows a precise representation of the fluctuation in the TE caused by the non-uniform distribution of the material below the meshing teeth due to the particular body geometry. The fluctuations in the body compliance causes additional excitation when the dynamic effects are considered. The FE computations allow moreover to include the microgeometry modifications effects, under the condition that the teeth flank geometry is properly dicretised. On the other side the high computational cost of the FE simulation is bounded to a pre-processing phase, where a stiffness map of the considered gear pair is created. The computational efficiency of the analytical representation of the body motion is then exploited.
The purpose of this analysis is not only to show how the different lightweight strategies can affect the dynamic response of a gear pair, but also to demonstrate that an analytical torsional model can predict detailed dynamic effects. This approach can easly be extended to more complex models, including three-dimensional motion of the gears as well as a lumped description of the stiffness of the supporting elements. A limitation of this approach, which is common to all the torsional models, is that the flexibility of the gear body is included as a lumped parameter in the motion equation, and the out-of-plane flexibility is not included in the formulation. The rigid body hypothesis behind this approach can represent a limit to the applicability of this formulation in particular conditions where thin web and thin rim gears are considered. In most of real application cases the gear geometry has a relatively high bending stiffness out of the plane. However when this condition is not satisfied, the user should be aware of the limitations.
In this dissertation an additional approach was considered, which is based on the general purpose MB formulation already implemented in the Siemens Simcenter 3D MB software [120]. This formulation is aimed at achieving high computational efficiency required to perform transient simulation of long events at a system level, such as speed-sweep simulations. In the perspective of this PhD dissertation this approach was developed in order to analyse lightweight gears. The method is extended, therefore, to the analysis of

gears with arbitrary shape of the gear body. This additional effort allows to investigate the static and dynamic effects of the gear topology on the system response. The advantages of the formulation compared to the analytical modelling of the mesh stiffness are in the three-dimensional multibody treatments of the system's equation of motion. The multibody modelling of the system covers most of the limitations raised by the analytical modelling. The three-dimensional description of the body motion implicitly considers the stiffness variation due to misalignments between the gear axis caused by compliant joints. This type of phenomena can be represented in a more precise manner if a flexible body formulation is included which is a standard technique in almost totality of commercial MB software. In this case the condensed mass and stiffness matrix of shafts and housings are computed exploiting a FE discretization. The resulting model consists of a detailed representation of the bodies flexibility. For instance it is possible to consider the motion field of the gear body when the transmission is loaded with the design's torques. The latter is the combination of the shafts, bearing and housing deformation, as well as the deformation of the gear body itself, that in the case of gears with optimized mass might be relevant. The coupling between all these effects causes to the meshing forces to change direction continuously, modifying accordingly the bodies deformed shape. The coupling effects are even more relevant when during the dynamic analysis the gear excitation is coupled with the modal models of the system, exciting the different mode shapes. This formulation is therefore suggested in all the cases where a detailed investigation is required with a focus on the effects of the dynamic coupling between the gears excitation and the system dynamics.

Another advantage of the FE-based formulation over the analytical one is the possibility to reconstruct the strain field from the nodal displacements in highly-loaded regions, such as the tooth root. The stress recovery phase additionally allows to evaluate the strength levels for different shapes of the gear body. The accuracy, and the level of detail of the method is comparable to FE simulations. An experimental campaign was performed, showing that the method provides reliable results in terms of overall displacement of the gears, using the TE as indicator. An additional validation phase involved the strain field on the tooth root. Even in this case the results obtained from the simulations matched the experimental ones.

It has to be noted that this increased level of detail in the numerical formulation brings an increase of the computational costs. This is due to the additional degrees-of-freedom required to discretize the distributed flexibility of the bodies. The computational complexity is also due to the more refined modelling of the contact constrain in the simulation compared to the analytical formulation. A penalty-based approach is implemented, allowing to consider the hertzian load distribution over the tooth flanks. This effects is particularly relevant when the gears rotate in a misaligned condition, or when the goal is to evaluate the effects of a microgeometry modification.

The MB formulation used in this dissertation has the drawback of not taking into account the dynamic coupling between the mode shapes of the gear body and its deflection under the meshing loads. More in detail, only static deformation patterns are used to condense

the stiffness matrix of the gear body, neglecting its dynamic contribution. It has to be pointed out that in most of the applications this effect is negligible, since the eigenmodes of the gear pair are located in a high frequency bandwidth, especially for the common industrial applications. In the applications where the dynamic coupling is a concern, more detailed simulations tools are available, but they require extremely long computational times.
In the last chapter of the dissertation the general purpose MB formulation was exploited to analyse the dynamic behaviour of a complete automotive transmission. The inclusion in the simulation of the flexible representation of key components, such as the gearbox housing is a key advantage over analytical tools. The dynamic simulation allows to simulate the coupling between the dynamic excitation generated by the meshing loads and the mode shapes of the analysed structure. The accurate prediction of the meshing loads, coupled with the flexible representation of the gearbox housing is a useful tool when the acoustic signature of the system is taken into account for NVH simulations. The formulation accuracy is evident when gears with different lightweight design are considered. The different orders corresponding to a specific numbers and shape of the holes in the gear body are visible also in the acoustic signature of the model.
Moreover the last chapter shows additionally that the proposed formulation can be efficiently integrated with already established simulation techniques, such as the ones used in the acoustic field, allowing to consider contribution of the gears excitation to the overall acoustic signature of the system, without affecting the computational efforts in a relevant manner.
To conclude, it is possible to state that the effects of a lightweight design can be a major concern for a mechanical transmission, especially when coupled with a dynamically compliant structure. However, the simulations required to catch these phenomena normally take extremely long computational times with standard FE methods. The methods showed in this dissertation, still keeping a good level of accuracy, make the simulation of long events feasible even on a standard desktop machine.

6.1 Future steps

In this thesis two exiting approaches, aimed at analysing the dynamics of geared transmission are considered and extend to enable the analysis of lightweight gears. The methods show good potential in term of computational efficiency and accuracy when compared to the state-of-the-art simulation tools.
The analytical model presented in this thesis is bounded to the analysis of cylindrical spur gears. The research might be extended to the analysis of helical and non cylindrical gears, being the approach suitable for such analysis without any additional limitation. This type of models require a more refined formulation of the body DOFs in order to take into account the multi-axial components of the meshing forces generated by the helical and non-cylindrical gears.
The approach based on a general purpose MB formulation showed great performances

in terms of computational efficiency obtained thanks to the analytical description of the hertzian loads on the tooth surface. Additionally a great accuracy of the results is reached, demonstrated by the good agreement with the experimental results, and additional validation of the dynamic and acoustic simulations might add value to the research. However a limitation of the method still lies in the decoupling of the stiffness and inertial terms in the gear body motion of the non rigid DOFs. A dedicated research path might easily overcome the limitation by including a set of mode shapes in the reduction space of the gear body. Even considering a potential increase of the problem complexity, it would still be orders of magnitude smaller compared to the standard FE simulation tools and could represent an attracting research topic.

Appendix A

Publications List

1. Palermo A., Toso A., Shweiki S., Mundo D., Desmet W., *Effects Of Transmitted Load On TheDynamic Behaviour Of A Spur Gear Pair*, Proceedings of ICeDyn 2015, Lagos, Algarve (Portugal).

2. S. Shweiki, A. Palermo, A. Toso, D. Mundo, W. Desmet, *Effect of center distance and microgeometry on the dynamic behaviour of a spur gear pair*, Proceedings of ICoEV 2015, Ljubliana (Slovenia).

3. J. Korta, A. Palermo, D. Mundo, S. Shweiki, *Combining Finite Element and Multibody Modeling Techniques for Time-Efficient Simulation of Nonlinear Gear Dynamics*, Proceedings of SIMUL 2015, Barcelona (Spain).

4. J. Korta, D. Mundo, G. Ambrogio, B. Folino, S. Shweiki, L. Filice, *Topology Optimization and Analysis of Static Transmission Error in Lightweight Gears*, Proceedings of IFToMM 2016, Vicenza (Italy).

5. S. Shweiki, D. Mundo, J. Korta, P. Oranges, A. Palermo, *Investigation of mesh phasing in a planetary gear train using a coupled FEM - Multibody simulation*, Proceedings of ISMA 2016, Leuven (Belgium).

6. A. Dabizzi, G.H.K. Heirman, A. Palermo, S. Manzato, E. Di Lorenzo, S. Shweiki, A. Toso, *Multibody Modeling Of A High Precision Gear Test Rig And Correlation To Experiments*, Proceedings of ISMA 2016, Leuven (Belgium).

7. S. Shweiki, J. Korta, A. Palermo, R. Adducci, D. Mundo, *Combining Finite Element analysis and analytical modelling for efficient simulations of non-linear gear dynamics*, Proceedings of ECCOMAS 2016, Crete (Greece).

8. S. Shweiki, J. Korta, A. Palermo, D. Mundo, G.H.K. Heirman, *On The Effects Of Blank Lightweighting On Gear Dynamics*, Proceedings of ICPT2016, Chongqing (China).

9. D. Mundo, S. Shweiki, P. Catera, *On the Impact of Transmission Error on the Dynamic Behaviour of Geared-Linkages*, Proceedings of MeTrApp 2017, Trabzon (Turkey).

10. S. Shweiki, D. Mundo, A. Palermo, *System-level Multi-Body simulations of a wind turbine gearbox*, Proceedings of ICSV24 2017, London (UK).

11. T. Tamarozzi, P. Jiranek, Ali Rezayat, S. Shweiki, *An efficient hybrid Approach to Gear Contact Simulation in Multibody Systems Leveraging Reduced Order Models*, Proceedings of ECCM6 2017, Glasgow (UK).

12. A. Rezayat, S. Shweiki, D. Park, M. Vivet, S. Donders, S. Flock, P. Jiranek, T. Tamarozzi, *A novel efficient high fidelity approach to gear contact simulation in multibody systems*, Proceedings of IGC 2018, Lyon (France).

13. S. Shweiki, A. Rezayat, T. Tamarozzi, D. Mundo, *Experimental and numerical validation of transmission error using advanced gear contact model*, Presented at IMSD 2018, Lisbon (Portugal).

14. S. Shweiki, D. Mundo, and A. Palermo, *A Study on the Dynamic Behaviour of Lightweight Gears*, Shock and Vibration (2017).

15. S. Shweiki, A. Rezayat, T. Tamarozzi, and D. Mundo, *Transmission Error and Strain Analysis of Lightweight Gears by using a Hybrid FE-Analytical Gear Contact Model*, Mechanical Systems and Signal Processing (2019).

Bibliography

[1] Palermo A., Anthonis J., Mundo D., and Desmet W. "A novel gear test rig with adjustable shaft compliance and misalignments. Part I: Design." In: *Proceedings of the CMMNO*. 2013.

[2] Mohamed Slim Abbes, Slim Bouaziz, Fakher Chaari, Mohamed Maatar, and Mohamed Haddar. "An acoustic–structural interaction modelling for the evaluation of a gearbox-radiated noise". In: *International Journal of Mechanical Sciences* 50.3 (2008), pp. 569–577.

[3] V. Abousleiman and P. Velex. "A hybrid 3D finite element/lumped parameter model for quasi-static and dynamic analyses of planetary/epicyclic gear sets". In: *Mechanism and Machine Theory* 41.6 (2006), pp. 725 –748.

[4] B. M. Abramov. "Vibration of gear transmissions caused by varying rigidity of meshing". In: *Trud. Sem. Tear. Mash. Mekh* 21.86 (1960).

[5] KissSoft AG. *Contact Analysis in the Cylindrical Gear Calculation*. `http://www.kisssoft.ch/italiano/home/index.php`. 2011.

[6] M. Ajmi and P. Velex. "A model for simulating the quasi-static and dynamic behaviour of solid wide-faced spur and helical gears". In: *Mechanism and Machine Theory* 40.2 (2005), pp. 173 –190.

[7] A. Al-Shyyab and A. Kahraman. "A non-linear dynamic model for planetary gear sets". In: *Proceedings of the Institution of Mechanical Engineers, Part K: Journal of Multi-body Dynamics* 221.4 (2007), pp. 567–576.

[8] Vijaya Kumar Ambarisha and Robert G. Parker. "Nonlinear dynamics of planetary gears using analytical and finite element models". In: *Journal of Sound and Vibration* 302.3 (2007), pp. 577 –595. ISSN: 0022-460X.

[9] A. Andersson and L. Vedmar. "A dynamic model to determine vibrations in involute helical gears". In: *Journal of Sound and Vibration* 260.2 (2003), pp. 195 –212.

[10] D. Appleyard. "Assessing drivetrain reliability". In: *Renewable Energy World - Wind Technology* (2011).

[11] M. Arra. *L'elicottero*. Biblioteca tecnica Hoepli. Hoepli, 2001. ISBN: 9788820325510. URL: `https://books.google.it/books?id=0tDiuJdsRjgC`.

[12] M. Bampton and R. Craig. "Coupling of substructures for dynamic analyses". In: *AIAA Journal* 6.7 (1968), pp. 1313–1319.

[13] S. Baud and P. Velex. "Static and Dynamic Tooth Loading in Spur and Helical Geared Systems-Experiments and Model Validation". In: *Journal of Mechanical Design* 124.2 (2002), pp. 334–346.

[14] N. Baydar and A. BALL. "Detection of Gear Failures via Vibration and Acoustic Signals Using Wavelet Transform". In: *Mechanical Systems and Signal Processing* 17.4 (2003), pp. 787 –804.

[15] G.W. Blankenship and A. Kahraman. "Steady state forced response of a mechanical oscillator with combined parametric excitation and clearance type non-linearity". In: *Journal of Sound and Vibration* 185.5 (1995), pp. 743 –765.

[16] B. Blockmans, T. Tamarozzi, F. Naets, and W. Desmet. "A nonlinear parametric model reduction method for efficient gear contact simulations". In: *International Journal for Numerical Methods in Engineering* 102.5 (2015), pp. 1162–1191.

[17] Giorgio Bonori, Marco Barbieri, and Francesco Pellicano. "Optimum profile modifications of spur gears by means of genetic algorithms". In: *Journal of Sound and Vibration* 313.3 (2008), pp. 603 –616.

[18] Christan Brecher, C Gorgels, Christian Carl, and M Brumm. "Benefit of psychoacoustic analyzing methods for gear noise investigation". In: *Gear Technology* 28.5 (2011).

[19] Y. Cai. "Simulation on the Rotational Vibration of Helical Gears in Consideration of the Tooth Separation Phenomenon (A New Stiffness Function of Helical Involute Tooth Pair)". In: 117 (Sept. 1995), pp. 460–469.

[20] Y. Cai and T. Hayashi. "The Linear Approximated Equation of Vibration of a Pair of Spur Gears (Theory and Experiment)". In: *Journal of Mechanical Design* 116.251 (1994), pp. 558–564.

[21] Brian Campbell, Wayne Stokes, Glen Steyer, Mark Clapper, R. Krishnaswami, and Nancy Gagnon. "Gear Noise Reduction of an Automatic Transmission Through Finite Element Dynamic Simulation". In: *SAE Transactions* 106 (1997), pp. 2883–2893.

[22] Niccolo' Cappellini, Tommmaso Tamarozzi, Bart Blockmans, Jakub Fiszer, Francesco Cosco, and Wim Desmet. "Semi-analytic Contact Technique in a Non-linear Parametric Model Order Reduction Method for Gear Simulations". In: *Meccanica – An International Journal of Theoretical and Applied Mechanics* (2017), pp. 1–27.

[23] A. Cardona. "Three-Dimensional Gears Modelling in Multibody Systems Analysis". In: *International Journal for Numerical Methods in Engineering* 40.2 (1997), pp. 357–381.

[24] P. Catera, F. Gagliardi, D. Mundo, L. De Napoli, A. Matveeva, and L. Farkas. "Multi-scale modeling of triaxial braided composites for FE-based modal analysis of hybrid metal-composite gears". In: *Composite Structures* 182 (2017), pp. 116 –123.

[25] Fakher Chaari, Walid Baccar, Mohamed Slim Abbes, and Mohamed Haddar. "Effect of spalling or tooth breakage on gearmesh stiffness and dynamic response of a one-stage spur gear transmission". In: *European Journal of Mechanics - A/Solids* 27.4 (2008), pp. 691 –705.

[26] Fakher Chaari, Tahar Fakhfakh, Riadh Hbaieb, Jamel Louati, and Mohamed Haddar. "Influence of manufacturing errors on the dynamic behavior of planetary gears". In: *The International Journal of Advanced Manufacturing Technology* 27.7 (2006), pp. 738–746.

[27] Yunxia Chen, Yi Jin, Xihui Liang, and Rui Kang. "Propagation path and failure behavior analysis of cracked gears under different initial angles". In: *Mechanical Systems and Signal Processing* 110 (2018), pp. 90 –109.

[28] T. F. Conry and A. Seireg. "A Mathematical Programming Technique for the Evaluation of Load Distribution and Optimal Modifications for Gear Systems". In: *Journal of Engineering for Industry* 95.4 (1973), pp. 1115–1122.

[29] Christopher G. Cooley and Robert G. Parker. "Vibration of high-speed rotating rings coupled to space-fixed stiffnesses". In: *Journal of Sound and Vibration* 333.12 (2014), pp. 2631 –2648. ISSN: 0022-460X. DOI: https://doi.org/10.1016/j.jsv.2014.01.005. URL: http://www.sciencedirect.com/science/article/pii/S0022460X14000273.

[30] John Coultate. "Wind turbine drivetrain technology and cost drivers". In: *Romax Technology* (2011).

[31] John Coultate. "Wind Turbine Gearbox Durability". In: *Wind Systems Magazine* (August 2009).

[32] Xiang Dai, Christopher G. Cooley, and Robert Parker. "Dynamic tooth root strains and experimental correlations in spur gear pairs". In: *Mechanism and Machine Theory* 101 (July 2016), pp. 60–74.

[33] G. Dalpiaz, A. Rivola, and R. Rubini. "Effectiveness and Sensitivity of Vibration Processing Techniques for Local Fault Detection in Gears". In: *Mechanical Systems and Signal Processing* 14.3 (2000), pp. 387 –412.

[34] P Davoli, Edoardo Conrado, and K Michaelis. "Recognizing gear failures". In: *Machine Design* 79 (June 2007), pp. 64–67.

[35] Jean-Luc Dion, Sylvie Le Moyne, Gaël Chevallier, and Hamidou Sebbah. "Gear impacts and idle gear noise: Experimental study and non-linear dynamic model". In: *Mechanical Systems and Signal Processing* 23.8 (2009), pp. 2608 –2628.

[36] D.W. Dudley and D.P. Townsend. *Dudley's Gear Handbook*. McGraw-Hill, 1991.

[37] Saeed Ebrahimi and Peter Eberhard. "Rigid-elastic modeling of meshing gear wheels in multibody systems". In: *Multibody System Dynamics* 16.1 (2006), pp. 55–71.

[38] K. Efstathiou, A. Basiakoulis, M. Efstathiou, M. Anastasiou, and J.H. Seiradakis. "Determination of the gears geometrical parameters necessary for the construction of an operational model of the Antikythera Mechanism". In: *Mechanism and Machine Theory* 52 (2012), pp. 219 –231.

[39] Tugan Eritenel and Robert G. Parker. "An investigation of tooth mesh nonlinearity and partial contact loss in gear pairs using a lumped-parameter model". In: *Mechanism and Machine Theory* 56 (2012), pp. 28 –51.

[40] Tugan Eritenel and Robert G. Parker. "Modal properties of three-dimensional helical planetary gears". In: *Journal of Sound and Vibration* 325.1 (2009), pp. 397 –420.

[41] Marcello Faggioni, Farhad S. Samani, Gabriele Bertacchi, and Francesco Pellicano. "Dynamic optimization of spur gears". In: *Mechanism and Machine Theory* 46.4 (2011), pp. 544 –557.

[42] Tony Freeth, Yanis Bitsakis, Xenophon Moussas, John H Seiradakis, Agamemnon Tselikas, Helen Mangou, Mary Zafeiropoulou, R Hadland, D Bate, Andrew Ramsey, et al. "Decoding the ancient Greek astronomical calculator known as the Antikythera Mechanism". In: *Nature* 444.7119 (2006), p. 587.

[43] GE. *GE Drivetrain Technologies*. Wind Turbine Gearbox Brochure.

[44] I. Gonzalez-Perez, Jose L. Iserte, and Fuentes A. "Implementation of Hertz theory and validation of a finite element model for stress analysis of gear drives with localized bearing contact". In: *Mechanism and Machine Theory* 46.6 (2011), pp. 765 –783.

[45] François Gérard, Michel Tournour, Naji Masri, Luc Cremers, Mario Felice, and Abbas Selmane. "Numerical Modeling of Engine Noise Radiation through the use of Acoustic Transfer Vectors - A Case Study". In: Apr. 2001.

[46] A. Grunwald. "Systematic optimization of gear boxes for hybrid and electric vehicles in terms of Efficiency, NVH and Durability". In: 2011.

[47] X. Gu and P. Velex. "On the dynamic simulation of eccentricity errors in planetary gears". In: *Mechanism and Machine Theory* 61 (2013), pp. 14 –29.

[48] Aydin Gunduz, Jason T. Dreyer, and Rajendra Singh. "Effect of bearing preloads on the modal characteristics of a shaft-bearing assembly: Experiments on double row angular contact ball bearings". In: *Mechanical Systems and Signal Processing* 31 (2012), pp. 176 –195.

[49] Yi Guo and Robert G. Parker. "Stiffness matrix calculation of rolling element bearings using a finite element/contact mechanics model". In: *Mechanism and Machine Theory* 51 (2012), pp. 32 –45.

[50] B. K. Han, M. K. Cho, C. Kim, C. H. Lim, and J. J. Kim. "Prediction of vibrating forces on meshing gears for a gear rattle using a new multi-body dynamic model". In: *International Journal of Automotive Technology* 10.4 (2009), pp. 469–474.

[51] Stephen L Harris. "Dynamic loads on the teeth of spur gears". In: *Proceedings of the Institution of Mechanical Engineers* 172 (1958), pp. 87–112.

[52] J. Helsen. "The Dynamics of High Power Density Gear Units with Focus on the Wind Turbine Application". PhD thesis. Katholieke Universiteit Leuven, Department of Mechanical Engineering, Division PMA, 2012.

[53] Jan Helsen, Frederik Vanhollebeke, Ben Marrant, Filip De Coninck, Dirk Vandepitte, and Wim Desmet. "Updated wind turbine gearbox multibody model with optimized flexible housing to deliver inputs for acoustic calculations". In: *Proceedings of the Multibody Dynamics Thematic Conference ECCOMAS* (2011).

[54] Bernd-Robert Hoehn, P Oster, S Radev, and T Griggel. "Tooth flanks corrections to counter excitation of noise by spur gears in theory and practice: Design of low noise toothing using the electronic data treatment (EDV) "Dynamic Tooth Forces Program" (DZP)". In: (Jan. 2006), pp. 235–250.

[55] "International Electrotechnical Commission Standard IEC 61400-11 and Other Procedures: Acoustic Noise Measurement Techniques". In: (2018).

[56] Korta J. and D. Mundo. "Multi-objective micro-geometry optimization of gear tooth supported by response surface methodology". In: *Mechanism and Machine Theory* 109 (2017), pp. 278 –295. ISSN: 0094-114X. DOI: https://doi.org/10.1016/j.mechmachtheory.2016.11.015. URL: http://www.sciencedirect.com/science/article/pii/S0094114X16305821.

[57] O J. Harris, M Douglas, B M. James, A M. Woolley, and L W. Lack. "Predicting the Effects of Transmission Housing Flexibility and Bearing Stiffness on Gear Mesh Misalignment and Transmission Error". In: *2nd MSC Worldwide Automotive Conference* (Jan. 2000).

[58] Barry James and Mike Douglas. "Development of a Gear Whine Model for the Complete Transmission System". In: *SAE Transactions* 111 (2002), pp. 1065–1074.

[59] Fred J Joachim and J C Boerner. "How to Minimize Power Losses in Transmissions , Axles and Steering Systems". In: 2012.

[60] K. L. Johnson. *Contact Mechanics*. Cambridge University Press, 1985. DOI: 10.1017/CBO9781139171731.

[61] A. Kahraman. "Planetary Gear Train Dynamics". In: *Journal of Mechanical Design* 116.3 (1994), pp. 713–720.

[62] A. Kahraman and G.W. Blankenship. "Interactions Between Commensurate Parametric And Forcing Excitations In A System With Clearance". In: *Journal of Sound and Vibration* 194.3 (1996), pp. 317 –336.

[63] A. Kahraman, A. Kharazi, and M. Umrani. "A deformable body dynamic analysis of planetary gears with thin rims". In: *Journal of Sound Vibration* 262 (May 2003), pp. 752–768. DOI: 10.1016/S0022-460X(03)00122-6.

[64] A. Kahraman and R. Singh. "Non-linear dynamics of a spur gear pair". In: *Journal of Sound and Vibration* 142.1 (1990), pp. 49 –75.

[65] Ma Ru Kang and Ahmet Kahraman. "Measurement of vibratory motions of gears supported by compliant shafts". In: *Mechanical Systems and Signal Processing* 29 (2012), pp. 391 –403.

[66] Jakub A Korta and Domenico Mundo. "A population-based meta-heuristic approach for robust micro-geometry optimization of tooth profile in spur gears considering manufacturing uncertainties". In: *Meccanica* 53.1-2 (2018), pp. 447–464.

[67] M. Kubur, A. Kahraman, D. M. Zini, and K. Kienzle. "Dynamic Analysis of a Multi-Shaft Helical Gear Transmission by Finite Elements: Model and Experiment". In: *Journal of Vibration and Acoustics* 126.3 (2004), pp. 398–406.

[68] US National Renewable Energy Laboratory. *Gearbox Reliability Collaborative*. `www.nrel.gov/wind/grc/`.

[69] Shuting Li. "Effects of machining errors, assembly errors and tooth modifications on loading capacity, load-sharing ratio and transmission error of a pair of spur gears". In: *Mechanism and Machine Theory* 42.6 (2007), pp. 698 –726.

[70] Shuting Li. "Experimental investigation and FEM analysis of resonance frequency behavior of three-dimensional, thin-walled spur gears with a power-circulating test rig". In: *Mechanism and Machine Theory* 43.8 (2008), pp. 934 –963.

[71] Xihui Liang, Hongsheng Zhang, Ming J. Zuo, and Yong Qin. "Three new models for evaluation of standard involute spur gear mesh stiffness". In: *Mechanical Systems and Signal Processing* 101 (2018), pp. 424 –434. ISSN: 0888-3270. DOI: `https://doi.org/10.1016/j.ymssp.2017.09.005`. URL: `http://www.sciencedirect.com/science/article/pii/S0888327017304818`.

[72] T.C. Lim and R. Singh. "Vibration transmission through rolling element bearings, part I: Bearing stiffness formulation". In: *Journal of Sound and Vibration* 139.2 (1990), pp. 179 –199.

[73] T.C. Lim and R. Singh. "Vibration transmission through rolling element bearings, part I: Bearing stiffness formulation". In: *Journal of Sound and Vibration* 139.2 (1990), pp. 179 –199.

[74] T.C. Lim and R. Singh. "Vibration transmission through rolling element bearings, part II: System studies". In: *Journal of Sound and Vibration* 139.2 (1990), pp. 201 –225.

[75] T.C. Lim and R. Singh. "Vibration transmission through rolling element bearings. Part III: Geared rotor system studies". In: *Journal of Sound and Vibration* 151.1 (1991), pp. 31 –54.

[76] Hsiang Hsi Lin, Fred B. Oswald, and Dennis P. Townsend. "Dynamic loading of spur gears with linear or parabolic tooth profile modifications". In: *Mechanism and Machine Theory* 29.8 (1994), pp. 1115 –1129.

[77] J. Lin and R. G. Parker. "Structured Vibration Characteristics of Planetary Gears with Unequally Spaced Planets". In: *Journal of Sound and Vibration* 233 (2000), p. 921.

[78] J. LIN and R.G. PARKER. "Analytical Characterization of the Unique Properties of Planetary Gear Free Vibration". In: *Journal of Vibration and Acoustics* 121.3 (1999), pp. 316 –321.

[79] J. LIN and R.G. PARKER. "Planetary Gear Parametric Instability Caused by Mesh Stiffness Variation". In: *Journal of Sound and Vibration* 249.1 (2002), pp. 129 –145.

[80] Tengjiao Lin, H. Ou, and Runfang Li. "A finite element method for 3D static and dynamic contact/impact analysis of gear drives". In: *Computer Methods in Applied Mechanics and Engineering* 196.9 (2007), pp. 1716 –1728.

[81] Faydor L. Litvin and Alfonso Fuentes. *Gear Geometry and Applied Theory*. 2nd ed. Cambridge University Press, 2004. DOI: 10.1017/CBO9780511547126.

[82] Gang Liu and Robert Parker. "Dynamic Modeling and Analysis of Tooth Profile Modification for Multimesh Gear Vibration". In: *Journal of Mechanical Design* 130.12 (2008), pp. 1–13.

[83] O. Lundvall, N. Strömberg, and A. Klarbring. "A flexible multi-body approach for frictional contact in spur gears". In: *Journal of Sound and Vibration* 278.3 (2004), pp. 479 –499.

[84] S. Mahalingam and R.E.D. Bishop. "Dynamic loading of gear teeth". In: *Journal of Sound and Vibration* 36.2 (1974), pp. 179 –189.

[85] D. Malkus, M. Plesha, R. Witt, and R. Cook. *Concepts and Applications of Finite Element Analysis*. Wiley, 2001.

[86] *Manual Transmission*. \protect\unhbox\voidb@x\penalty\@M\http://auto.howstuffworks.com/transmission4.htm. 2017.

[87] Jeffrey A. Morgan, Maruthi R. Dhulipudi, Refaat Y. Yakoub, and Alan D. Lewis. "Gear Mesh Excitation Models for Assessing Gear Rattle and Gear Whine of Torque Transmission Systems with Planetary Gear Sets". In: *SAE Technical Paper* 5 (2007).

[88] E. Mucchi and A. Vecchio. "Acoustical signature analysis of a helicopter cabin in steady-state and run up operational conditions". In: *Proceedings of ISMA Conference, Leuven Belgium* (2008), pp. 1345–1358.

[89] *Simpack modeling elements*. 2010.

[90] R.G. Munro. "The dynamic Behaviour of spur gears". PhD thesis. University of Cambridge.

[91] Katta G. Murty, Feng Yu, and umich edu emurty. "Linear Complementarity, Linear and Nonlinear Programming Internet Edition". In: 2010.

[92] Z. Neusser, M. Sopouch, Thomas Schaffner, and Hans-Herwig Priebsch. "Multibody Dynamics Based Gear Mesh Models for Prediction of Gear Dynamics and Transmission Error". In: *SAE Technical Paper*. SAE International, Apr. 2010.

[93] Takayuki Nishino. "Vibration Analysis of the Helical Gear System Using the Integrated Excitation Model". In: *Journal of Advanced Mechanical Design, Systems, and Manufacturing* 1.4 (2007), pp. 541–552.

[94] Norman C. Otto, Richard Simpson, and Jason Wiederhold. "Electric Vehicle Sound Quality". In: *SAE Technical Paper* (1999).

[95] A. Palermo, D. Mundo, R. Hadjit, and W. Desmet. "Multibody element for spur and helical gear meshing based on detailed three-dimensional contact calculations". In: *Mechanism and Machine Theory* 62 (2013), pp. 13 –30.

[96] Antonio Palermo, Laurent Britte, Karl Janssens, Domenico Mundo, and Wim Desmet. "The measurement of Gear Transmission Error as an NVH indicator: Theoretical discussion and industrial application via low-cost digital encoders to an all-electric vehicle gearbox". In: *Mechanical Systems and Signal Processing* 110 (2018), pp. 368 –389.

[97] Sungho Park, Seokgoo Kim, and Joo-Ho Choi. "Gear fault diagnosis using transmission error and ensemble empirical mode decomposition". In: *Mechanical Systems and Signal Processing* 108 (2018), pp. 262 –275.

[98] R G. Parker and X. Wu. "Parametric Instability of Planetary Gears Having Elastic Continuum Ring Gears". In: *Journal of Vibration and Acoustics* 134.4 (2012), pp. 041011–1 –041011–11.

[99] R.G. Parker, V. Agashe, and S.M. Vijayakar. "Dynamic Response of a Planetary Gear System Using a Finite Element/Contact Mechanics Model". In: *Journal of Mechanical Design* 122.3 (1999), pp. 304 –310.

[100] R.G. Parker and J. Lin. "Mesh Phasing Relationships in Planetary and Epicyclic Gears". In: *Journal of Mechanical Design* 126.2 (2004), pp. 365 –370.

[101] R.G. Parker, S.M. Vijayakar, and T. Imajo. "Non-Linear Dynamic Response of a Spur Gear Pair: Modelling and Experimental Comparisons". In: *Journal of Sound and Vibration* 237.3 (2000), pp. 435 –455.

[102] J. Pears, S. Curtis, A. Poon, A. Smith, D. Poon, and D. Palmer. "Investigation of Methods to Predict Parallel and Epicyclic Gear Transmission Error". In: *SAE Technical Paper*. SAE International, Apr. 2005. DOI: 10.4271/2005-01-1818.

[103] José I. Pedrero, Miguel Pleguezuelos, Mariano Artés, and Juan A. Antona. "Load distribution model along the line of contact for involute external gears". In: *Mechanism and Machine Theory* 45.5 (2010), pp. 780 –794.

[104] J. L. M. Peeters. "Simulation of dynamic drive train loads in a wind turbine". PhD thesis. Katholieke Universiteit Leuven, Department of Mechanical Engineering, Division PMA, 2006.

[105] Jesús María Pinar Pérez, Fausto Pedro García Marquez, Andrew Tobias, and Mayorkinos Papaelias. "Wind turbine reliability analysis". In: *Renewable and Sustainable Energy Reviews* 23 (2013), pp. 463 –472.

[106] Amani Raad, Jérôme Antoni, and Ménad Sidahmed. "Indicators of cyclostationarity: Theory and application to gear fault monitoring". In: *Mechanical Systems and Signal Processing* 22.3 (2008), pp. 574 –587.

[107] B. Randall R. "State of the art in monitoring rotating machinery-part 1". In: *Sound and vibration* 38.3 (2004), pp. 14–21.

[108] B. Randall R. "State of the art in monitoring rotating machinery-part 2". In: *Sound and vibration* 38.5 (2004), pp. 10–17.

[109] J. Reswick. "Dynamic loads in spur and helical gear teeth". In: *Trans. Amer. Soc. mech. Engrs* 77.635 (1954).

[110] A. Rezaei and A. Dadouche. "Development of a turbojet engine gearbox test rig for prognostics and health management". In: *Mechanical Systems and Signal Processing* 33 (2012), pp. 299 –311. ISSN: 0888-3270. DOI: https://doi.org/10.1016/j.ymssp.2012.05.013. URL: http://www.sciencedirect.com/science/article/pii/S0888327012002312.

[111] A. Fernandez del Rincon, P. Garcia, A. Diez-Ibarbia, A. de Juan, M. Iglesias, and F. Viadero. "Enhanced model of gear transmission dynamics for condition monitoring applications: Effects of torque, friction and bearing clearance". In: *Mechanical Systems and Signal Processing* 85 (2017), pp. 445 –467. ISSN: 0888-3270. DOI: https://doi.org/10.1016/j.ymssp.2016.08.031. URL: http://www.sciencedirect.com/science/article/pii/S0888327016303132.

[112] Rolls-Royce. *The Jet Engine*. Key Publishing, 2005.

[113] P. Sainsot, P. Velex, and O. Duverger. "Contribution of Gear Body to Tooth Deflections—A New Bidimensional Analytical Formula". In: *Journal of Mechanical Design* 126.4 (2004), pp. 748 –752.

[114] Paul D Samuel and Darryll J Pines. "A review of vibration-based techniques for helicopter transmission diagnostics". In: *Journal of sound and vibration* 282.1-2 (2005), pp. 475–508.

[115] *State-of-the-Art Techniques used for Determining Reliable Load Assumptions in Wind Turbines using SIMPACK*. 2010.

[116] Dennis Schurr, Philip Holzwarth, and Peter Eberhard. "Investigation of dynamic stress recovery in elastic gear simulations using different reduction techniques". In: *Computational Mechanics* (2017). ISSN: 1432-0924. DOI: 10.1007/s00466-017-1507-z. URL: https://doi.org/10.1007/s00466-017-1507-z.

[117] D. L. Seager. "Conditions for the Neutralization of Excitation by the Teeth in Epicyclic Gearing". In: *Journal of Mechanical Engineering Science* 17.5 (1975), pp. 293–299.

[118] S. Shweiki, D. Mundo, and A. Palermo. "A Study on the Dynamic Behaviour of Lightweight Gears". In: *Shock and Vibration* 2017 (2017).

[119] S. Shweiki, A. Rezayat, T. Tamarozzi, and D. Mundo. "Transmission Error and strain analysis of lightweight gears by using a hybrid FE-analytical gear contact model". In: *Mechanical Systems and Signal Processing* 123 (2019), pp. 573 –590.

[120] Siemens PLM Software. *Boosting productivity in gearbox engineering*. \protect\unhbox\voidb@x\penalty\@M\https://community.plm.automation.siemens.com/siemensplm/attachments/siemensplm/Simcenter_event_tkb/117/2/Siemens-PLM-Boosting-Productivity-in-Gearbox-Engineering.pdf. 2017.

[121] Avinash Singh. "Load sharing behavior in epicyclic gears: Physical explanation and generalized formulation". In: *Mechanism and Machine Theory* 45.3 (2010), pp. 511 –530.

[122] Chen Siyu, Tang Jinyuan, Luo Caiwang, and Wang Qibo. "Nonlinear dynamic characteristics of geared rotor bearing systems with dynamic backlash and friction". In: *Mechanism and Machine Theory* 46.4 (2011), pp. 466 –478.

[123] J.D. Smith. *Gear Noise and Vibration*. Dekker Mechanical Engineering. Taylor & Francis, 2003.

[124] M. E. Stegemiller and D. R. Houser. "A Three-Dimensional Analysis of the Base Flexibility of Gear Teeth". In: *Journal of Mechanical Design* 115.1 (1993), pp. 186 – 192.

[125] H. Strauch. "Zahnradschwingungen". In: *Z. Yer. dtsch* 159.395 (1954).

[126] T. Tamarozzi, G.H.K. Heirman, and W. Desmet. "An on-line time dependent parametric model order reduction scheme with focus on dynamic stress recovery". In: *Computer Methods in Applied Mechanics and Engineering* 268 (2014), pp. 336 –358.

[127] V. K. Tamminana, A. Kahraman, and S. Vijayakar. "A Study of the Relationship Between the Dynamic Factors and the Dynamic Transmission Error of Spur Gear Pairs". In: *Journal of Mechanical Design* 129.1 (2006), pp. 75 –84.

[128] Christoph Tobias and Peter Eberhard. "Stress recovery with Krylov-subspaces in reduced elastic multibody systems". In: *Multibody System Dynamics* 25.4 (2011), pp. 377–393.

[129] W. A. Tuplin. "Gear-Tooth Stresses at High Speed". In: *Proceedings of the Institution of Mechanical Engineers* 163.1 (1950), pp. 162–175.

[130] Kiyohiko Umezawa, Toshio Suzuki, and Taichi Sato. "Vibration of Power Transmission Helical Gears : Approximate Equation of Tooth Stiffness". In: *Bulletin of JSME* 29.251 (1986), pp. 1605–1611.

[131] *ISO 21771. Gears – Cylindrical involute gears and gear pairs – Concepts and geometry*. Intenational Standard. Geneva, CH: International Organization for Standardization, 2007.

[132] *ISO 6336-1. Calculation of load capacity of spur and helical gears — Part 1: Basic principles, introduction and general influence factors*. Intenational Standard. Geneva, CH: International Organization for Standardization, 2006.

[133] M. Utagawa. "Dynamic Loads on Spur Gear Teeth". In: *Bulletin of JSME* 1.4 (1958), pp. 397–403.

[134] Lars Vedmar. "On the design of external involute gears". English. PhD thesis. Division of Machine Elements, Department of Mechanical Engineering, Lund Institute of Technology, 1981.

[135] P. Velex and M. Ajmi. "Dynamic tooth loads and quasi-static transmission errors in helical gears – Approximate dynamic factor formulae". In: *Mechanism and Machine Theory* 42.11 (2007), pp. 1512 –1526.

[136] P. Velex and M. Ajmi. "On the modelling of excitations in geared systems by transmission errors". In: *Journal of Sound and Vibration* 290.3 (2006), pp. 882 –909.

[137] P. Velex and M. Maatar. "A Mathematical Model for Analyzing the Influence of Shape Deviations and Mounting Errors on Gear Dynamic Behaviour". In: *Journal of Sound and Vibration* 191.5 (1996), pp. 629 –660.

[138] Philippe Velex and Avinash Singh. "Top Gear". In: *Journal of Mechanical Design* 132.6 (2010), p. 060301.

[139] Sandeep Vijayakar. "A combined surface integral and finite element solution for a three-dimensional contact problem". In: *International Journal for Numerical Methods in Engineering* 31.3 (1991).

[140] H. Vinayak and R. Singh. "Multi-body Dynamics and Modal Analysis of Compliant Gear Bodies". In: *Journal of Sound and Vibration* 210.2 (1998), pp. 171 –214.

[141] R W Gregory, S L Harris, and R G Munro. "Dynamic Behaviour of Spur Gears". In: *Proceedings of the Institution of Mechanical Engineers* 178 (1963), pp. 207–226.

[142] Lassâad Walha, Tahar Fakhfakh, and Mohamed Haddar. "Nonlinear dynamics of a two-stage gear system with mesh stiffness fluctuation, bearing flexibility and backlash". In: *Mechanism and Machine Theory* 44.5 (2009), pp. 1058 –1069.

[143] Jiande Wang and Ian Howard. "Finite Element Analysis of High Contact Ratio Spur Gears in Mesh". In: *Journal of Tribology* 127.3 (2005), pp. 469 –483.

[144] C Weber, K. Banaschek, and G. Niemann. "Formänderung und Profilrücknahme bei gerad-und schrägverzahnten Rädern". In: *F. Vieweg* (1955).

[145] Agusta Westland. *AW101 VVIP Helicopter*. Product Brochure.

[146] Wikipedia contributors. *Dual-mass flywheel — Wikipedia, The Free Encyclopedia*. [Online; accessed 12-September-2018]. 2018.

[147] Wikipedia contributors. *Emblem of Italy — Wikipedia, The Free Encyclopedia*. [Online; accessed 12-September-2018]. 2018.

[148] P. Wriggers. *Computational Contact Mechanics*. Wiley, 2002. ISBN: 9780471496809. URL: https://books.google.it/books?id=8e9eNEpvVdYC.

[149] J. Zeman. "Dynamische Zusatzkrafter in Zahnradgetrieben". In: *Yer. dtsch, Ing.* 18.161 (1957).

[150] ZF. *ZF 8HP 8-Speed Automatic Transmission*. Product Brochure.

[151] H. Nevzat Özgüven and D.R. Houser. "Mathematical models used in gear dynamics—A review". In: *Journal of Sound and Vibration* 121.3 (1988), pp. 383 –411.

[152] H.N. Özgüven. "A non-linear mathematical model for dynamic analysis of spur gears including shaft and bearing dynamics". In: *Journal of Sound and Vibration* 145.2 (1991), pp. 239 –260.

[153] H.Nevzat Özgüven and D.R. Houser. "Dynamic analysis of high speed gears by using loaded static transmission error". In: *Journal of Sound and Vibration* 125.1 (1988), pp. 71 –83.

[154] J.J. Zhang, I.I. Esat, and Y.H. Shi. "Load analysis with varying mesh stiffness". In: *Computers and Structures* 70.3 (1999), pp. 273 –280.

[155] Pascal Ziegler and Peter Eberhard. "Simulative and experimental investigation of impacts on gear wheels". In: *Computer Methods in Applied Mechanics and Engineering* 197.51 (2008), pp. 4653 –4662.

[156] Pascal Ziegler, Peter Eberhard, and Bernhard Schweizer. "Simulation of impacts in geartrains using different approaches". In: *Archive of Applied Mechanics* 76.9 (2006), pp. 537–548.